APPENDIX N
FATE & TRANSPORT ANALYSIS

TABLE OF CONTENTS

LIST OF FIGURES

LIST OF TABLES

1.0 INTRODUCTION

A three-layer, three-dimensional steady-state numerical groundwater flow model of the region of the former Loring Air Force Base (Loring or Site) was developed to evaluate the current and future distributions of per- and polyfluoroalkyl substances (PFAS) compounds within the surface and subsurface waters at the Site. Work was performed on behalf of the Air Force Civil Engineer Center (AFCEC) under Contract Number FA8903-16-D-0027, Task Order FA8903-21-F-1048, Per- and Polyfluroalkyl Substances Response, Former Loring Air Force Base, Limestone, Maine.

2.0 BACKGROUND

PFAS are a group of synthetic fluorinated compounds used to make products more resistant to heat, grease, and water, and were detected in various sample media as part of the Site Inspection investigation (Wood E&I, 2018). PFAS are classified as hazardous substances and are therefore regulated under the Comprehensive Environmental Response, Compensation, and Liability Act (CERCLA). In response, WSP USA Environment & Infrastructure Inc. (WSP), has prepared this Remedial Investigation (RI) Summary Report to document the nature and extent of per- and polyfluoroalkyl substances (PFAS) contaminants in soil, groundwater, surface water, sediment, stormwater, and biota at the former Loring Air Force Base located in Limestone, Maine, and depicted on Figure N-1.

3.0 GEOLOGIC AND HYDROGEOLOGIC SETTING

The geologic and hydrogeologic settings are described in detail in Section 2 of the *RI Summary Report*. A summary is included below.

3.1 GEOLOGIC SETTING

Loring lies in the lower Aroostook River Basin. Topography of the basin is typified by a succession of gently rolling to steeply sloping ridges separated by narrow valleys. Elevations of the ridges range from 600 to 800 feet above sea level (referenced elevations are based on the National Geodetic Vertical Datum [NGVD]). Narrow swamps and bogs extend between the ridges. The valleys range in elevation from 500 to 600 feet above the NGVD.

Most of Loring is located on a relatively flat plateau, particularly between the Runway and Nose Dock areas in the central portion of the base, which generally represent the highest elevations of the base between 700 and 750 feet NGVD. The most significant changes in relief occur in the western portions of the base, where westerly flowing drainage with the Little Madawaska has formed incised valleys and swales.

3.1.1 Overburden Geology

The regional overburden geology, as shown in Figure N-2, reflects the surficial geology of northeastern Maine, shaped by Pleistocene glacial and post-glacial processes. These surface deposits mainly consist of glacial tills, stratified sand and gravel, as well as alluvial or peat deposits formed after the glaciers retreated.

At Loring, the uppermost Pleistocene deposits generally include either unstratified till directly overlying bedrock, glaciofluvial sediments, or stagnation moraine deposits (Maine Geological Survey, 2002). Among these, glacial till is the most prevalent unconsolidated material. The thickness of the glacial till varies greatly, ranging from a thin veneer to much greater depths in bedrock depressions.

3.1.2 Bedrock Geology

Beneath Loring and its surrounding region, the bedrock is classified as the Carys Mill Formation, as shown in Figure N-3. This formation consists of thinly interlayered micritic limestone—often termed ribbon limestone—and calcareous phyllitic slate. The limestone within this sequence ranges in character from strong and lightly fractured to areas that are extensively fractured and weathered.

The regional structural geology includes a series of mapped anticlines and synclines, which are occasionally interrupted and displaced by faults and fault zones trending generally from the northeast to the southwest. This structural system is especially well-documented to the west and southwest of Loring.

Within the Loring area, the trends observed in the subsurface bedrock are consistent with this wider regional pattern—a sequence of anticlines and synclines of varying scales, intersected by northeast-southwest oriented faults. The Basewide Groundwater Operable Unit (OU 12) Remedial Investigation at Loring made extensive use of borehole geophysical logging, which enabled geologists to identify the locations of several large-scale folds and the areas where fold limbs have been offset by faulting (ABB-ES, 1997). These investigations provided comprehensive information across the base, including the orientation of bedding within the Carys Mill Formation and the arrangement of joint and fracture systems critical to groundwater movement through the bedrock.

High-altitude aerial photography further assisted in tracing both local and regional fault-related lineaments throughout Loring (ABB-ES, 1997). Altogether, these studies have led to a detailed structural geologic interpretation, which forms the basis for understanding the hydrologic Conceptual Site Model (CSM) at Loring—a model dominated by the bedrock groundwater system. The principal structural features of the bedrock at the base are depicted in Figure N-4.

3.2 Hydrogeologic Setting

The site hydrogeology is described in detail in Section 2 of the *RI Summary Report*. The conceptual model presented in Section 2 and simplified for purposes of this groundwater numerical model consists of the following primary elements:

1. Groundwater base-wide is recharged primarily by infiltrating precipitation.
2. The base lies within the watersheds of Butterfield Brook-Limestone Stream, Greenlaw Brook, and Wolverton and Brandy Brooks. Greenlaw Brook, and Wolverton-Brandy Brooks, flow west into the Little Madawaska River, which is assumed to form a flow boundary to shallow groundwater flow moving west from the base.
3. The watershed areas adequately define separate flow regimes in the shallow flow systems at the base.
4. The streams and associated tributaries, ponds, wetlands, and lakes form principal hydrogeologic controls for shallow groundwater flow at the base.
5. Recharge of groundwater by infiltration of precipitation is further controlled by storm water interception, facility development promoting runoff, and extensive underdrain systems through the Nose Dock Area (NDA) and the Flightline Area.

4.0 SITE-SPECIFIC INFORMATION

Much of the applicable site-specific information presented here is summarized from the *OU-12 RI Report* (ABB-ES, 1997) and includes data from site investigations related to that investigation. New information from the current PFAS RI, described in the main body of this document, is also included and summarized below.

4.1 Geologic Information

Available and pertinent site data was compiled into data visualization platform Earth Volumetric Studio (EVS) to serve as a basis for refining and communicating the site conceptual model (CSM). Major components of the visualization included a representation of ground surface from digital elevation models, top of bedrock based on interpretations from the OU-12 RI augmented and updated with observations from the PFAS RI, and overburden and bedrock aquifer potentiometric surfaces from six synoptic water level measurement rounds from 2022 through 2024.

4.2 Aquifer Tests

WSP performed slug tests at the site in overburden and bedrock wells. The results of these tests are included here. Wells where slug tests were performed at Loring are shown on Figure N-5.

4.2.1 Slug Tests

Slug tests were performed in conjunction with synoptic sampling at the site. In total, 32 locations were tested (13 in overburden and 19 in bedrock). Full test results are presented in Appendix H.

5.0 NUMERICAL MODEL DEVELOPMENT

A three-dimensional groundwater flow model was developed for Loring to provide a framework for evaluating the site hydrogeology and for testing the soundness of the Site groundwater conceptual model for shallow groundwater movement at Loring and environs, and the fate and transport modeling of constituents found onsite. WSP developed the groundwater model using the following steps:

- Adopted the groundwater model domain from the OU-12 model as the domain for the revised groundwater model.
- Incorporated hydraulic conductivity values and distributions from the OU-12 model as starting values for the revised groundwater model.
- Updated bedrock lithologies which were incorporated into the model layering structure
- Incorporated boundary conditions reflecting current hydrological conditions.
- Added Connected Linear Network (CLN) elements to represent regional surface water features such as creeks, streams, ditches, and ponds.
- Calibrated the model using both manual and inverse methods, the latter available in Parameter ESTimation code (PEST) software.

A steady-state flow model was used for the flow portion of the simulation. A steady-state model applies constant stresses to the model and calculates long-term constant groundwater heads in the model. There is no transient pumping or other transient stresses within the model domain, so a steady-state model using average hydrologic conditions is appropriate.

The groundwater model was constructed using the graphical user interface Groundwater Vistas version 8.30 (Rumbaugh, 2024) as the pre- and post-processor.

5.1 Model Code

The numerical code used to construct the three-dimensional model was MODFLOW-USG, version 1.40 (Panday, 2020). MODFLOW-USG makes use of a robust solver, has the advantage of allowing for the creation of an unstructured (locally variable spaced) grid and can simulate unconfined (i.e., water table) conditions while using an upstream weighting function to smooth cell connections during drying and re-wetting of cells. This in turn helps with model convergence.

The XMD solver was used as the linear solution method, and the non-linear solver used was delta-bar-delta with the Newton-Raphson method. Other packages used were Layer-Property Flow (LPF), Recharge (RCH), Drain (DRN), General Head Boundary (GHB) (Harbaugh, 2005), and Connected Linear Network (CLN) (Panday, 2020).

5.2 Model Grid and Domain

The three-dimensional model grid includes a parent grid with areas of refinement around the source locations and surface water features. The parent grid cells are 500 x 500 feet and the most refined cells are 31.25 x 31.25 feet. Details of the model grid are provided in Table N-1. The model grid is rotated clockwise 36.78 degrees to be approximately parallel to the inferred average angle of the major fractures and lineaments within the model area. The horizontal datum of the model is feet (ft) North American Datum of 1983 (NAD83) and the vertical datum is ft NAVD 88.

Figure N-6 shows the model grid. The active domain corresponds to the interpreted extent of the local watershed areas. The exceptions to this are small segments representing connections of the Butterfield Brook/Limestone Stream system which extend beyond the model domain, and which are expected to have some local influence on flow into and out of the model.

5.3 Model Layers

The model is discretized in three layers representing overburden, fractured bedrock, and competent bedrock.

Layer 1 represents the overburden at the site. The top of Layer 1 represents the current ground surface elevation of the model, which was determined from 1/3 arc-second digital elevation model (DEM) data (USGS, 2025). Along streams, sand and gravel and alluvial deposits fill in much of the incised stream channels. These typically represent highly conductive zones, and, due to the lower bedrock surface in these channels, the sand and gravel deposits include much of the area where a groundwater table actually persists in the overburden. Elsewhere in the overburden, till and till-like fill are present. The denser and less conductive fill/till promotes runoff, and, particularly in the higher bedrock elevations, the water table is likely to be present in the upper rock.

Layer 2 represents the upper, more conductive fractured bedrock at the site. The top of bedrock was borings throughout the site, both historic from the OU-12 investigation and more recent as part of the current RI effort. The top of bedrock surface was interpolated in EVS and imported into the model. In areas of the model where the new EVS surface was absent, the bedrock surface used in the OU-12 model was incorporated, with some smoothing between the two. Layer 2 is a uniform 20 feet thick throughout the model.

Layer 3 represents the less conductive competent bedrock at the site. Layer 3 is a uniform 50 feet thick throughout the model and represents the bottom of the transmissive zones at the site and the area likely to affect contaminant transport.

5.4 Model Properties

Model properties dictate how water moves through the model. Groundwater recharge and hydraulic conductivity properties were assigned to the Loring model.

5.4.1 Groundwater Recharge

A Soil Water Balance (SWB) code, developed by the United States Geologic Survey (USGS), was used to estimate recharge on a basin-wide scale (Westenbroek et al., 2010). The USGS SWB calculates components of the water balance at daily increments using the Thornwaite-Mather water balance methodology (Thornwaite et al., 1957). Data requirements for estimating recharge with the SWB code include at minimum: 1) precipitation and temperature; 2) land cover; 3) hydrologic soil group; 4) soil-water capacity, and 5) flow direction. The SWB output provides annual recharge distribution for the specified model domain and time period. For the Loring model, the time period was January 2022 to December 2023, corresponding with the period of record for model calibration data (discussed below).

The SWB code calculates recharge as the difference between the change in soil moisture and sources and sinks:

$$\text{Recharge} = \text{Sources} - \text{Sinks} - \Delta\text{soil moisture}$$

Sources of water include precipitation and inflow from an adjacent model cell. Sinks include evapotranspiration (ET), interception of water assumed to be trapped and used by plants, and surface-run-off. A brief discussion of the components of sources and sinks are provided below. A more detailed description of the SWB code is provided by Westenbroek et al., 2010.

5.4.1.1 Precipitation

Precipitation for the simulated time period was obtained from the National Oceanic and Atmospheric Administration (NOAA) National Center for Environmental Information Climate Data Online (NOAA, 2024). Climate data (precipitation and temperature) has been recorded at the National Weather Service Forecast Office in Caribou, ME since 1939. Daily precipitation and temperature data was downloaded for the recorded time-period. Average annual precipitation from 1939 to 2022 is 38.2 inches.

5.4.1.2 SWB Inflow and Outflow

For every cell within the SWB model domain, the model calculates inflow to that cell and outflow out if it. Calculations are made to determine inflows and outflows, as well as the direction the water is moving. Flow direction, surface runoff, soil type, and land cover are used together to calculate inflow and outflow from a model cell. Flow direction was generated from digital elevation data using Environmental Systems Research Institute (ESRI) ArcGIS software using the current digital elevation model (DEM). Surface runoff is calculated using U.S. Department of Agriculture (USDA), Natural Resource Conservation Service (NRCS) run-off curve number (CN) method (USDA, 1986). Soil data was downloaded from the NRCS (Soil Survey Staff NRCS USDA, 2024). The National Land Cover Database (NLCD) (Dewitz, 2021) provides land cover data.

5.4.1.3 Evapotranspiration

Evapotranspiration (ET) is the loss of water from the land surface due to evaporation and the transpiration from plants. Although ET is a property that can be assigned directly to the groundwater flow model, the SWB model includes ET in the water balance calculations. The SWB model was run using the Thornthwaite-Mather (1957) method.

5.4.1.4 Soil Moisture

Soil moisture is the amount of water held in soil storage. The change in soil moisture is the amount of water that can be extracted from the soil and is tabulated using several intermediary calculations based on Thornthwaite and Mather (1957). The upper and lower bounds of soil moisture correspond to soils maximum soil water-holding capacity and a soils' wilting capacity (Westenbroek, et al. 2010). If the soil moisture value exceeds the maximum water holding capacity, the excess moisture is converted to groundwater recharge.

5.4.1.5 SWB Model Results

After the SWB model was run for the period of January 2022 to December 2023, the calculated average recharge rate was applied to the steady-state flow model. The recharge distribution is shown in Figure N-7.

While using a water balance method is a reasonable approach to estimating recharge on a basin-wide scale; there are some limitations to using the SWB code:

1. The code does not account for storm water management in areas of urbanization; and therefore, may be routing too much overland flow to adjacent, lower-lying areas. This is particularly important regarding the Nose Dock Area. Potential storm inflows are not accounted for in the SWB model nor the groundwater flow model.

2. The SWB code does not account for time of travel in the unsaturated zone which could be significant to timing of recharge applied to the groundwater flow model.

3. Water routed to a closed depression may result in an unrealistic amount of recharge. Although recharge applied to a grid cell is restricted by specifying a maximum recharge rate to the cell, the rejected recharge in a closed depression is ultimately removed from the model on the same day it originated as precipitation. Modeled recharge in stream channels were as high as 150+ inches/year. A maximum recharge rate of 30 inches per year was used in the flow model where higher values were calculated by SWB.

5.4.2 Hydraulic Conductivity

Initial model hydraulic conductivity values for the model were based on the OU-12 groundwater model. Hydraulic conductivity (K) data are available for each of the three layers but are widely variable. For Layer 1, representing overburden material comprised of till, alluvium, and sand and gravel, 23 data points were available, with K values ranging from 0.027 to 260 feet per day (ft/d). Lower values are believed to represent till, while the upper values are for alluvium and sand and gravel. For Layer 2, representing the upper fractured bedrock, 46 data points were available, with K values ranging from 0.0016 to 170 ft/d. For Layer 3, representing the deeper competent bedrock, only 4 points were available, with one value about 4 ft/ d and the other three ranging from about 0.2 to 0.9 ft/d.

WSP performed slug testing at Loring, targeting overburden and fractured bedrock. In all, 32 locations were tested with 19 locations in bedrock and 13 in overburden. A summary of the data is shown in Table N-2. The results were used to inform the assignment of hydraulic conductivity. Slug tests, while useful for quickly estimating hydraulic conductivity near a well, have limitations. They primarily provide information about the immediate area surrounding the well and may not be representative of the entire aquifer.

5.5 Boundary Conditions

Boundary conditions typically represent specific physical features (e.g., rivers, lakes, recharge, etc.), that influence the groundwater system where water either enters or leaves the model domain and are required to close the equation solution set. Four types of boundaries were used in the model; constant head, general head, drains, and no-flow.

5.5.1 General Head

General head boundaries (GHB) represent, conceptually, a fixed head far from the model where it is assumed to be constant with time (i.e., the river or head will not be affected by the model stresses over time). The purpose of using this boundary condition is to avoid unnecessarily extending the model domain outward to meet the actual physical feature influencing the head in the model domain. As a result, the general head condition is usually assigned along the outside edge of the model domain. GHB cells were used on the north side of the model domain to simulate regional groundwater levels north of the active portion of the model where Dagget Brook, Masters Brook, and Willard Brook enter the model. GHB cells are also used to represent alluvial underflow where Butterfield Brook and Little Madawaska River exit the model. Specified elevations for the GHB boundary cells were approximated from potentiometric surface maps and adjusted as part of the calibration process. GHB boundary calls are shown in Figure N-8.

5.5.2 Streams

Streams and surface water bodies play a significant role in the hydrology of the Site, and the interaction of surface water and groundwater can accelerate the transport of compounds. MODFLOW-USG's Connected Linear Network (CLN) package was used to model surface water boundaries. The CLN package was developed for MODFLOW–USG to provide the framework for incorporating one-dimensional connected features into a three-dimensional groundwater model grid. A one-dimensional CLN feature is any hydrogeologic or hydrologic water conveyance feature that has a cross-sectional dimension which is much smaller than the encompassing model cell (Panday et al., 2017). The CLN package also models transport through the features, which is well suited to Loring.

Streams and surface water bodies within the model domain were digitized in ArcGIS. Stage values were assigned where known, and approximated based on surface elevation elsewhere. Stream widths were approximated from satellite imagery. For surface water features that originate outside the model boundary (Little Madawaska River, Dagget Brook, Masters Brook, and Willard Brook) a constant head boundary condition was applied at the point of inflow. Constant head value was based on stage if known, or approximated from surface elevation elsewhere, and values were adjusted during calibration. Drain boundary conditions were used to manage surface water flow out of the model in Little Madawaska River and Butterfield Brook. Drain elevation was set to stream or river stage and drain conductance was set sufficiently high to allow water to exit the model without restriction. The CLN representation of streams is shown in Figure N-9.

5.5.3 Storm Drains

Storm drains near the nose dock area, south of the nose dock area, and adjacent to the runway are thought to have a role in the transport of PFAS compounds at the Site. The CLN package was used to simulate storm drains. Drain elevation was based on invert elevations measured at the Site, with slight adjustments made to ensure a correct gradient. A storm drain diameter of 4 feet was used. Upgradient boundary conditions intended to supply constant flow, such as those described for streams, were not used because constant inflow values were not known. Instead, groundwater can infiltrate when groundwater elevations are above the storm drain elevation and exfiltrate when groundwater elevations fall below the storm drain elevation, or flow out to the outfall in the Flightline Drainage Ditch. CLNs representing storm drains are shown in Figure N-10.

5.6 Model Calibration

The groundwater model must be calibrated to observed conditions to demonstrate its ability to reasonably replicate the hydrogeologic responses at the Site. Calibration is a process whereby model parameters are adjusted until the model output reasonably matches field observations. This is necessary to build confidence and credibility in the subsequent prediction of future conditions after construction.

Generally, calibration of the Loring model focused on adjusting hydraulic conductivity, recharge, and streambed leakance. During manual calibration, only one or two parameters could be adjusted at once because making more changes at one time made it difficult to isolate the effect that each change had on the calibration results. After each model run, the calibration statistics were analyzed, and a new set of parameter values were defined for the next model run. The process was then repeated to improve model fit and approach calibration goals.

5.6.1 Calibration Targets

Field investigations at the site from September 2022 to October 2023 recorded groundwater level measurements at 437 locations. Measurement density in parts of the model domain was high so the original list of locations was thinned using automated methods within Groundwater Vistas and manual methods. The final list of measurement locations used for model calibration contained data from 284 locations. Table N-3 shows construction information and water level measurements from those wells. Water level target measurements used for calibration are shown in Table N-4. Figures N-11, N-12, and N-13 show calibration target locations for overburden, fractured bedrock, and competent bedrock, respectively.

Calibration was performed by a combination of manual adjustments and automated parameter fit adjustments using the PEST software.

5.6.2 Calibration Results

Model calibration consists of comparing measured groundwater levels described above to model-calculated water levels as well as comparing model output with interpreted gradients and flow directions derived from observational data. Model calibration includes adjusting model parameters and boundary conditions to minimize statistical deviation from observed conditions and data.

The results of the calibration were evaluated based on analysis of residual statistics and comparison of modeled and observed groundwater potentiometric surfaces. A residual is defined as the observed piezometric level minus the modeled value. Thus, a negative residual indicates the model over-predicted the piezometric head at this location. An average residual of near zero indicates a balance of under- and over-prediction.

Residual statistics for the calibrated model run are shown in Table N-5.

A model is considered reasonably well-calibrated if the scaled root mean squared error (RMSE) is below 0.1 or 10% of the difference between the maximum and minimum of the piezometric heads in the target data set (Anderson et al. 2015). RMSE is calculated as:

$$RMSE = \sqrt{\frac{1}{N}\sum_{i=1}^{N}\left(h_i^m - h_i s\right)^2}$$

Where:

N is the number of measured values from observation points (for this CRN model N = 18)

h_i^m is the measured head in feet NAVD88

h_i^s is the simulated head at the corresponding location

The scaled RMSE for the calibrated model is 4.1%. The residual mean is 2.8 feet, indicating that the model is biased slightly low, although the bias is acceptable given the range in of observed values of 226.3 feet.

In addition to the quantitative calibration to groundwater levels, a qualitative comparison of modeled and observed surface water flow was also performed. Modeled flows generally match field-measured values, and relative changes in flow, such as above and below a stream confluence, are well represented, Table N-6. Stretches of streams that are gaining water through groundwater baseflow or losing water through infiltration also match inferred data as well.

The modeled potentiometric surface for overburden and bedrock are shown in Figure N-14 and Figure N-15. Observed versus modeled water levels for overburden, fractured bedrock, and competent bedrock are shown on Figure N-16.

5.6.3 Calibrated Model Parameter Values

Model calibration can take the form of adjustments to model properties within reasonable bounds and is an iterative process. The hydraulic conductivity zones of the calibrated model are shown in Figures N-17, N-18, and N-19. The final calibrated model parameter values are presented in Table N-7.

5.6.4 Model Water Balance

The modeled groundwater budget, presented in Table N-8, is consistent with the conceptual site model. The primary sources of inflow to the model are direct areal recharge (57 percent) and incoming flow of Little Madawaska River (41 percent) with the remainder coming in at the northern GHB. With no groundwater pumping in the model, the main discharge of groundwater is to the streams and rivers, with some alluvial underflow associated with Butterfield Brook and Little Madawaska River also present.

6.0 FATE AND TRANSPORT ASSESSMENT

The fate and transport of PFAS from source area soils to groundwater and along groundwater flow paths, including interaction with surface water, was assessed for Loring using a combination of data collected as part of this RI and data reported in literature. The PFAS assessed include perfluorooctanoic acid (PFOA) and perfluorooctanesulfonic acid (PFOS) with respect to United States Environmental Protection Agency (USEPA) Maximum Contaminant Levels (MCL). The combined data was used to determine the leaching to groundwater mass flux, develop USEPA soil screening level (SSL) calculations, and define source term input for the numerical model transport simulations. The approach, calculations, and data used in the soil leaching assessment are provided in the following sections.

6.1 Source Area Vadose Zone Soil Leaching

The leaching of PFAS from soils to groundwater at the four identified source areas (Fire Training Area [FTA], Structural Fire Station, Crash Fire Station, and Nose Dock Area [NDA]) was assessed using a combination of data collected as part of this RI. This data included soil PFAS concentrations, lysimeter porewater PFAS concentrations, PFAS leaching concentrations from column testing, recharge rates, and water levels, as well as soil physical properties such as hydraulic conductivity, bulk density, total porosity, effective porosity from grain size data, and soil moisture content. Additionally, data reported in literature was used to support calculations where site specific information was not available. The PFAS assessed include PFOA and PFOS with respect to USEPA Maximum Contaminant Levels (MCL). The combined data was used to define the source term input for the numerical model transport simulations, leaching to groundwater mass flux, and USEPA soil screening level (SSL) calculations. The approach, calculations, and data used in the soil leaching assessment is provided in the following sections.

6.2 Source Area Soil Leaching Areal Extent

The four source areas (FTA, Structural Fire Station, Crash Fire Station, and NDA) were assessed for their individual areal extent of PFAS in soils using ArcGIS and soil PFAS data from this RI to support fate and transport modeling and risk assessment. A convex hull polygon around each PFAS at each source area was created based on detections of each PFAS to define the source areas, Figures N-20 and N-21. The resulting calculated source areas range in size from 2.9 acres for PFOA at the Structural Fire Station up to 74 acres for PFOS at the FTA, Table N-9.

6.3 Source Area Soil Leaching Lysimeter Assessment

The PFAS results from six semi-annual sampling events were reported for porewater suction-lysimeter sampling that occurred in summer and fall of 2022, 2023, and 2024 for three of the four source areas (FTA, Crash Fire Station, and Structural Fire Station). An unsuccessful attempt was made to install a lysimeter at the NDA and thus there are no lysimeter results for that location. Qualitative assessment of the lysimeter porewater concentration results indicates that there is wide variability in the porewater concentrations throughout any single year, indicating potential seasonality, Figures N-22 through N-27. The results show a mix of temporal PFAS concentration trends with some PFAS increasing over time, others decreasing, and some showing an increase followed by a decrease. The ranges in concentrations are likely associated with the variable precipitation, soil heterogeneity, saturation within the vadose zone throughout the year as it relates to seasonal variation in precipitation and the flushing of PFAS from contaminated soils, and the variable distribution of PFAS in soils at each source area.

Plotting of the PFAS concentration distributions using univariate box plots indicates variability among the different source areas as well as the different PFAS and depths at which they were collected, Figures N-28 and N-29. The lysimeter PFAS concentration distributions for the four primary PFAS of interest in lysimeter porewater samples show that the leaching to groundwater is dominated by PFOS followed by PFOA at approximately an order of magnitude lower concentrations. The plots also show that the concentrations are generally normally distributed with median and mean concentrations being relatively similar. The shallow lysimeter concentrations for PFOS are consistently higher compared to deep concentrations for the three source areas with lysimeters installed, Figure N-29. The opposite is true for PFOA where concentrations from deep lysimeters are typically higher, Figure N-28. The higher PFOA at depth is likely a reflection of its typically lower adsorption to soils compared to PFOS allowing greater leaching to occur while more PFOS is retained higher in the soil column. The highest concentrations of both PFOS and PFOA are observed at the Crash Fire Station source area with relatively similar ranges for the other two source areas.

The median PFAS mass flux rate to groundwater per square foot, representing the median condition from August 2022 to October 2024, was calculated for both PFOA and PFOS at each lysimeter for the three source areas that have lysimeters installed. The median flux rate is based on the median concentrations from two years of data collection in combination with the calculated recharge rate for each source area using the SWB model (details provided as part of the numerical model development section), Table N-10. The per square foot flux rates for each lysimeter were then multiplied by the source areas determined from the convex hull polygons assessment to provide a total mass flux rate for each of the PFAS compounds at each of the three source area lysimeters resulting in loading of 10 to 506 grams per year (g/yr) for PFOS and 7.5 to 115 g/yr for PFOA. The greatest PFOA mass flux is at Crash Fire Station and the greatest PFOS mass flux is at Fire Training Area. The recharge rate at Structural Fire Station is the highest but has the lowest mass flux for both PFOA and PFOS due to higher PFOA and PFOS porewater concentrations.

6.4 Soil Screening Levels (SSLs) Assessment

The USEPA Soil Screening Guidance (U.S. EPA 1996) was used in combination with the revised screening method reported by Brusseau and Guo (2023) as an initial assessment in the determination of soil PFAS concentrations that will result in groundwater PFAS values below the regulatory values, Tables N-11 to N-14. The resulting calculated soil PFAS concentrations are referred to as the Soil Screening Levels (SSLs). The USEPA Soil Screening Guidance on developing SSLs is conservative in that the results likely indicate biased low residual soil concentrations necessary to meet groundwater regulatory values but serves as a basis for further evaluation. In part the evaluation is conservative in that the vadose zone calculated K_d values are the only mechanism used to account for attenuation of PFAS. The USEPA methodology does not capture or consider other potential mechanisms such as those occurring at the air water interface that can lead to significantly increased retention in the vadose zone. Thus, the revised method by Brusseau and Guo (2023) is used to calculate revised SSLs ($SSLs^{Rev}$) to consider the increased attenuation by soils due to air water interface interactions and provide more realistic PFAS soil concentrations that will result in meeting groundwater PFAS concentration regulatory criteria. The SSLs and $SSLs^{Rev}$ are both calculated and summarized for comparison, Table N-15.

While results are provided for estimates of soil concentrations needed to meet groundwater regulatory criteria, they should be taken as a low-end estimate that requires additional assessment, such as vadose zone numerical modeling that provides a more robust assessment, during subsequent efforts.

The SSL and SSL^{Rev} calculations were performed using the USEPA MCLs current as of April 2024, as the target groundwater concentrations for select PFAS (PFOA and PFOS). This soil screening assessment is used to estimate contaminant release to groundwater at a receptor based on a linear equilibrium soil/water partition equation referred to as the SSL (eq. 1), a linear equilibrium soil/water partition equation taking into account air water interface based on the work by Brusseau and Guo (2023) and referred to as the SSL^{REV} (eq. 2) for comparison to the traditional SSL, with both equations incorporating a combination of a water-balance and dilution attenuation factor (DAF) equation (eq. 3 and 4) to account for reduction of soil leachate concentration from mixing in an aquifer.

Soil Screening Level (SSL) = $C_{gw}DAF[K_d+(\theta_w+\theta_a H')/\rho_b]$ eq. 1

Where: C_{gw} is the target groundwater concentration

DAF is the dilution attenuation factor (from eqs. 3 & 4)

K_d is the distribution coefficient

θ_w is the water filled porosity

θ_a is the air-filled porosity

H' is Henry's constant at 20 degrees Celsius

ρ_b is the dry bulk density

Soil Screening Level Revised (SSL^{REV}) = $C_wDAF[K_d+(K_{aw}a_w+\theta_w+\theta_a H')/\rho_b]$ eq. 2

Where: C_{gw} is the target groundwater concentration

DAF is the dilution attenuation factor (from eqs. 3 & 4)

K_d is the distribution coefficient

K_{aw} is the air-water interfacial adsorption coefficient

a_w is the air-water interfacial area

θ_w is the water filled porosity

θ_a is the air-filled porosity

H' is Henry's constant at 20 degrees Celsius

ρ_b is the dry bulk density

Dilution Attenuation Factor (DAF) = $1 + [Kid_m]/[IL]$ eq. 3

Where: K is the saturated hydraulic conductivity

i is the groundwater gradient

d_m is the mixing depth (from eq. 4)

I is the infiltration rate or recharge rate

L is the length of the source

Mixing depth (d_m) = (0.0112L2)0.5 + d_a{1 - exp[(-LI)/(Kid_a)]} eq. 4

Where: L is the length of the source

d_a is the aquifer saturated thickness

I is the infiltration or recharge rate

K is the saturated hydraulic conductivity

i is the hydraulic gradient

The calculated SSL is a simplistic and conservative estimate of soil concentrations required to meet the set C_{gw}, and the SSL^{Rev} is somewhat less conservative, depending on the soil and PFAS properties, and degree of saturation, by considering potentially greater sorption at the air water interface in the vadose zone to meet the C_{gw}. The C_{gw} is set to the USEPA MCLs for both PFOS and PFOA (4 nanograms per liter [ng/L]). The SSL and SSL^{Rev} equations are solved based on site data for the other parameters including the site-specific calculated K_d values.

The DAF is one parameter within the SSL and SSL^{Rev} equations that is based on its own equation and set of parameters. The DAF considers dilution of PFAS porewater concentrations by groundwater once the leachate reaches groundwater and mixes with groundwater prior to being measured at a monitoring well or point of compliance. The DAF is also a function of the mixing depth equation such that the d_m is first calculated and then used in the DAF calculation. The SSL and SSL^{Rev} are then calculated using the site-specific DAF values in combination with the other parameters, Tables N-11 to N-14. Additionally, a target soil porewater concentration (C_{pw}) was calculated from the C_{gw} and DAF, Tables N-11 to N-15. The C_{pw} represents the PFAS porewater concentration that would result in a groundwater PFAS concentration at or below the groundwater regulatory criteria due to dilution and attenuation that can be related back to measured PFAS concentrations in lysimeter porewater samples.

The development of the SSL and SSL^{Rev} input parameters for the Loring source areas, including inputs to the DAF and d_m equations, are discussed in the following subsections.

6.4.1 DAF Specific Parameters

The input values for DAF calculations were determined from the numerical groundwater flow model and monitoring well water level and boring logs. The numerical groundwater model recharge rates and simulated groundwater contours were brought into ArcGIS to determine the infiltration rate (I) by averaging the recharge rates from the numerical model at each source zone area, and the hydraulic gradient (i) for each source area by taking the difference in contour elevations and measuring the distance between contours across the source areas. The numerical model recharge rates were determined from the SWB model developed by the USGS that uses daily temperature and precipitation input along with climatological, land use, and topography data to determine recharge (Section 2). The source areas were calculated by importing the direct push soil sampling locations into ArcGIS, creating convex hulls around the samples with detections for each PFAS of interest, and then calculating the associated areas. The source length (L) was also measured using ArcGIS by taking the distance from one end to the other across each convex hull generated from soils borings with detected PFAS at each source area. The boring logs indicating the depth to top of bedrock for source areas where the first groundwater is in the unconsolidated soils and the depth of boring for bedrock wells in combination with water level data to determine depth to groundwater and combined were used to determine the saturated thickness.

Hydraulic conductivity (K) values used in the DAF calculations were determined for each source area based on slug testing results from wells at or near each source area. The wells used to apply a K value in the calculations include JBW8003B and BW01005 for the FTA, OW05003 for the Structural Fire Station, OW07001 for the Crash Fire Station, and OW12002 for NDA.

6.4.2 Vadose Zone Distribution Coefficients

The median lysimeter water samples collected from biannual sampling over three years (2022 to 2024) were combined with collocated soil PFAS concentrations to calculate an apparent vadose zone K_d for the four PFAS having an MCL for drinking water for each of the three source zones with lysimeters. However, there is no lysimeter at the NDA and several soil analyses resulted in PFAS being below the detection limits such that a K_d could not be calculated. Thus, K_d values were also calculated based on the median of literature organic carbon-water partitioning coefficients (K_{oc}) reported by Interstate Technology and Regulatory Council (ITRC) PFAS physical and chemical properties table, Table 4-1 (2023) and average site-specific fraction of organic carbon (foc) where K_d is equal to the product of K_{oc} and foc. The resulting K_d values from both sources, lysimeter porewater with collocated soil pairs and organic carbon content with literature K_{oc} values, were then averaged for a final set of K_d values to use in the SSL calculations. The resulting K_d values are estimates and provide a first approximation but may be considered apparent due to the complex characteristics of PFAS interactions. The determination of K_d values from lysimeter porewater samples with collocated soil pairs assumes the concentration of PFAS in soils does not significantly change over the relatively short time of lysimeter sample collection and that the measured soil concentrations are due to the adsorption onto soils. Additionally, it is assumed that the variability observed in the lysimeter porewater sample concentrations is related to changing vadose zone saturation associated with precipitation events throughout the year and that the median concentration represents an annual average that can be related back to the soil concentrations migrating downward to groundwater.

The K_d values for each collocated soil sample with lysimeter porewater samples from the same sample depth, were calculated by dividing the soil concentration by the median of the six lysimeter porewater concentrations, Table N-16. Soil and lysimeter porewater concentrations with non-detect values were not used in the calculations. The calculated median K_d values range from 0.77 to 2.1 for PFOA and from 2.5 to 25 for PFOS. The range of calculated K_d values is relatively small and are associated with the variability in soil and lysimeter porewater concentrations which in part could be related to the air-water interface interactions, spatial and temporal differences in PFAS releases, soil type heterogeneity, and or in porewater saturation due to varying precipitation and snow melt events.

The K_d values calculated from lysimeter porewater pairs with soil concentrations were then supplemented with median K_d values calculated from literature data values of K_{oc} from the ITRC multiplied by the foc determined from site soils collected as part of this RI, Table N-17. The final set of K_d values used in the SSL and SSL^{Rev} calculations were then calculated as the median of the to data sets from lysimeter porewater and soil pairs, and from the product of K_{oc} with foc, Table N-18.

6.4.3 Vadose Zone Bulk Density and Porosity Values

The bulk density (ρ_b), air filled porosity (Θ_a), and water filled porosity (Θ_w) values for the unconsolidated vadose zone soils were taken as the median from the analysis of soils collected during lysimeter installation at each source area and attempted lysimeter installation at NDA, Table N-19. The bulk density for each source area was determined as the median value derived from laboratory analyses. Water-filled porosity was determined from the median laboratory soil moisture content, while air-filled porosity was calculated by subtracting water-filled porosity from total porosity measured in the lab.

6.4.4 Henry's Constant

Henry's constant (H') values for the four PFAS of interest were taken as the median of values from ITRC PFAS physical and chemical properties table, Table 4-1 (ITRC 2023). These values do not play an important role due to the relatively low volatility of the PFAS compounds of interest.

6.4.5 Air-Water Interfacial Adsorption

The air-water interfacial adsorption coefficient (K_{aw}) and air-water interfacial area (a_w) were determined from data provided in the ITRC's PFAS physical and chemical properties table, Table 4-1 (ITRC 2023), the relationship between K_{aw} and molar volume of each PFAS compound as reported by Brusseau and Van Glubt (2021), and a_w and grain size data reported by Silva et al. (2022). The data provided in ITRC's Table 4-1 includes K_{aw} values compiled from different sources for each PFAS compound that were used to calculate a median K_{aw} of 0.020 for PFOA and 0.045 for PFOS. The a_w values were calculated using the grain size data D_{50}, porosity, and soil saturation (S_w) determined from soil samples collected as part of this RI based on equations 5 and 6. The grain size data includes grain size analyses for soil samples collected from each source area during drilling for lysimeter installation. Soil samples were collected at up to three different depth intervals: shallow (0-3 feet), intermediate (6-8 feet at NDA, 8-10 feet at Structural Fire

Station and Crash Fire Station, and 11-13 feet at FTA), and deep (18-20 feet). The calculated a_w values and associated input used are presented in Table N-20.

Air-water interfacial area (a_w) = GSA(1-S_w) eq. 5

Where: a_w is the target groundwater concentration

GSA is the geometric surface area of the medium

S_w is the volumetric water content divided by total porosity

GSA = 6(1-n)/D_{50} eq. 6

GSA is the geometric surface area of the medium

n is the porosity

D_{50} the particle size where 50% of the total particles are smaller

6.5 Numerical Transport Model Parameters

There are several additional parameter inputs required for setting up the three-dimensional numerical groundwater transport model in addition to what is already included in the numerical flow model. The additional parameters characterize the current distribution of PFAS concentrations in groundwater, continuing source inputs to groundwater, and how the PFAS compounds interact with the aquifer media and therefore how quickly the PFAS compounds transport through the aquifer. The additional parameters required for transport simulations include effective porosity, bulk density, saturated K_d, dispersivity, recharge concentrations associated with each of the five source areas, and an initial concentration condition. The additional parameters were developed from Site specific data collected during this RI. Derivation of the additional transport modeling parameters and their input values for the three-dimensional numerical groundwater transport model are provided.

6.5.1 Effective Porosity

Effective porosity is a property of the aquifer sediments and bedrock units and is necessary to simulate the advection and sorption aspects of transport. The effective porosity values applied in the groundwater transport model were determined from a combination of site-specific data for the unconsolidated surficial soils, collected as part of this RI, and literature sources for the upper weathered and deeper more competent bedrock at the site.

The effective porosity values for the unconsolidated surficial soils represented by model layer 1 were determined from grain size data of soil samples collected during this RI using the method outlined by Urumovic and Urumovic (2014). The grain size data and calculated values are provided in Tables N-21 to N-30. The resulting calculated median effective porosity value is 0.23 and is used in model layer 1 representing the unconsolidated surficial soils for transport simulations.

Effective porosity values for the upper fractured bedrock (model layer 2), and competent bedrock (model layer 3) were determined from previous studies performed at the site and reported in literature (Thompson et al. 2004, Lane Jr. et al. 1996). The bedrock matrix porosity values reported by Thompson et al. (2004) range from 0.2 to 2.4 percent and are based on geotechnical laboratory analysis of 43 rock samples from 11 cored boreholes. It is reported that 88 percent of the measured values were less than 0.9 percent and a weak correlation of decreasing matrix porosity with increasing depth was noted. An additional porosity assessment for weathered and fractured bedrock reported by Thompson et al. (2004) indicated porosity values exceeding 3 percent. Lane Jr. et al. (1996) report a secondary porosity of the fractured-bedrock at the site on the order of 1 percent based on square-array resistivity data. A value of 0.9 percent was selected for use in the transport for the deep bedrock model layer (layer 2) because the bedrock matrix porosity and secondary porosity values reported from the two studies have similar values. Additionally, the deep bedrock in the model is still relatively shallow at an average depth of approximately 91 feet. This shallow depth supports the use of a higher porosity value given the correlation of decreasing porosity with increasing depth based on results from testing bedrock samples at relatively greater depths from 20 to 300 feet below ground surface. The reported higher end of the bedrock porosity range, 2.4 percent, from Thompson et al. (2004) was selected for the upper weathered and fractured bedrock represented in model layer 2. The upper end of the range accounts for the increased connected void space due to fracturing and weathering and is in line with the values just exceeding 3 percent in a limited area reported by Lane Jr. et al. (1996).

6.5.2 Bulk Density

The bulk density is a property of the aquifer sediments and is necessary to simulate sorption in the transport model. The bulk density values applied in the model are from a combination of site-specific data for the unconsolidated surficial soils, collected as part of this RI, and literature sources for the upper weathered and deeper competent bedrock at the site.

The calculated median bulk density for the consolidated surficial soils represented by layer 1 in the model is 1.6 grams per cubic centimeter, as shown on Table N-19. The median value was calculated from the analysis of ten soil samples collected across the site at the different source areas.

The weathered upper bedrock and deeper more competent bedrock bulk density values were taken from Thompson et al. (2004). Thompson et al. (2004) reported a range and average of bulk density measurements from seven bedrock cores collected from various locations across the site and tested by a geophysical laboratory. The measured values ranged from 2.69 to 2.98 grams per cubic centimeter with an average of 2.84 grams per cubic centimeter. No details are provided on the bulk density with respect to the samples being from fractured weathered bedrock versus more competent bedrock at depth, therefore the average value was assigned to both the upper weathered bedrock in model layer 2 and more competent bedrock in model layer 3.

6.5.3 Saturated Model Distribution Coefficients

The median K_d values were calculated for PFOA and PFOS to calculate soil concentrations needed to meet groundwater regulatory values based on the SSL and SSL^{Rev} equations using vadose zone data which are influenced by a different set of conditions including lithology, partial saturation, and potentially air water interface interactions. The K_d values for saturated flow transport modeling were determined using laboratory batch testing results for soil samples as part of this RI. The K_d is determined from the batch testing results by taking the slope from plotting the mass adsorbed versus the aqueous concentration after agitation, Figures N-30 and N-31. The batch testing made use of site soil samples collected from saturated conditions and PFAS-free groundwater collected from the Site. The main K_d batch testing performed after two initial tests were setup to identify an optimal liquid to solid ratio and kinetics. The final batch testing used 125 grams of each soil sample combined with 250 milliliters of groundwater sample (a liquid to solid ratio of 0.5 determined after initial testing ratios of 0.04, 0.2 and 0.5) spiked with a series of known PFAS concentrations at ratios typically observed across the site and agitated for 8-hours (determined sufficient after initial kinetic testing using times from 4 to 96 hours). The PFAS spike concentrations included 8 different spike concentrations that were from 2 to 4,000 ng/L for PFOA and from 10 to 20,000 ng/L for PFOS. The laboratory batch samples were centrifuged after agitation, and the supernatant and soils were then analyzed to determine the amount of PFAS compound sorbed and remaining in solution. The results are provided for PFOA and PFOS Table N-31.

6.5.4 Dispersivity

Dispersivity is used to characterize the local variations in the velocity field of a groundwater solute with longitudinal dispersivity in the direction of fluid flow and transverse perpendicular to flow direction. The longitudinal dispersivity was calculated using the power function (eq. 6) taken from Schulze-Makuch (2005).

$$\alpha = 0.2 \times L^n \qquad \text{eq. 6}$$

Where: α is the longitudinal dispersivity

L is the flow path length

n is the scaling exponent

The longitudinal dispersivity used is 8.2 ft and was calculated using a length of 1,700 ft that represents the approximate plume length from the source areas, and the scaling exponent of 0.5 that Schulze-Makuch (2005) states is closer to the values associated with higher reliability data sets. The transverse dispersivity is typically an order magnitude lower resulting in a value of 0.82 ft (Gelhar et al. 1992).

6.6 Source Zone Recharge PFAS Concentrations

The predictive transport modeling includes the continued leaching of PFAS from the vadose zone to groundwater at each of the four source zones based on laboratory Leaching Environmental Assessment Framework (LEAF) testing results combined with recharge rates, thickness of vadose contamination, soil density, and median deep lysimeter porewater concentrations.

The temporal leaching behavior of PFAS from site soils for use in the numerical modeling was determined using SW-846 LEAF Method 1314 to evaluate PFAS leaching from contaminated site soils with results reported as a function of liquid-solid ratio (L/S). SW-846 Method 1314 is an up-flow percolation column test designed to obtain liquid-solid partitioning (LSP) information as a function of L/S. The L/S is represented as the cumulative volume of leaching solution, PFAS free water in this case, passing through a column containing a known mass of soil contaminated with PFAS. The eluate is collected from the outlet of the column and analyzed for PFAS. The LEAF analyses were performed on soils collected during two different sampling events and include both shallow (0 to 3 feet below ground surface) and deep samples (8 to 15 feet below ground surface depending on location). The first soil sampling event occurred in 2022 and included samples for LEAF analysis from areas of greater PFAS at each of the four source areas with additional soil samples collected from areas of lower soils concentrations at each source area for LEAF testing in 2024, resulting in a total of fourteen LEAF analyses. The LEAF samples from each source area during the first sampling event were collocated with soil sampling and lysimeter installations for a comparison between soil and porewater concentrations in the field to the LEAF results generated in the laboratory. The deep median lysimeter porewater concentrations provide an estimation of PFAS concentrations currently leaching from the vadose zone soils to groundwater at each source area and can be used for comparison to LEAF concentrations generated from the first L/S ratio.

The LEAF PFAS concentrations reported as the L/S ratio provides a prediction of the leaching concentrations over time at a source zone from the vadose zone to groundwater using the rate of water passing through the soils, in this case the recharge rate, that interacts with the specific mass of soils based on the vadose zone thickness and bulk density of the vadose zone soils. The recharge rate provides a water flux in contact with the mass of soil in per unit area extending down through the entire length of the vadose zone represented by the measured depth to water. The mass of soil is determined by bulk density analysis and is used with the flux recharge rate to calculate the time to reach groundwater. The L/S ratio was converted to a time in years for plotting and calculating a source term for the numerical modelling effort using the numerical model recharge rate determined from the Soil Water Balance model, an average bulk density of 1.6 gram per cubic centimeter (g/cm3) for site samples, and the depth to water at each source area. The PFAS leaching concentrations were plotted versus the calculated time on log-log axes, Figures N-32 to N-45. The LEAF testing results indicate that PFAS porewater concentrations from source zone soils will decline significantly within the 50-year simulation period. The second set of soil samples collected in 2024 and analyzed by the LEAF method had lower concentrations compared to the first set of soils samples collected in 2022, confirming that the highest concentrations of PFAS for the source areas is associated with the location of the lysimeters. Additionally, the LEAF analyses for the soils collected during the first sampling event show relatively linear declines over time with log axes resulting in using power functions to fit the data and predict more continuous source terms for the numerical model with input on an annual basis.

The initial sample collected from the LEAF testing is associated with the smallest L/S ratio of 0.2 and in most cases is the maximum concentration and provides an estimate of the initial concentration of PFAS leaching from the soils. This initial dissolved PFAS concentration can be compared to in-situ measured PFAS concentrations from the porewater results from lysimeter sampling, Figures N-32 through N-37.

The resulting power functions for each PFAS at each source area were used in combination with the lysimeter concentrations to relate the laboratory results back to the field observed concentrations resulting in an adjusted set of temporal PFAS leaching to groundwater concentrations in the numerical groundwater model, Tables N-32 and N-33.

The power functions developed from the LEAF PFOA and PFOS concentrations were adjusted based on the median deep lysimeter concentrations at each source area to develop site specific declining source term concentrations at each of the four source areas for the predictions up to 50 years in the future simulated in the model. The declining source terms were applied to recharge in the model in each of the defined source areas with recharge rates based on the SWB model ranging between approximately 8.6 and 22.7 inches per year.

6.7 Initial Concentration Distribution of Compounds

The predictive modeling of PFAS transport in groundwater requires the input of an initial concentration for each PFAS compound simulated to represent current conditions. The model predictions of future concentrations are strongly dependent on the initial concentrations assigned in the model. The initial concentrations of each PFAS were developed using EVS and PFAS data collected as part of this RI from across the Site. The most recent and comprehensive groundwater sampling round was performed in October of 2024 and was comprised of samples from 78 overburden and 212 bedrock monitoring wells. Plume volumes were estimated for each groundwater sampling round via kriging of all data into a convex hull grid. The same grid geometry was used for all sampling rounds and a 10:1 horizontal to vertical, simple anisotropy was applied. The resulting interpolated plumes were imported directly into the groundwater transport model as an initial current condition for predictive modeling.

6.8 Contaminant Migration

Contaminant migration was assessed using the three-dimensional numerical groundwater fate and transport model using a combination of site specific and literature-based data described in previous sections. The transport of PFAS was predicted using the numerical model with a steady state flow field employing advection, dispersion, and sorption, but not degradation. A declining source term for leaching from source zone vadose zone soils, assigned to recharge, for each of the four main source areas, for 50 years into the future was applied. The initial conditions, PFAS interpolated plume using EVS, is considered representative of the Site PFAS concentrations as of the development of this report. Therefore, the numerical model times referenced will be with respect to the end of 2025 simulated predictions moving forward 50 years. Modeled PFOA and PFOS extents in groundwater at the current time (Day 1), and in 10, 25, and 50 years for PFOA and PFOS are shown in Figure N-46 and Figure N-47. Polygons represent the greatest extent of each compound present above the MCL of 4 ng/L in all three model layers at each time.

The transport of PFOA and PFOS is relatively limited in the groundwater over the simulated duration of 50 years. However, transport is increased where the plumes intersect surface water features in gaining reaches of streams. Greenlaw Brook, and to a lesser extent Flightline Drainage Ditch, both receive contaminated groundwater and transport it downstream to a point that it reinfiltrates. Concentrations are predicted in groundwater along Greenlaw Brook after 10 years and Little Madawaska River after 25 years, earlier than would be expected with groundwater transport alone. There is little to no reduction in the size of the PFOA or PFOS plumes at the site over the 50-year simulation period.

7.0 CONCLUSIONS AND RECOMMENDATIONS

The objectives of the current modeling effort were to update the conceptual site model, construct and calibrate a steady-state groundwater flow model of current conditions, and perform modeling to predict the fate and transport of PFAS compounds PFOA and PFOS. The model has been shown to simulate the regional groundwater system reasonably well based on the steady-state calibration and can also simulate surface water/groundwater interaction reasonably well.

Given the acceptable ability of the model to simulate groundwater at the Site, the model’s ability to evaluate PFAS compound migration and travel time to potential downgradient receptors is also acceptable. The interaction of surface water and groundwater plays a significant part of regional hydrology and fate and transport, allowing solutes to travel further via surface water than would otherwise occur when traveling within groundwater alone.

Continued development of the model to incorporate new data, including groundwater levels, PFAS concentrations, and lithology is recommended. Additional data, particularly beyond the area of focus thus far will increase confidence of model predictions in those areas.

8.0 REFERENCES

ABB-ES, 1997. Basewide Groundwater Operable Unit (OU 12) Remedial Investigation Report, Portland, Maine; December.

Anderson, Mary P., Woessner, William W., and Hunt, Randall J., 2015. Applied Groundwater Modeling: Simulation of Flow and Advective Transport, 2nd Edition, Academic Press; 564 pp.; August.

Brusseau, M .L. and S. Van Glubt. 2021. The influence of molecular structure on PFAS adsorption at air-water interfaces in electrolyte solutions. Chemosphere, 281: 130829.

Brusseau, M.L. and Guo, B. 2023. Revising the EPA dilution-attenuation soil screening model for PFAS. Journal of Hazardous Materials Letters, 4: article 100077.

Dewitz, J., 2021, National Land Cover Database (NLCD) 2019 Products: U.S. Geological Survey data,, available online at the following link https://www.mrlc.gov/national-land-cover-database-nlcd-2016 and accessed December 2024.

Gelhar, L. W., C. Welty, and K. R. Rehfeldt, 1992, A critical review of data on field-scale dispersion in aquifers, 28(7), 1955-1974.

Harbaugh, A.W., 2005, MODFLOW-2005, the U.S. Geological Survey modular ground-water model -- the Ground-Water Flow Process: U.S. Geological Survey Techniques and Methods 6-A16. https://doi.org/10.3133/tm6A16

Interstate Technology and Regulatory Council (ITRC), 2023. PFAS physical and chemical properties table, Table 4-1.

Lane Jr., J.W., Haeni, F.P., Soloyanis, S., Placzek, G., Williams, J.H., Johnson, C.D., Buursnick, M.L., Joesten, P.K., and Knutson, K.D., 1996. Geophysical Characterization of a Fractured-Bedrock Aquifer and Blast-Fractured Contaminant-Recovery Trench, in Bell, R.S., and Cramer, M.H., eds., Symposium on the Application of Geophysics to Engineering and Environmental Problems, Keystone, Colo., April 28-May 2, 1996, Proceedings: Wheat Ridge, Colorado, Environmental and Engineering Geophysical Society, p. 429-441.

Maine Geological Survey, 2002. Surficial Materials, Fort Fairfield NW Quadrangle, Maine, mapping by Michael E. Foley, Open-File No. 02-75, 22 State House Station, Augusta, Maine.

National Oceanic and Atmospheric Administration (NOAA), 2024. Climate Data Available online at https://www.ncdc.noaa.gov/cdo-web/ and accessed December 2024.

Panday, Sorab, Langevin, C.D., Niswonger, R.G., Ibaraki, Motomu, and Hughes, J.D., 2017. MODFLOW-USG version 1.4.00: An unstructured grid version of MODFLOW for simulating groundwater flow and tightly coupled processes using a control volume finite-difference formulation: U.S. Geological Survey Software Release, 27 October 2017, https://dx.doi.org/10.5066/F7R20ZFJ

Panday, S., 2020. USG-Transport Version 1.40.0: The Block-Centered Transport Process for MODFLOW-USG, GSI Environmental; July.

Rumbaugh, J., 2024. Guide to Using Groundwater Vistas Version 9, Environmental Simulations Inc., https://www.groundwatermodels.com/Groundwater_Vistas.php

Schulze-Makuch, D., 2005. Longitudinal Dispersivity Data and Implications for Scaling Behavior. Groundwater, Volume 43, Issue3, pages 443-456.

Silva, J., J. Simůnek, J. McCray, 2022. Comparison of methods to estimate air-water interfacial areas for evaluating PFAS transport in the vadose zone. Journal of Contaminant Hydrology 247: 103984.

Soil Survey Staff, Natural Resources Conservation Services (NRCS), U.S. Department of Agriculture (USDA), 2024. Web Soil Survey, Available online at the following link: https://websoilsurvey.sc.egov.usda.gov/, accessed December 2024.

Thompson, Peter, Baker, P., Calkin, S., and Forbes, P., 2004. The Regional Bedrock Structure at Loring Air Force Base, Limestone, Maine; The Unifying Model for the Study of Base-Wide Ground Water Contamination. 2004 U.S. EPA/NGWA Fractured Rock Conference: State of the Science and Measuring Success in Remediation. Portland, Maine.

Thornthwaite, C.W. and Mather, J.R., 1957. Instructions and tables for computing potential evapotranspiration and the water balance: Centerton, N.J., Laboratory of Climatology, Publications in Climatology, v. 10, no. 3, p. 185-311.

U.S. EPA. 1996. Soil Screening Guidance: User's Guide. Office of Solid Waste and Emergency and Remedial Response, Washington, DC. EPA/540/R-96/018.

United States Geologic Survey, 2025. USGS 3D Elevation Program Digital Elevation Model, accessed August 14, 2024 at URL https://www.usgs.gov/the-national-map-data-delivery.

Urumovic, K. and Urumovic, K. Sr., 2014. The effective porosity and grain size relations in permeability functions. Hydrol. Earth Syst. Sci. Discuss., 11, 6675–6714.

Westenbroek, S.M., Kelson V.A., Dripps W.R., Hunt R.J, and Bradbury, K.R., 2010. SWB- A modified Thornwaite-Mather Soil-Water-Balance Code for estimating groundwater recharge: U.S. Geologic Survey Techniques and Methods 6-A31, 60 p.

Wood Environment & Infrastructure, Inc. (Wood E&I), 2018. Site Inspection Report for Aqueous Film-Forming Foam Areas at Former Loring Air Force Base, Maine, Final; December.

FIGURES

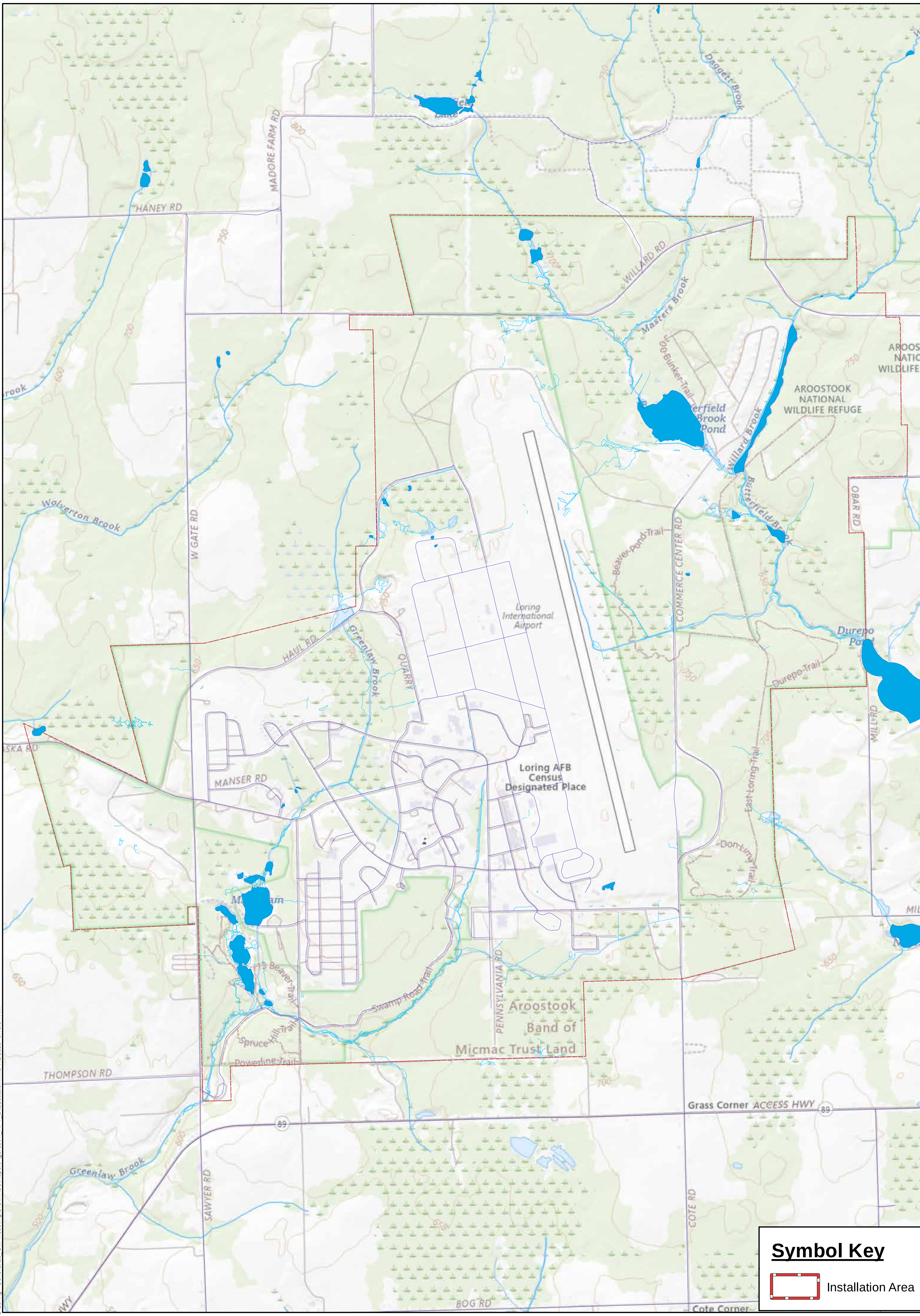

Air Force Civil Engineer Center
2261 Hughes Ave., Suite 163
JBSA Lackland, TX 78236

Figure N-1
Site Location
Groundwater Model Development Report
Former Loring Air Force Base, Limestone, ME

0 500 1,000 2,000 3,000 Meters
0 1,000 2,000 4,000 6,000 8,000 Feet

N

NOTES:
-Aerial Imagery obtained from NAIP, USDA-FSA. Published September, 2021

Drawn: JL

Drawn Date: 07/02/2025

PROJ: 775361701

Document: C:\Users\USJL717025\WSP O365\WDS-Loring - General\15_GW Modeling\GIS\MXDs\ReportFigures\RI_RPT_SiteLocation.mxd 7/2/2025 8:48:54 AM

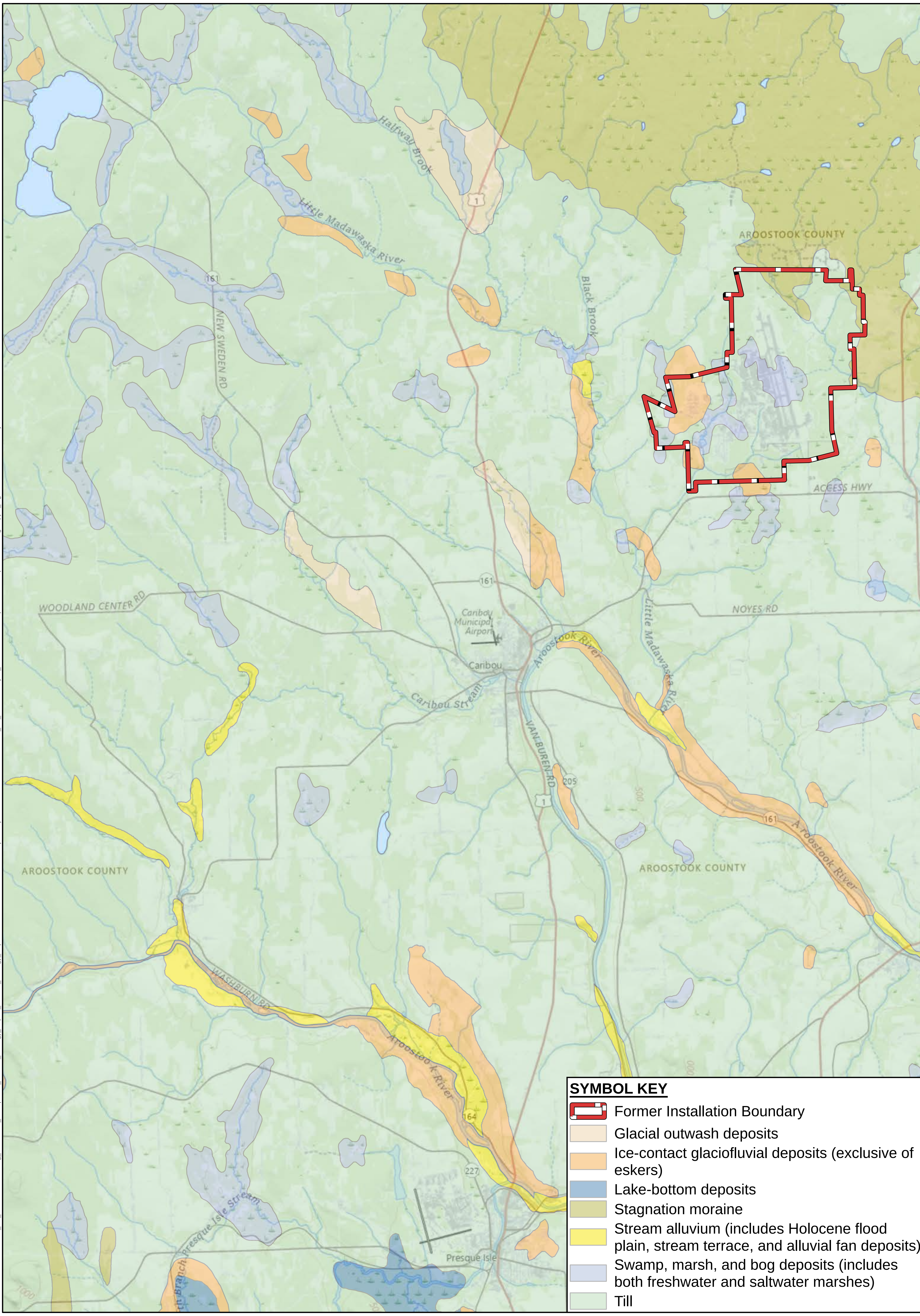

Air Force Civil Engineer Center
2261 Hughes Ave., Suite 163
JBSA Lackland, TX 78236

Figure N-2
Surficial Geology
Groundwater Model Development Report
Former Loring Air Force Base, Limestone, ME

NOTES:
-Topographic basemap obtained from ESRI Services, USGS National Map
-Surficial geology data sourced from Maine Geological Survey: Maine Surficial Geology 500K Units

Drawn: FD

Drawn Date: 06/11/2025

PROJ: 775361701

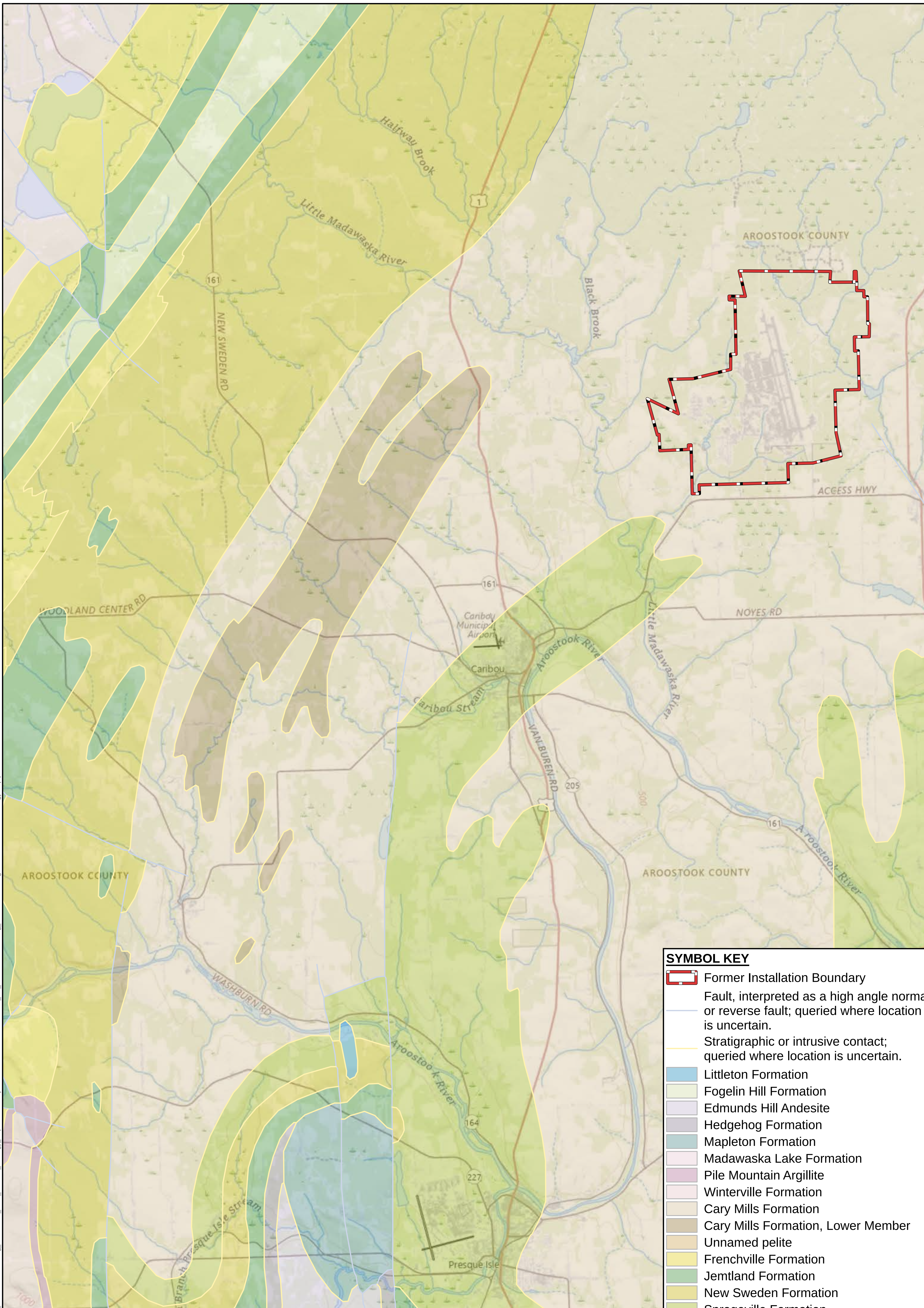

Air Force Civil Engineer Center
2261 Hughes Ave., Suite 163
JBSA Lackland, TX 78236

Figure N-3
Bedrock Geology
Groundwater Model Development Report

Former Loring Air Force Base, Limestone, ME

0 1,500 3,000 6,000 9,000 Meters

0 5,000 10,000 20,000 30,000 40,000 Feet

N

NOTES:
-Topographic basemap obtained from ESRI Services, USGS National Map
-Bedrock geology data sourced from Maine Geological Survey: Maine Bedrock Geology 500K Units

Drawn: FD

Drawn Date: 07/03/2025

PROJ: 775361701

Document: P:\Projects\AFCEE\LORING PFAS RI\1_TO_10484\4.0 Data\Loring_GIS\APRX_RI\RI_Bedrock_Geology_Map PDF: P:\Projects\AFCEE\LORING PFAS RI\1_TO_10484\4.0 Data\Loring_GIS\PDF\2025\Figure 2.7.2I - Bedrock Geology Map.pdf 3/5/2025 12:11PM ariel.anderson

SYMBOL KEY

- Borehole geophysics location
- Former Installation Boundary
- Modeled Bedrock Surface Contour
- Approximate Location of Photolineaments
- Projected Anticline
- Projected Syncline

Water Features:

- Stream
- Surface Water Body

ROSE DIAGRAM LEGEND

- Strike of feature
- Dip direction of feature

Label Notes:
White Label - Indicates rose diagrams created from PFAS RI borehole geophysics data.
Yellow Label - Indicates rose diagram reconstructed from OU12 RI Report borehole geophysics data logs.

Air Force Civil Engineer Center
2261 Hughes Ave., Suite 163
JBSA Lackland, TX 78236

N

Figure N-4
Bedrock Structural Features
Groundwater Model Development Report
Former Loring Air Force Base, Limestone, ME

0 200 400 800 1,200 1,600 Meters
0 675 1,350 2,700 4,050 5,400 Feet

NOTES:
-Aerial Imagery obtained from NAIP, USDA-FSA. Published September, 2021.
-Projected bedrock folds and photolineaments sourced from OU12 RI Report

Drawn: FD
Drawn Date: 6/10/2025
PROJ: 775361701

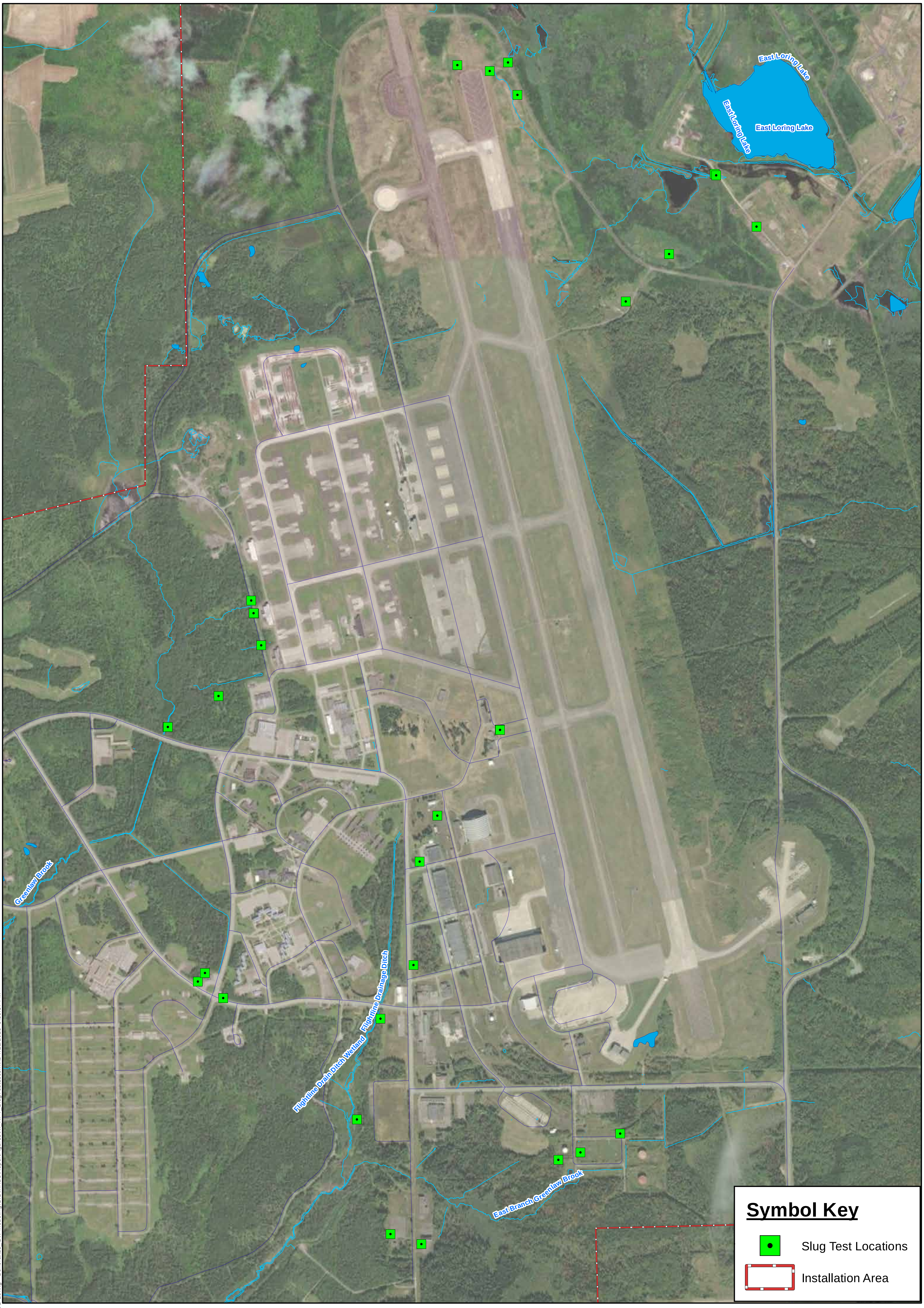

Air Force Civil Engineer Center
2261 Hughes Ave., Suite 163
JBSA Lackland, TX 78236

Figure N- 5
Slug Test Locations
Groundwater Model Development Report
Former Loring Air Force Base, Limestone, ME

0 200 400 800 1,200 Meters
0 500 1,000 2,000 3,000 4,000 Feet

N

NOTES:
-Aerial Imagery obtained from NAIP, USDA-FSA. Published September, 2021

Drawn: JL

Drawn Date: 07/21/2025

PROJ: 775361701

Document: C:\Users\USJL717025\WSP O365\WDS-Loring - General\15_GW Modeling\GIS\MXDs\ReportFigures\RI_RPT_SlugTestLocs.mxd 7/21/2025 5:56:57 PM

Air Force Civil Engineer Center
2261 Hughes Ave., Suite 163
JBSA Lackland, TX 78236

Figure N-6
Numerical Groundwater Model Grid Spacing
Groundwater Model Development Report
Former Loring Air Force Base, Limestone, ME

0 500 1,000 2,000 3,000 4,000 5,000 Meters
0 2,000 4,000 8,000 12,000 16,000 Feet

N

NOTES:
-Aerial Imagery obtained from NAIP, USDA-FSA. Published September, 2021

Drawn: JL
Drawn Date: 07/01/2025
PROJ: 775361701

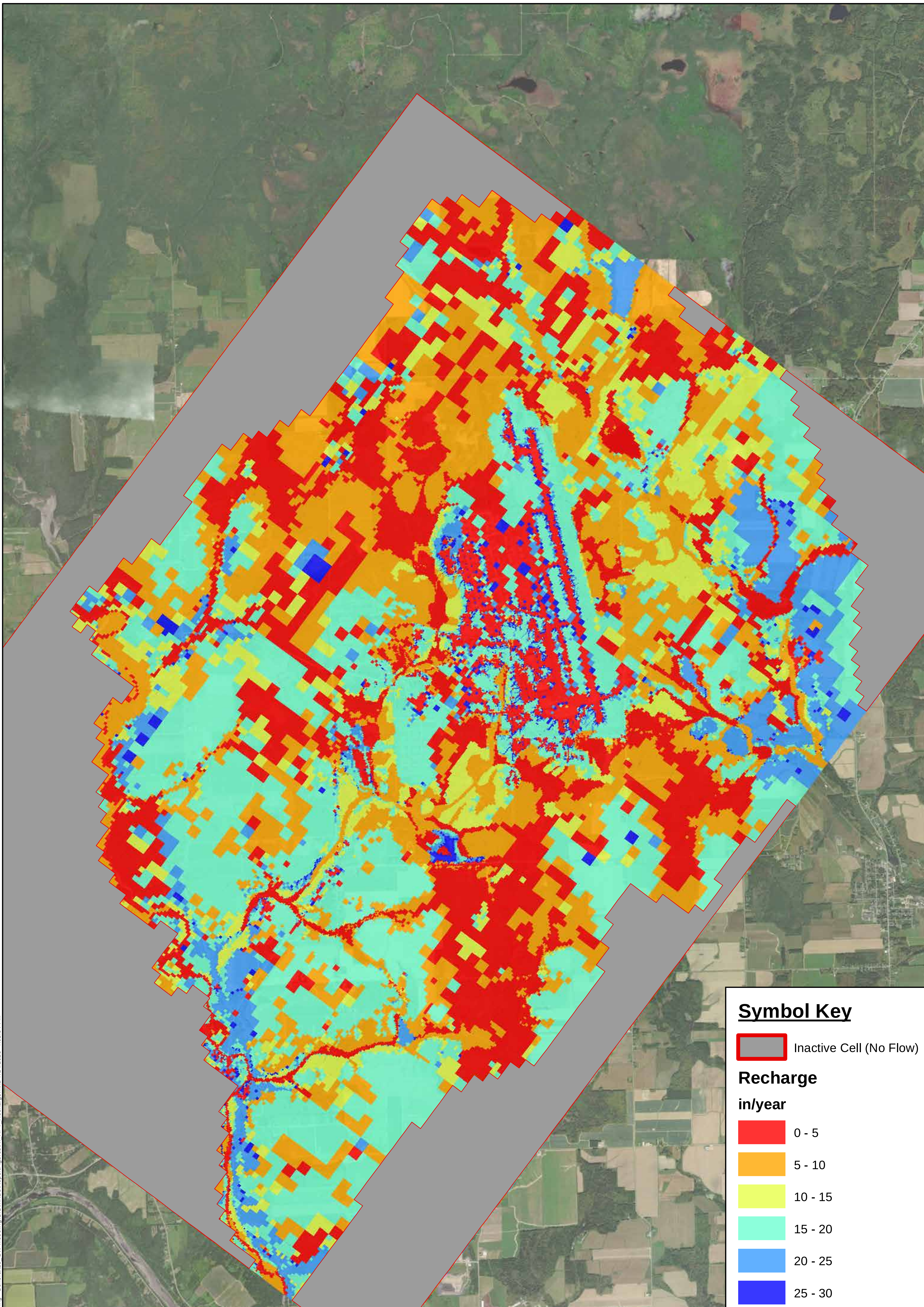

Air Force Civil Engineer Center
2261 Hughes Ave., Suite 163
JBSA Lackland, TX 78236

Figure N-7
Modeled Groundwater Recharge
Groundwater Model Development Report
Former Loring Air Force Base, Limestone, ME

0 500 1,000 2,000 3,000 Meters

0 1,000 2,000 4,000 6,000 8,000 Feet

N

NOTES:
-Aerial Imagery obtained from NAIP, USDA-FSA. Published September, 2021

Drawn: JL

Drawn Date: 7/14/2025

PROJ: 775361701

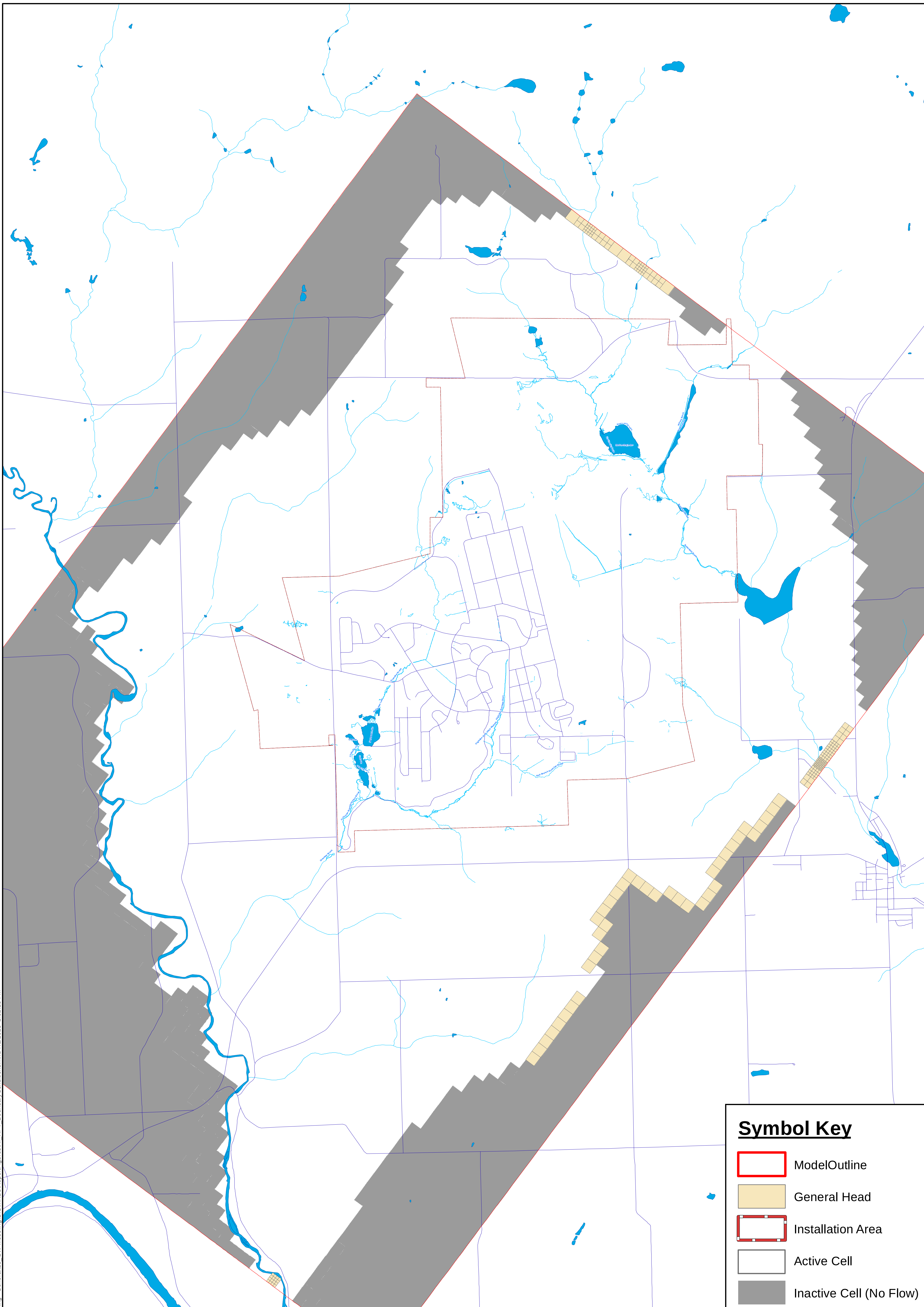

Air Force Civil Engineer Center
2261 Hughes Ave., Suite 163
JBSA Lackland, TX 78236

Figure N- 8
Model Boundary Conditions
Groundwater Model Development Report
Former Loring Air Force Base, Limestone, ME

0 500 1,000 2,000 3,000 Meters

0 1,000 2,000 4,000 6,000 8,000 Feet

N

NOTES:
-Aerial Imagery obtained from NAIP, USDA-FSA. Published September, 2021

Drawn: JL

Drawn Date: 07/02/2025

PROJ: 775361701

Document: C:\Users\USJL717025\WSP O365\WDS-Loring - General\15_GW Modeling\GIS\MXDs\ReportFigures\RI_RPT_BoundaryConditions.mxd 7/2/2025 2:52:15 PM

Air Force Civil Engineer Center
2261 Hughes Ave., Suite 163
JBSA Lackland, TX 78236

Figure N-9
Modeled Streams and Surface Water Bodies
Groundwater Model Development Report
Former Loring Air Force Base, Limestone, ME

0 500 1,000 2,000 3,000 Meters
0 1,000 2,000 4,000 6,000 8,000 Feet

N

NOTES:
-Aerial Imagery obtained from NAIP, USDA-FSA. Published September, 2021

Drawn: JL
Drawn Date: 07/02/2025
PROJ: 775361701

Document: C:\Users\USJL717025\WSP O365\WDS-Loring - General\15_GW Modeling\GIS\MXDs\ReportFigures\RI_RPT_CLNstreams.mxd 7/2/2025 3:35:09 PM

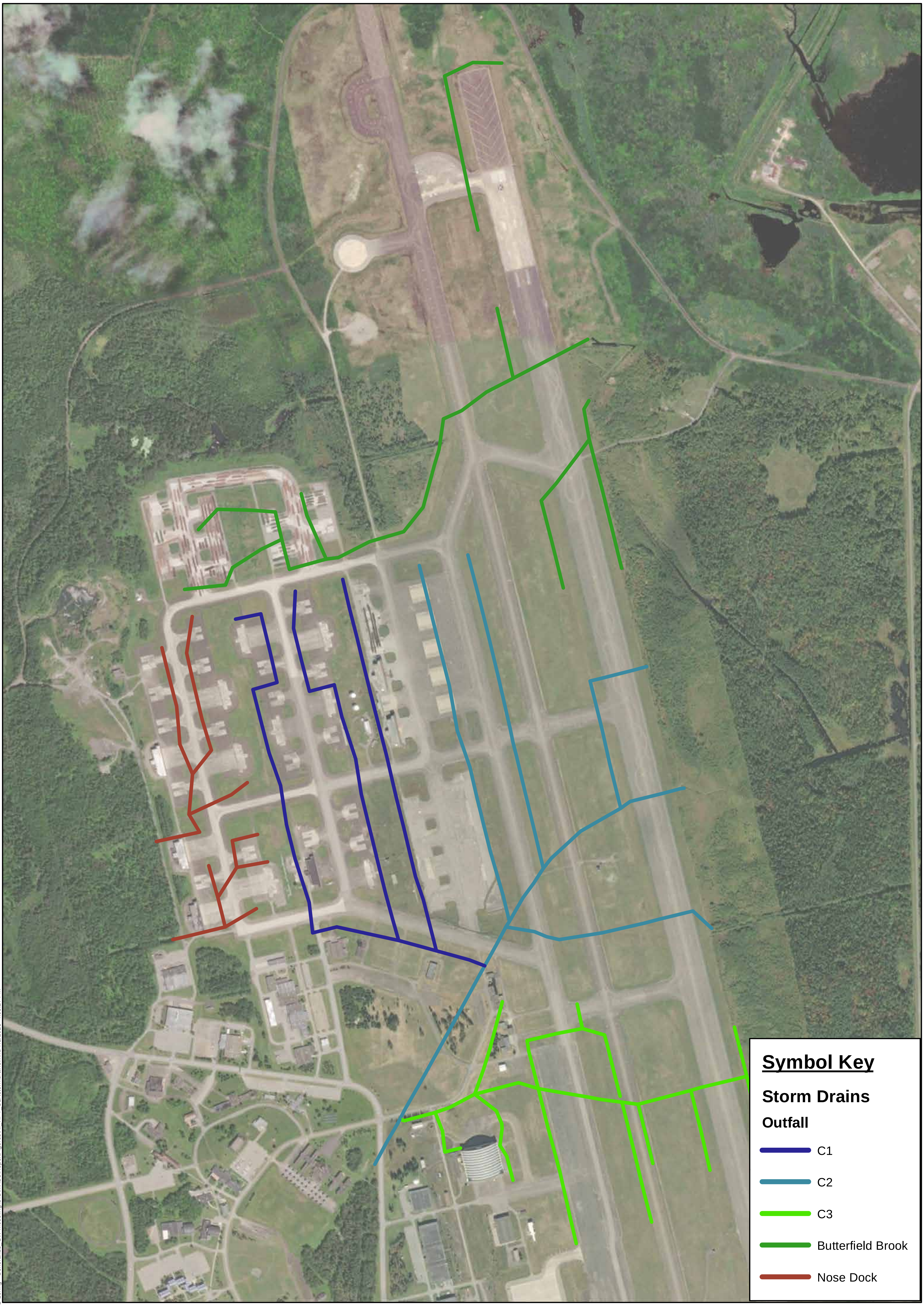

Air Force Civil Engineer Center
2261 Hughes Ave., Suite 163
JBSA Lackland, TX 78236

Figure N-10
Modeled Streams and Surface Water Bodies
Groundwater Model Development Report
Former Loring Air Force Base, Limestone, ME

0 150 300 600 900 Meters
0 250 500 1,000 1,500 2,000 2,500 Feet

N

NOTES:
-Aerial Imagery obtained from NAIP, USDA-FSA. Published September, 2021

Drawn: JL

Drawn Date: 07/02/2025

PROJ: 775361701

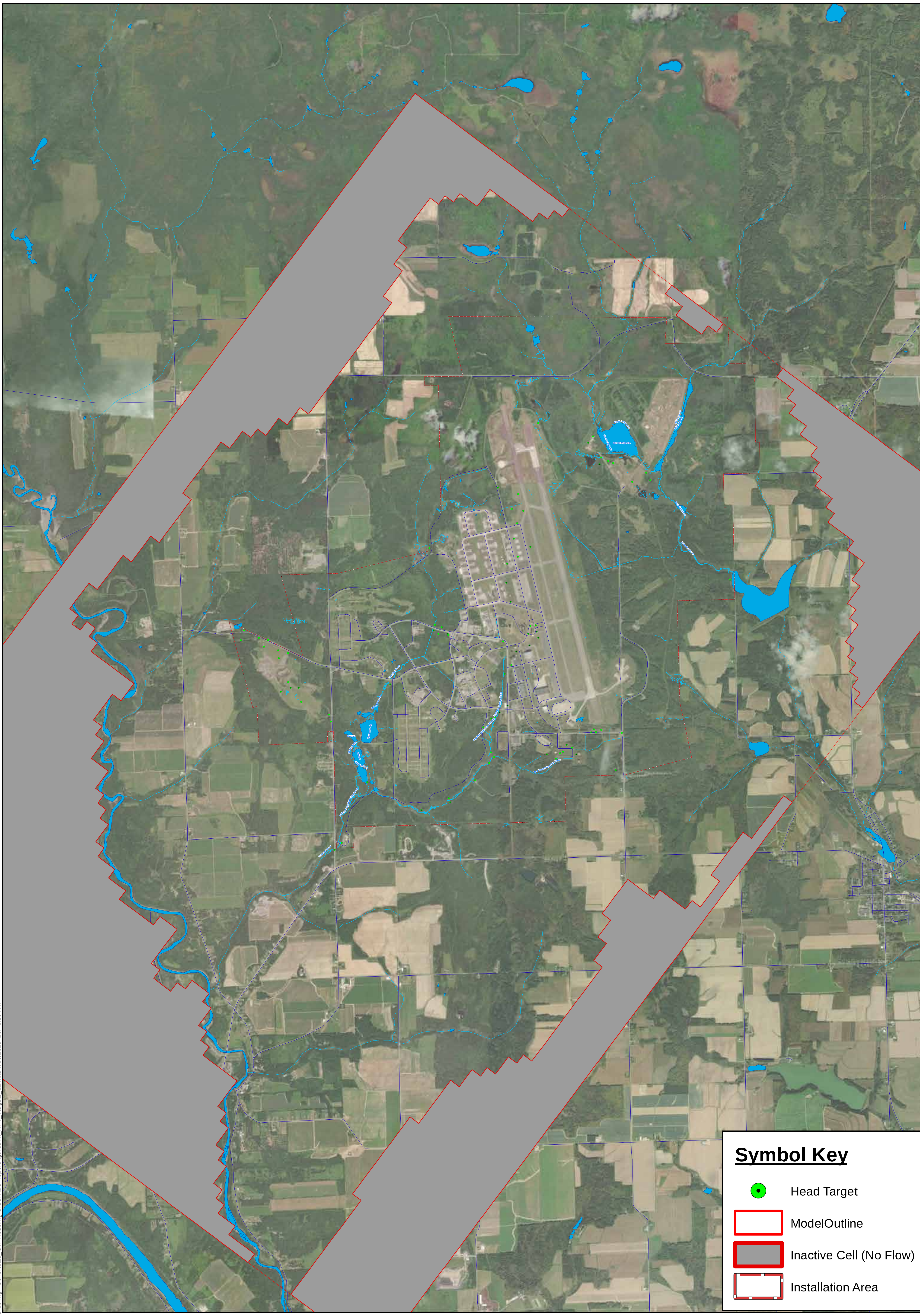

Air Force Civil Engineer Center
2261 Hughes Ave., Suite 163
JBSA Lackland, TX 78236

Figure N - 11
Head Target Wells, Layer 1
Groundwater Model Development Report
Former Loring Air Force Base, Limestone, ME

0 500 1,000 2,000 3,000 Meters

0 1,000 2,000 4,000 6,000 8,000 Feet

N

NOTES:
-Aerial Imagery obtained from NAIP, USDA-FSA. Published September, 2021

Drawn: JL

Drawn Date: 07/15/2025

PROJ: 775361701

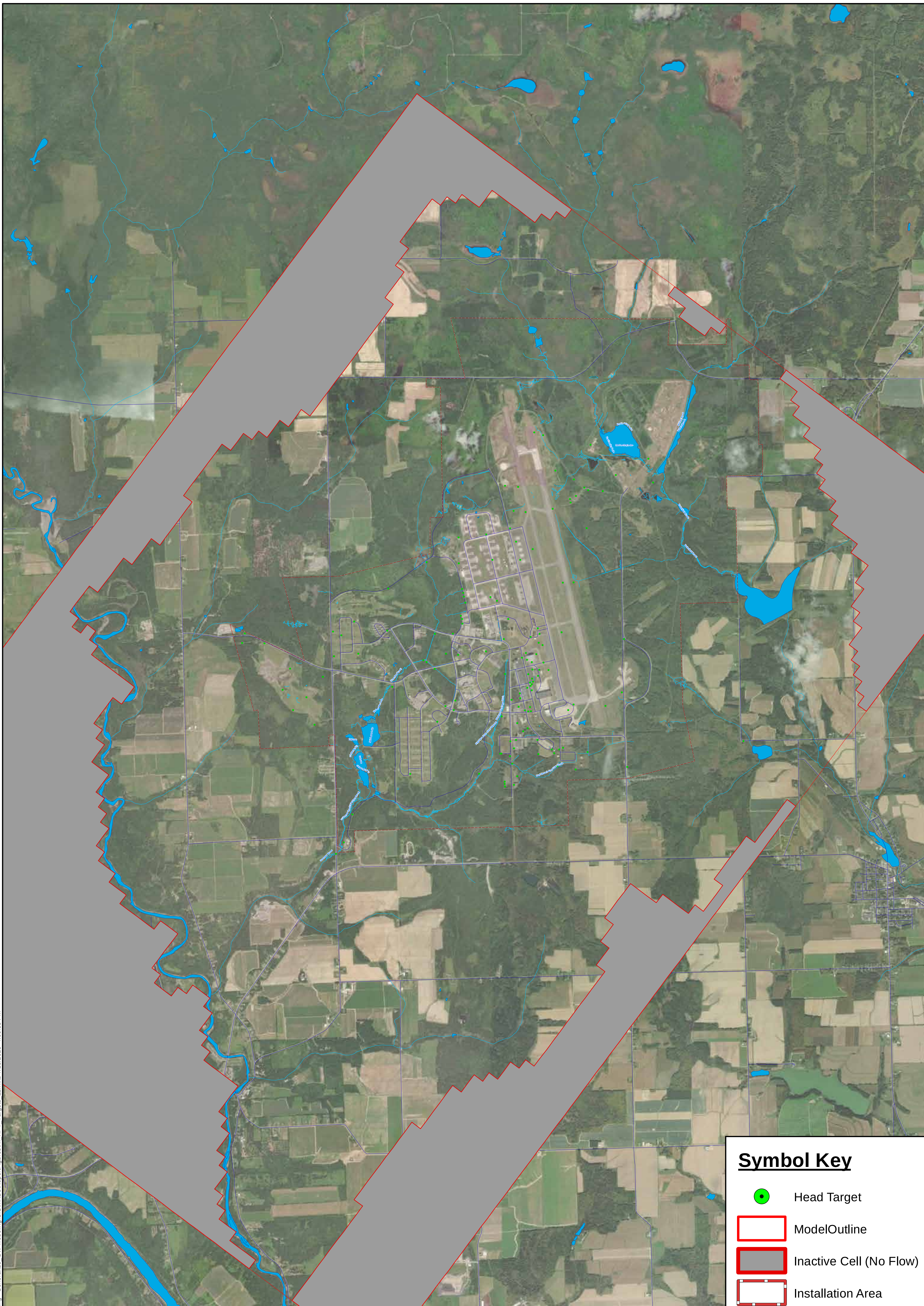

Air Force Civil Engineer Center
2261 Hughes Ave., Suite 163
JBSA Lackland, TX 78236

Figure N-12
Head Target Wells, Layer 2
Groundwater Model Development Report
Former Loring Air Force Base, Limestone, ME

0 500 1,000 2,000 3,000 Meters

0 1,000 2,000 4,000 6,000 8,000 Feet

N

NOTES:
-Aerial Imagery obtained from NAIP, USDA-FSA. Published September, 2021

Drawn: JL

Drawn Date: 07/15/2025

PROJ: 775361701

Document: C:\Users\USJL717025\WSP O365\WDS-Loring - General\15_GW Modeling\GIS\MXDs\ReportFigures\RI_RPT_Targets_L2.mxd 7/15/2025 4:06:53 PM

Air Force Civil Engineer Center
2261 Hughes Ave., Suite 163
JBSA Lackland, TX 78236

Figure N - 13
Head Target Wells, Layer 3
Groundwater Model Development Report
Former Loring Air Force Base, Limestone, ME

NOTES:
-Aerial Imagery obtained from NAIP, USDA-FSA. Published September, 2021

Drawn: JL

Drawn Date: 07/15/2025

PROJ: 775361701

Document: C:\Users\USJL717025\WSP O365\WDS-Loring - General\15_GW Modeling\GIS\MXDs\ReportFigures\RI_RPT_Targets_L3.mxd 7/15/2025 4:05:34 PM

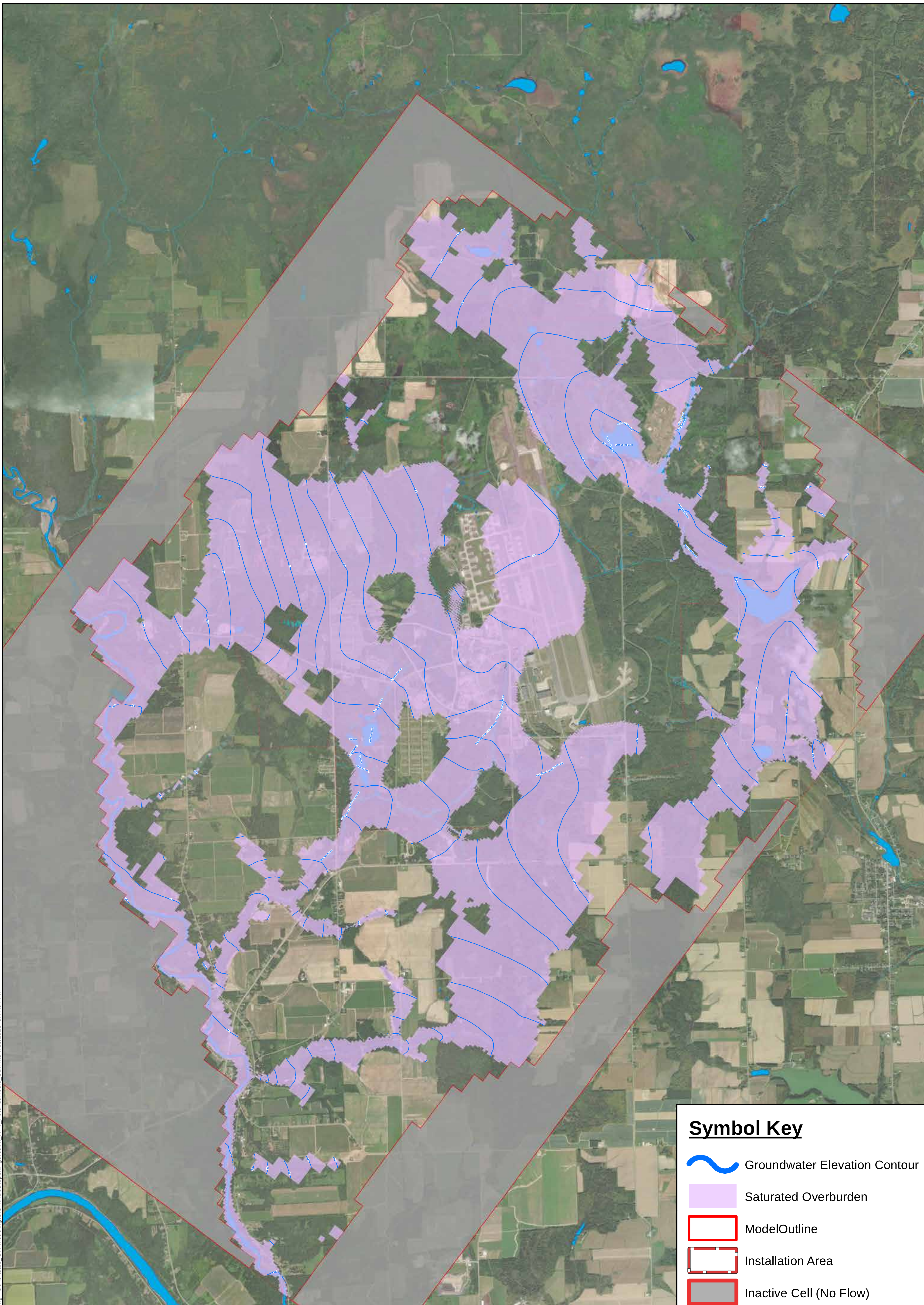

Air Force Civil Engineer Center
2261 Hughes Ave., Suite 163
JBSA Lackland, TX 78236

Figure N- 14
Modeled Overburden Potentiometric Elevation
Groundwater Model Development Report
Former Loring Air Force Base, Limestone, ME

0 500 1,000 2,000 3,000 Meters
0 1,000 2,000 4,000 6,000 8,000 Feet

N

NOTES:
-Aerial Imagery obtained from NAIP, USDA-FSA. Published September, 2021

Drawn: JL
Drawn Date: 07/15/2025
PROJ: 775361701

Document: C:\Users\USJL717025\WSP O365\WDS-Loring - General\15_GW Modeling\GIS\MXDs\ReportFigures\RI_RPT_Potentiometric_OB.mxd 7/15/2025 5:47:54 PM

Air Force Civil Engineer Center
2261 Hughes Ave., Suite 163
JBSA Lackland, TX 78236

Figure N - 15
Modeled Competent Bedrock Potentiometric Elevation
Groundwater Model Development Report
Former Loring Air Force Base, Limestone, ME

0 500 1,000 2,000 3,000 Meters
0 1,000 2,000 4,000 6,000 8,000 Feet

N

NOTES:
-Aerial Imagery obtained from NAIP, USDA-FSA. Published September, 2021

Drawn: JL
Drawn Date: 07/15/2025
PROJ: 775361701

Document: C:\Users\USJL717025\WSP O365\WDS-Loring - General\15_GW Modeling\GIS\MXDs\ReportFigures\RI_RPT_Potentiometric_BR.mxd 7/15/2025 5:44:06 PM

Figure N-16
Observed versus Modeled Water Level - Layers 1, 2, and 3

Groundwater Model Development Report
Former Loring Air Force Base, Limestone, ME

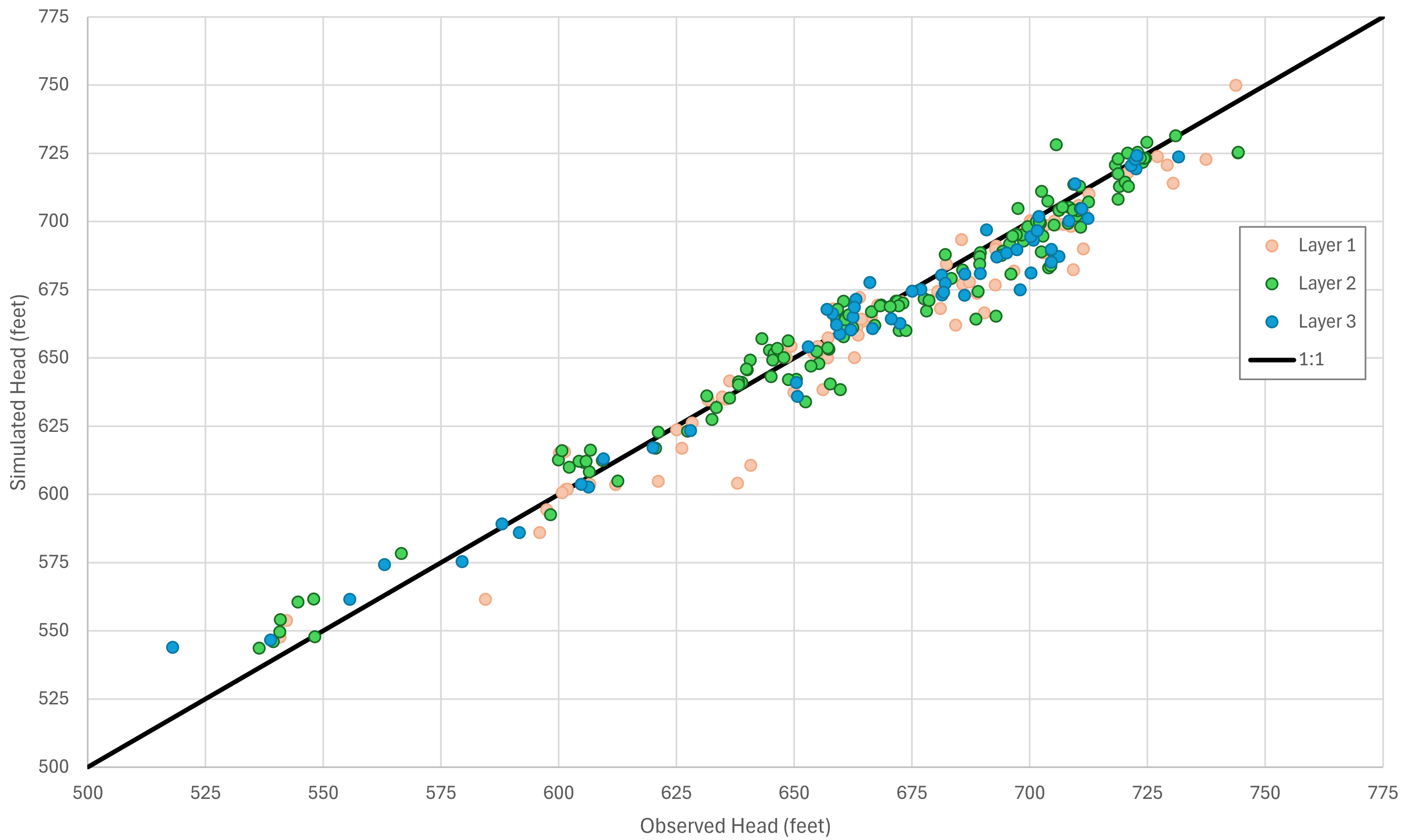

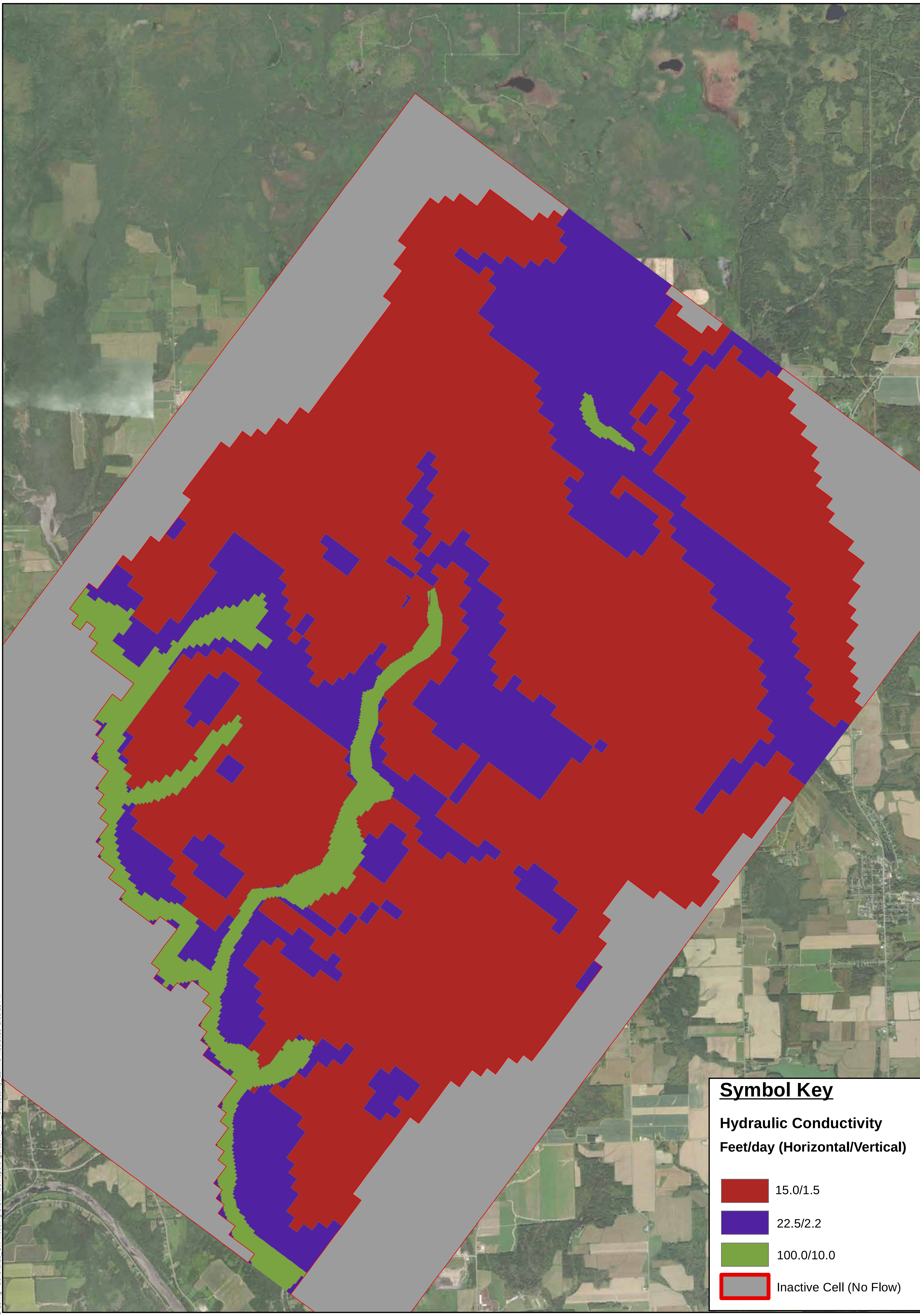

Air Force Civil Engineer Center
2261 Hughes Ave., Suite 163
JBSA Lackland, TX 78236

Figure N- 17
Modeled Horizontal Conductivity, Layer 1
Groundwater Model Development Report
Former Loring Air Force Base, Limestone, ME

0 500 1,000 2,000 3,000 Meters
0 1,000 2,000 4,000 6,000 8,000 Feet

N

NOTES:
-Aerial Imagery obtained from NAIP, USDA-FSA. Published September, 2021

Drawn: JL
Drawn Date: 07/15/2025
PROJ: 775361701

Document: C:\Users\USJL717025\WSP O365\WDS-Loring - General\15_GW Modeling\GIS\MXDs\ReportFigures\RI_RPT_Conductivity_L1.mxd 7/15/2025 2:03:13 PM

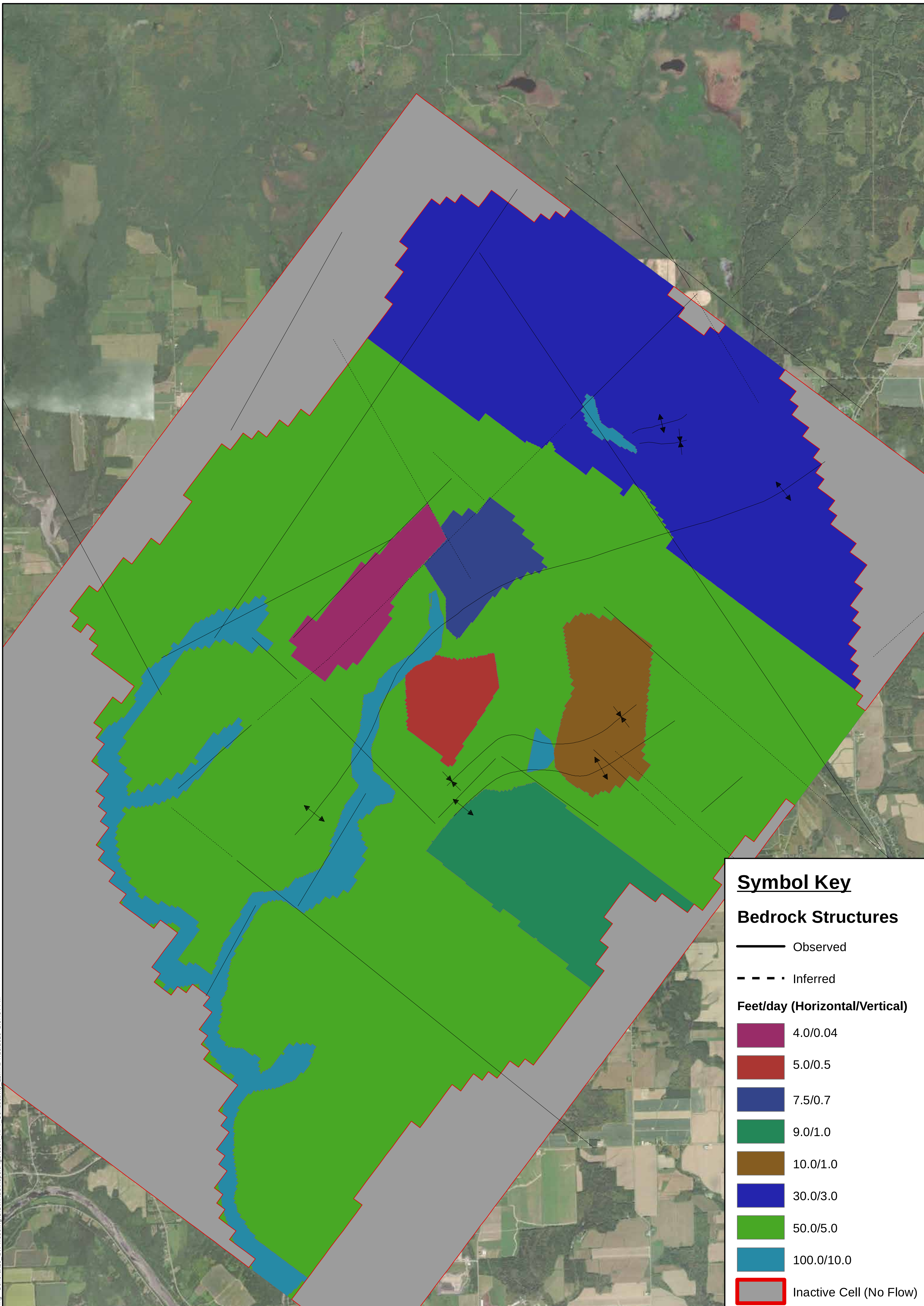

Air Force Civil Engineer Center
2261 Hughes Ave., Suite 163
JBSA Lackland, TX 78236

Figure N - 18
Modeled Horizontal Conductivity, Layer 2
Groundwater Model Development Report
Former Loring Air Force Base, Limestone, ME

0 500 1,000 2,000 3,000 Meters

0 1,000 2,000 4,000 6,000 8,000 Feet

N

NOTES:
-Aerial Imagery obtained from NAIP, USDA-FSA. Published September, 2021

07/15/2025	RI_RPT_Conductivity_L2
Drawn: JL	PROJ: 775361701

Document: C:\Users\USJL717025\WSP O365\WDS-Loring - General\15_GW Modeling\GIS\MXDs\ReportFigures\RI_RPT_Conductivity_L2.mxd 7/15/2025 1:37:54 PM

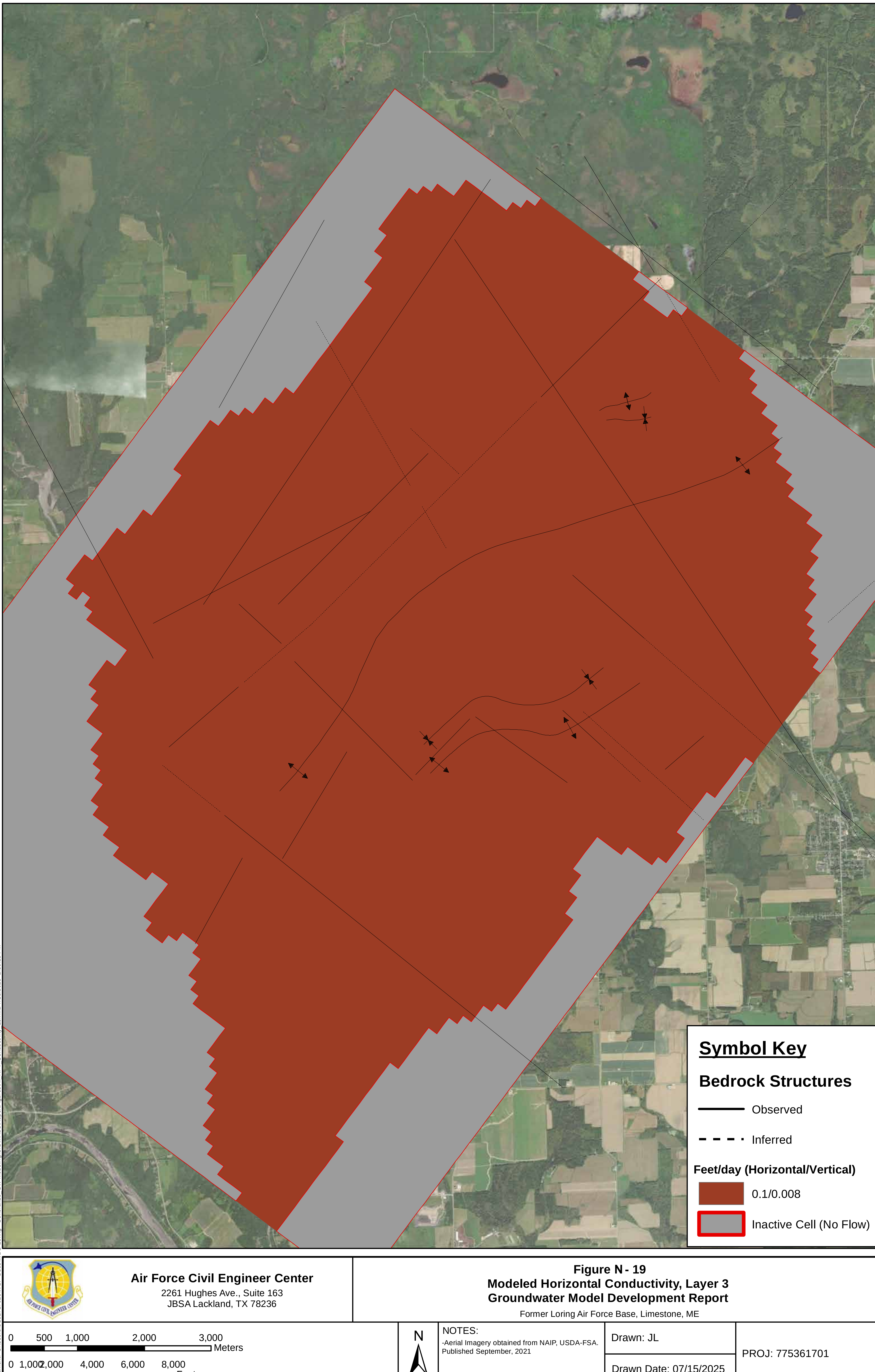

Air Force Civil Engineer Center
2261 Hughes Ave., Suite 163
JBSA Lackland, TX 78236

Figure N - 19
Modeled Horizontal Conductivity, Layer 3
Groundwater Model Development Report
Former Loring Air Force Base, Limestone, ME

NOTES:
-Aerial Imagery obtained from NAIP, USDA-FSA. Published September, 2021

Drawn: JL

Drawn Date: 07/15/2025

PROJ: 775361701

Document: C:\Users\USJL717025\WSP O365\WDS-Loring - General\15_GW Modeling\GIS\MXDs\ReportFigures\RI_RPT_Conductivity_L3.mxd 7/15/2025 2:36:16 PM

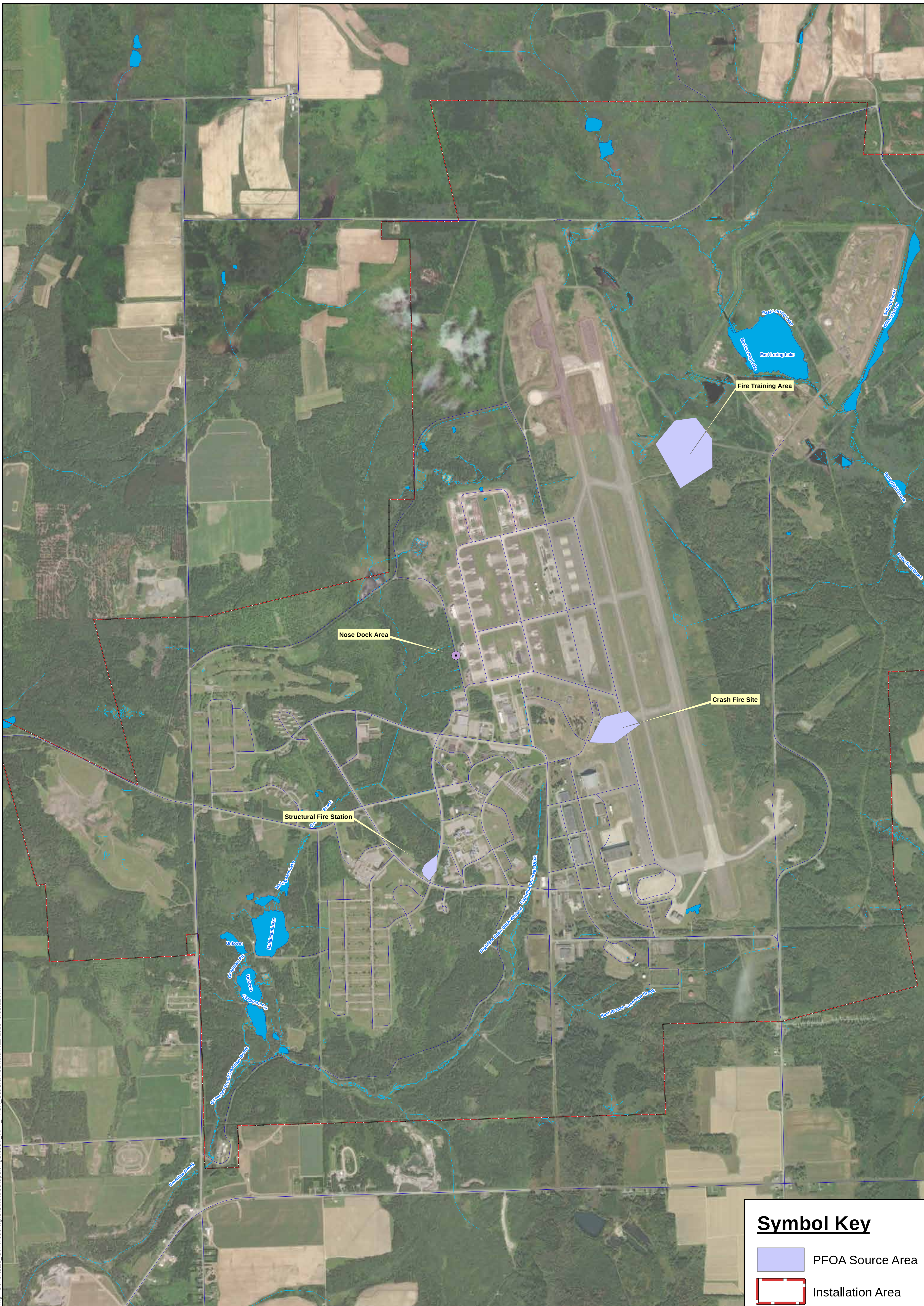

Air Force Civil Engineer Center
2261 Hughes Ave., Suite 163
JBSA Lackland, TX 78236

Figure N-20
PFOA Source Areas
Groundwater Model Development Report
Former Loring Air Force Base, Limestone, ME

0 250 500 1,000 1,500 2,000 2,500 Meters
0 1,000 2,000 4,000 6,000 8,000 Feet

N

NOTES:
-Aerial Imagery obtained from NAIP, USDA-FSA. Published September, 2021

Drawn: JL
Drawn Date: 07/22/2025
PROJ: 775361701

Document: C:\Users\USJL717025\WSP O365\WDS-Loring - General\15_GW Modeling\GIS\MXDs\ReportFigures\RI_RPT_PFOA_SedSrcArea.mxd 7/22/2025 8:33:22 AM

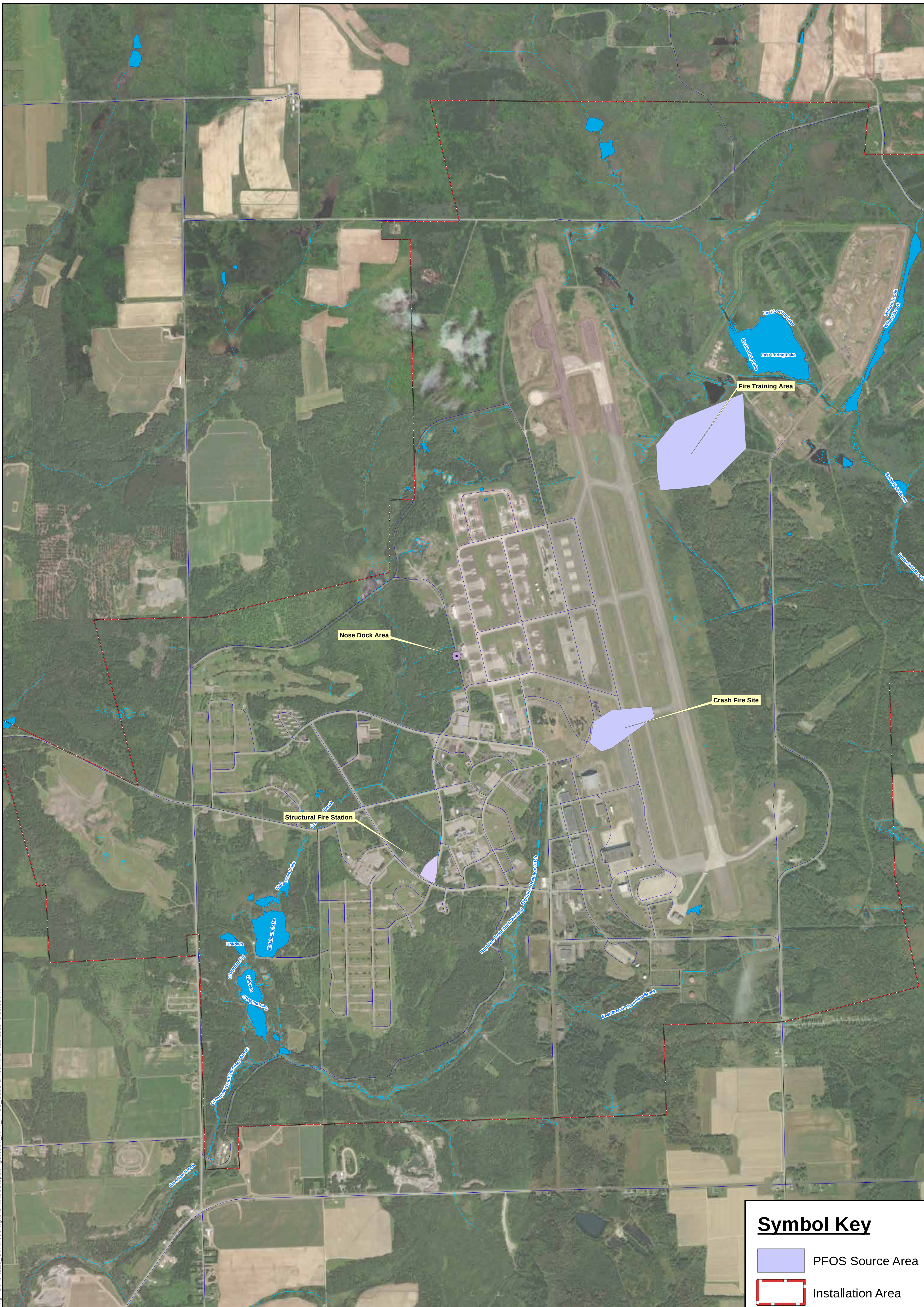

Air Force Civil Engineer Center
2261 Hughes Ave., Suite 163
JBSA Lackland, TX 78236

Figure N-21
PFOS Source Areas
Groundwater Model Development Report
Former Loring Air Force Base, Limestone, ME

0 250 500 1,000 1,500 2,000 2,500 Meters
0 1,000 2,000 4,000 6,000 8,000 Feet

N

NOTES:
-Aerial Imagery obtained from NAIP, USDA-FSA. Published September, 2021

Drawn: JL
Drawn Date: 07/22/2025
PROJ: 775361701

Document: C:\Users\USJL717025\WSP O365\WDS-Loring - General\15_GW Modeling\GIS\MXDs\Report\Figures\RI_RPT_PFOS_SedSrcArea.mxd 7/22/2025 8:36:39 AM

Figure N-22
FTA Shallow Lysimeter Porewater Concentrations

Groundwater Model Development Report
Former Loring Air Force Base, Limestone, Maine

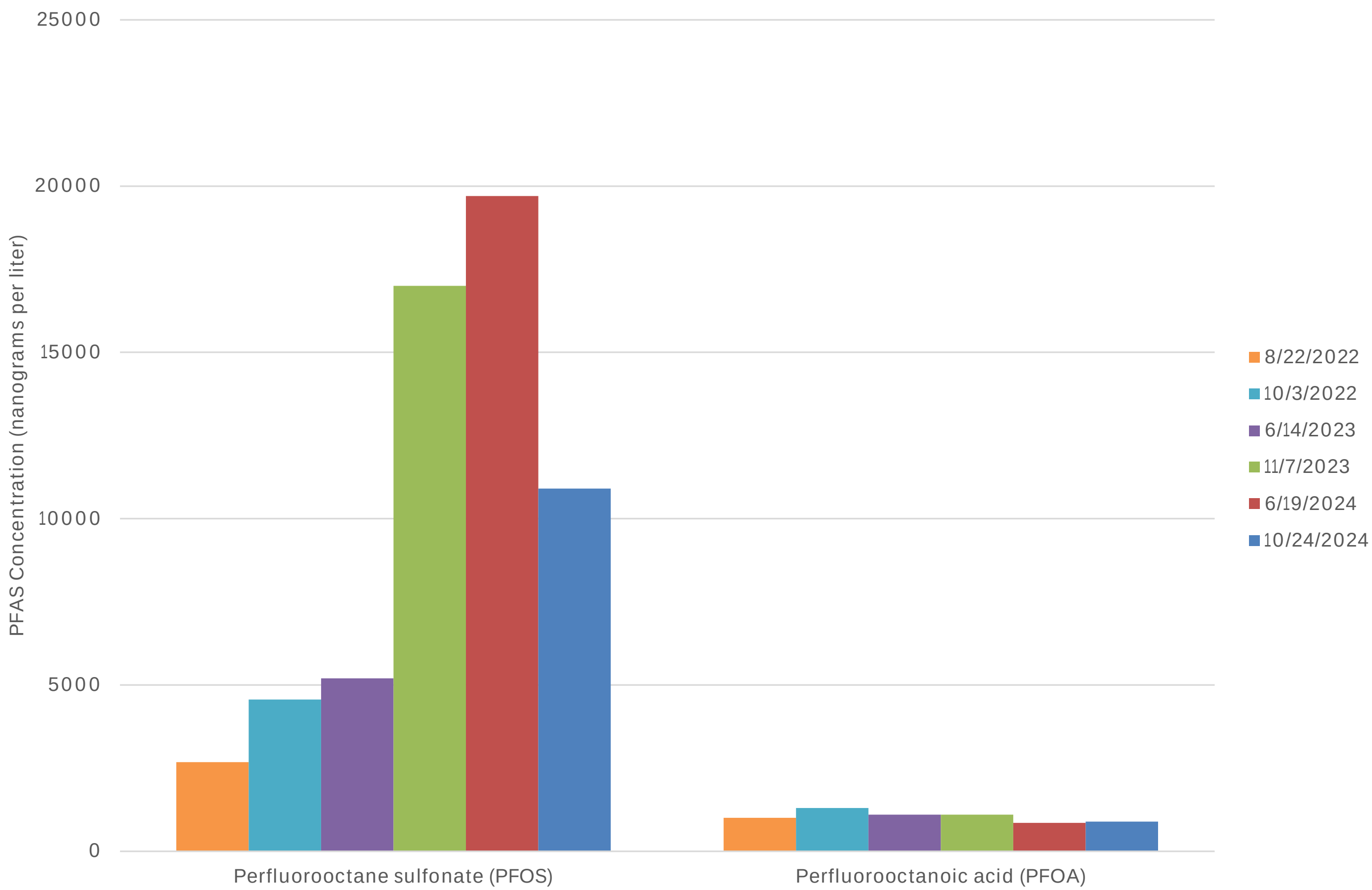

Figure N-23
FTA Deep Lysimeter Porewater Concentrations

Groundwater Model Development Report
Former Loring Air Force Base, Limestone, Maine

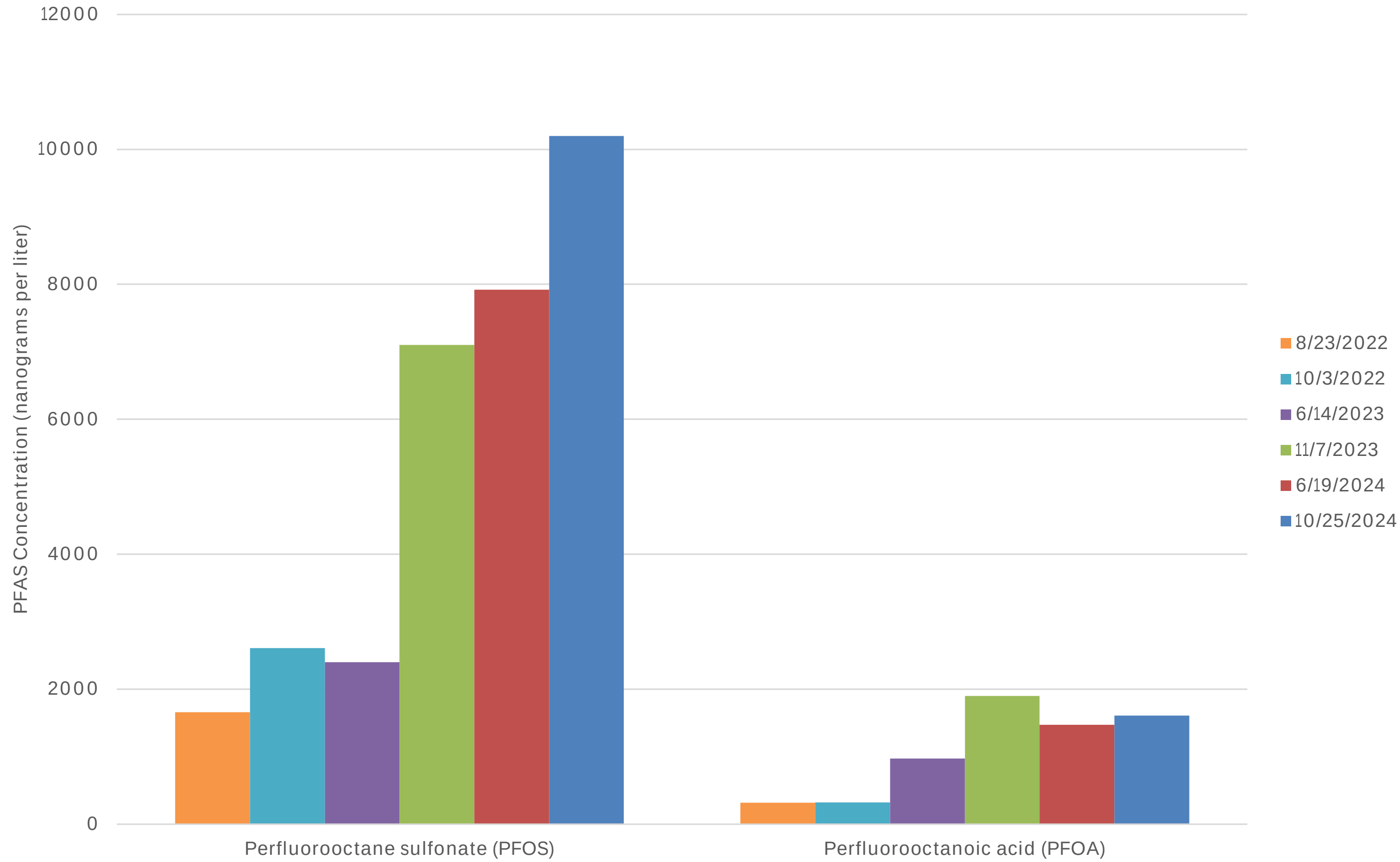

Figure N-24
Structural Fire Station Shallow Lysimeter Porewater Concentrations

Groundwater Model Development Report
Former Loring Air Force Base, Limestone, Maine

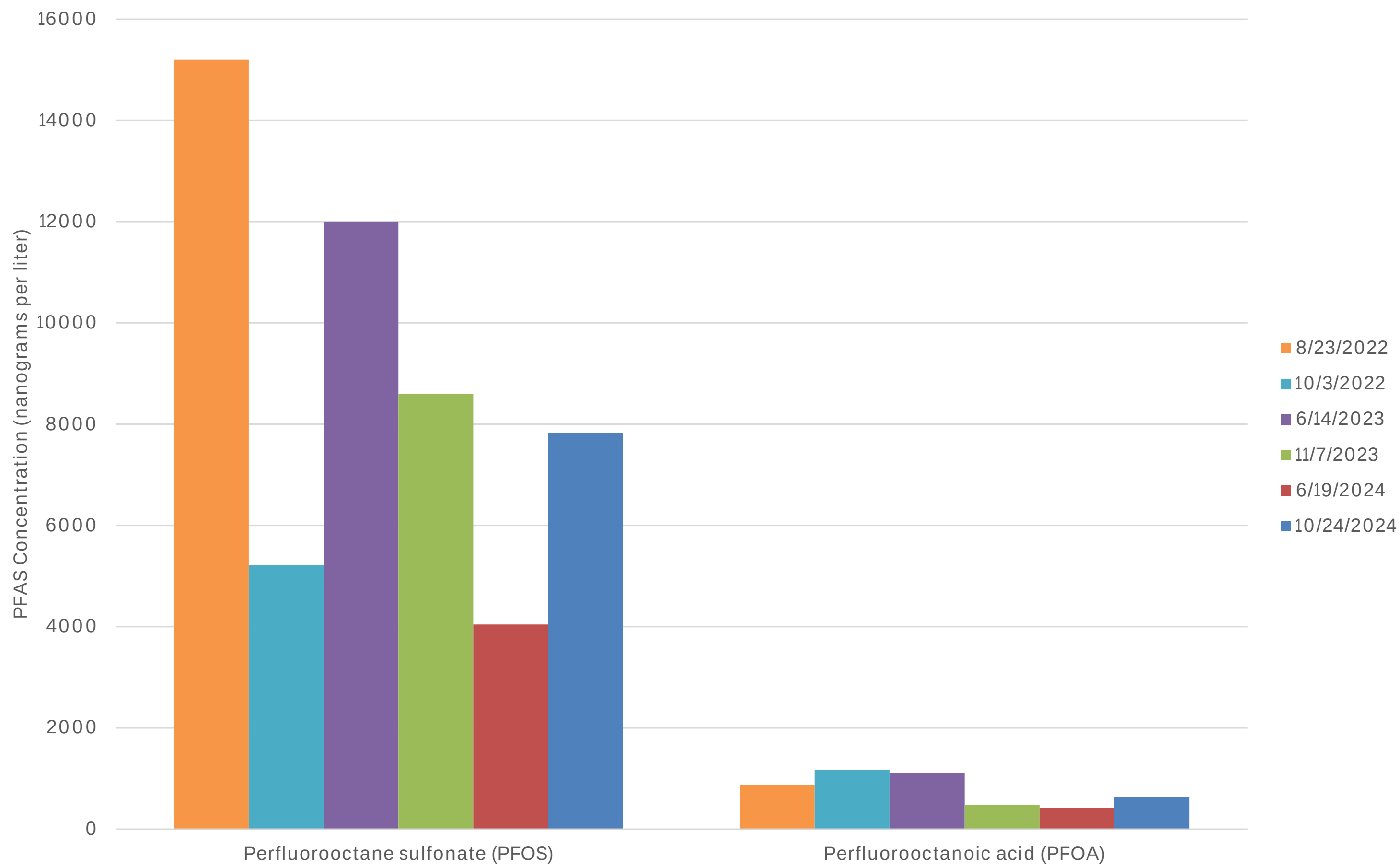

Figure N-25
Structural Fire Station Deep Lysimeter Porewater Concentrations

Groundwater Model Development Report
Former Loring Air Force Base, Limestone, Maine

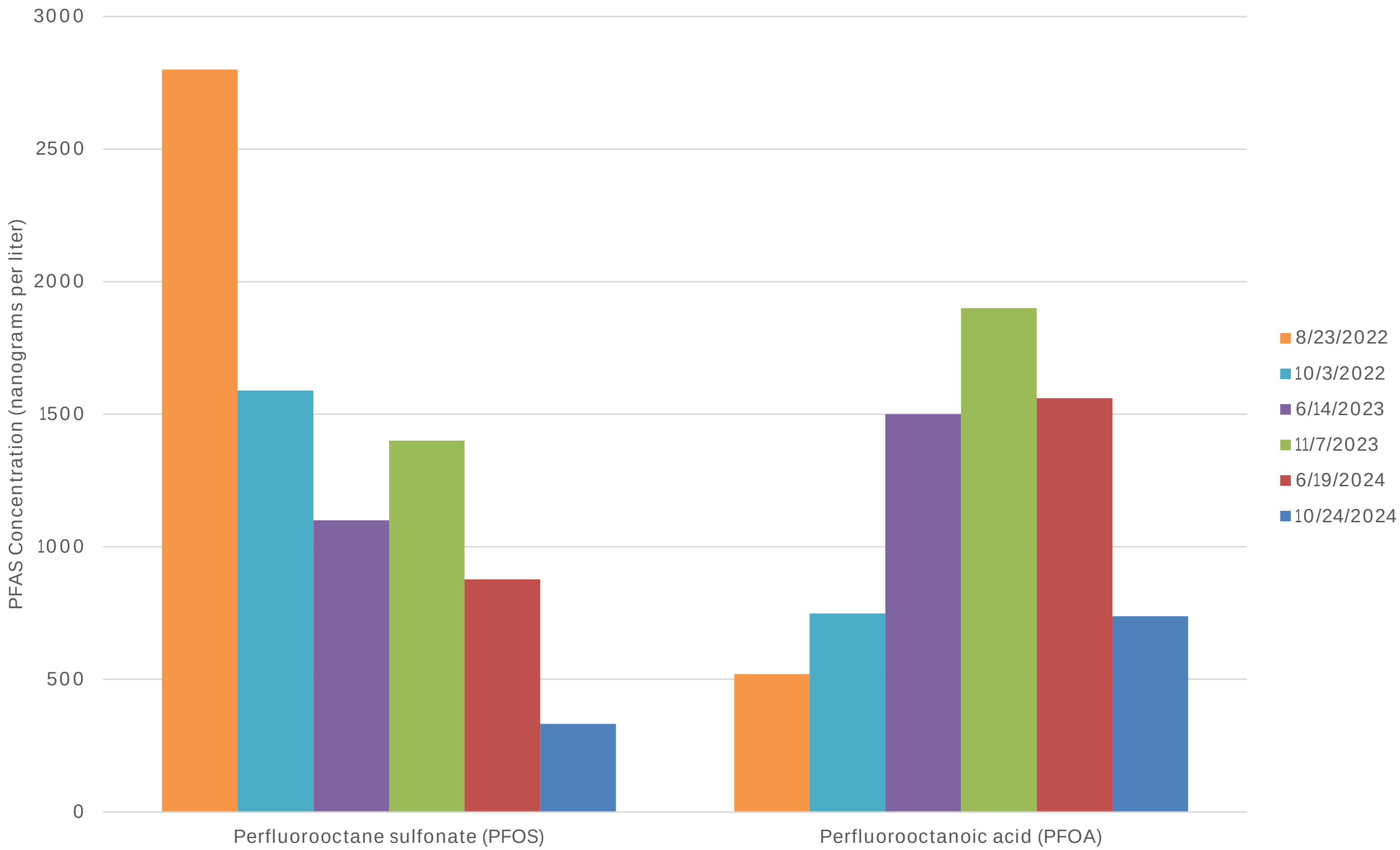

Figure N-26
Crash Fire Station Shallow Lysimeter Porewater Concentrations

Groundwater Model Development Report
Former Loring Air Force Base, Limestone, Maine

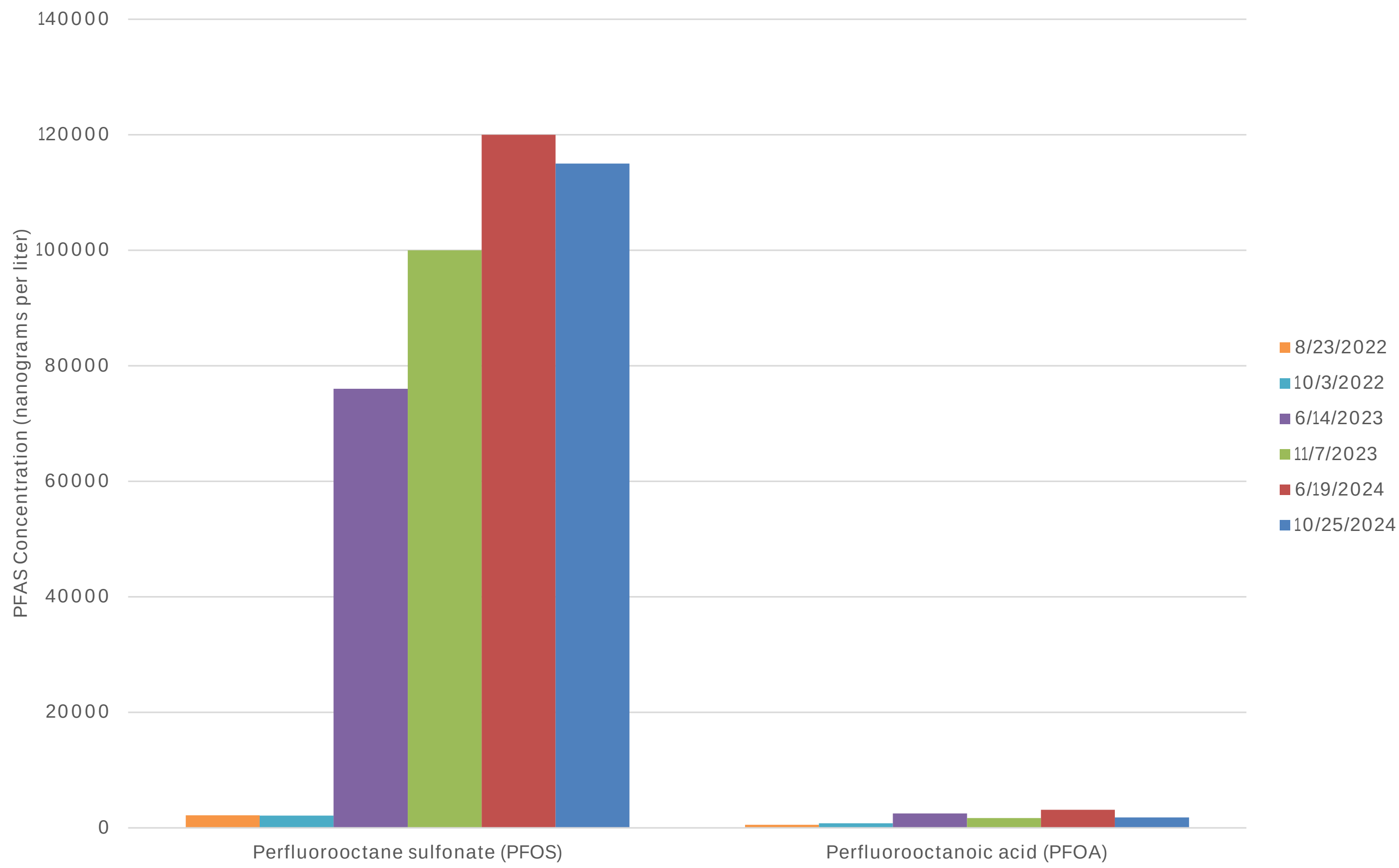

Figure N-27
Crash Fire Station Deep Lysimeter Porewater Concentrations

Groundwater Model Development Report
Former Loring Air Force Base, Limestone, Maine

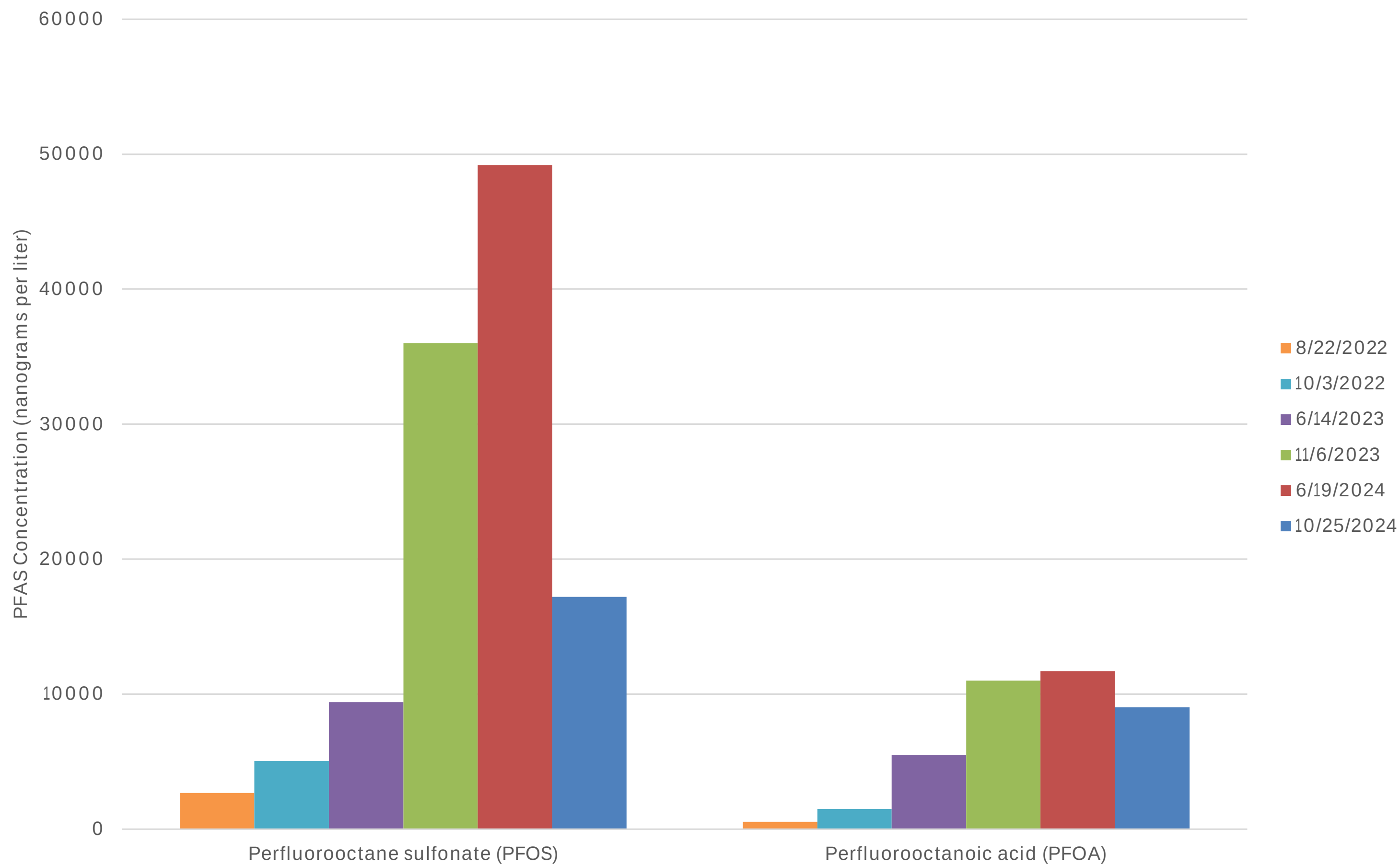

Figure N-28
Univariate Box Plot of Lysimeter Porewater PFOA Concentrations

Groundwater Model Development Report
Former Loring Air Force Base, Limestone, Maine

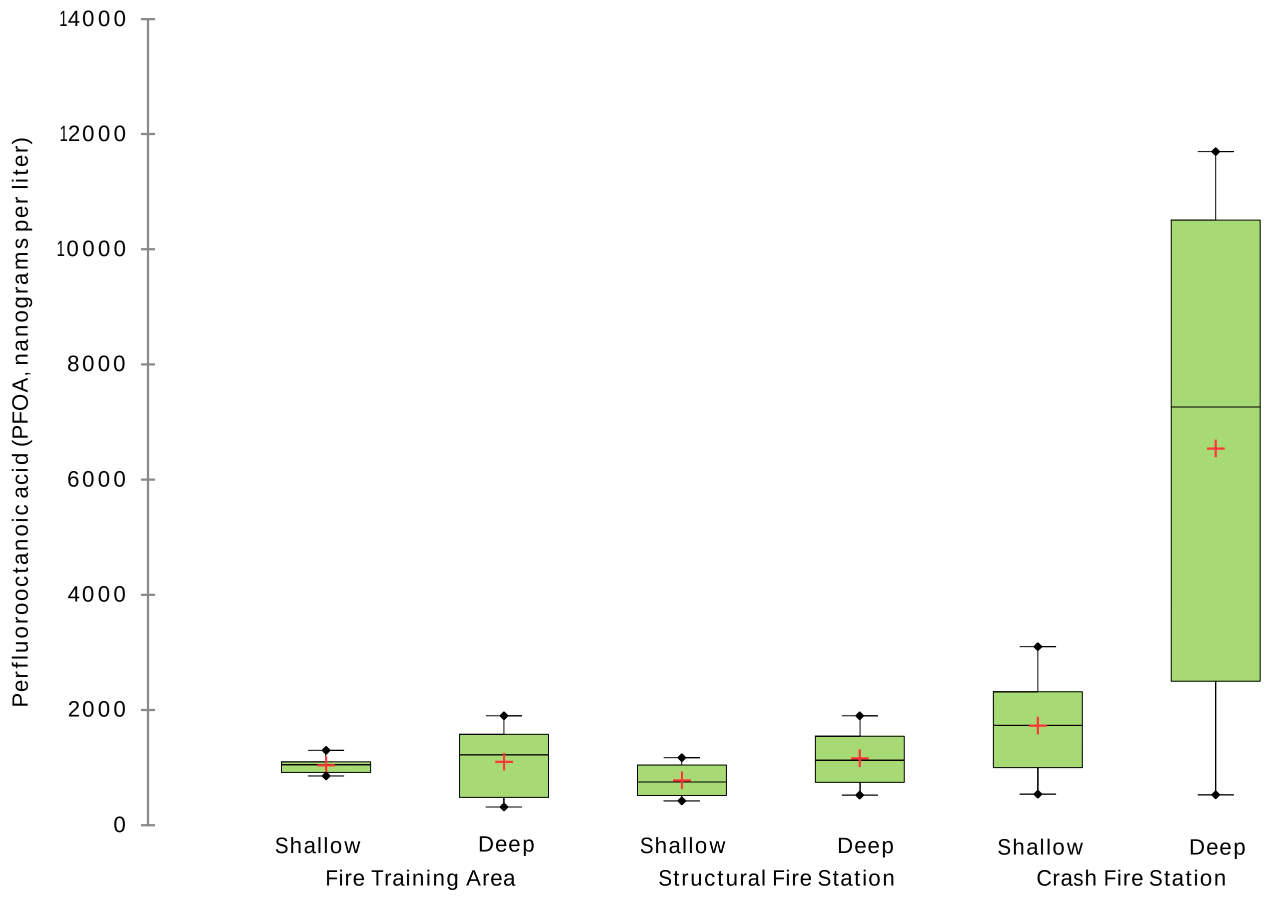

Figure N-29
Univariate Box Plot of Lysimeter Porewater PFOS Concentrations

Groundwater Model Development Report
Former Loring Air Force Base, Limestone, Maine

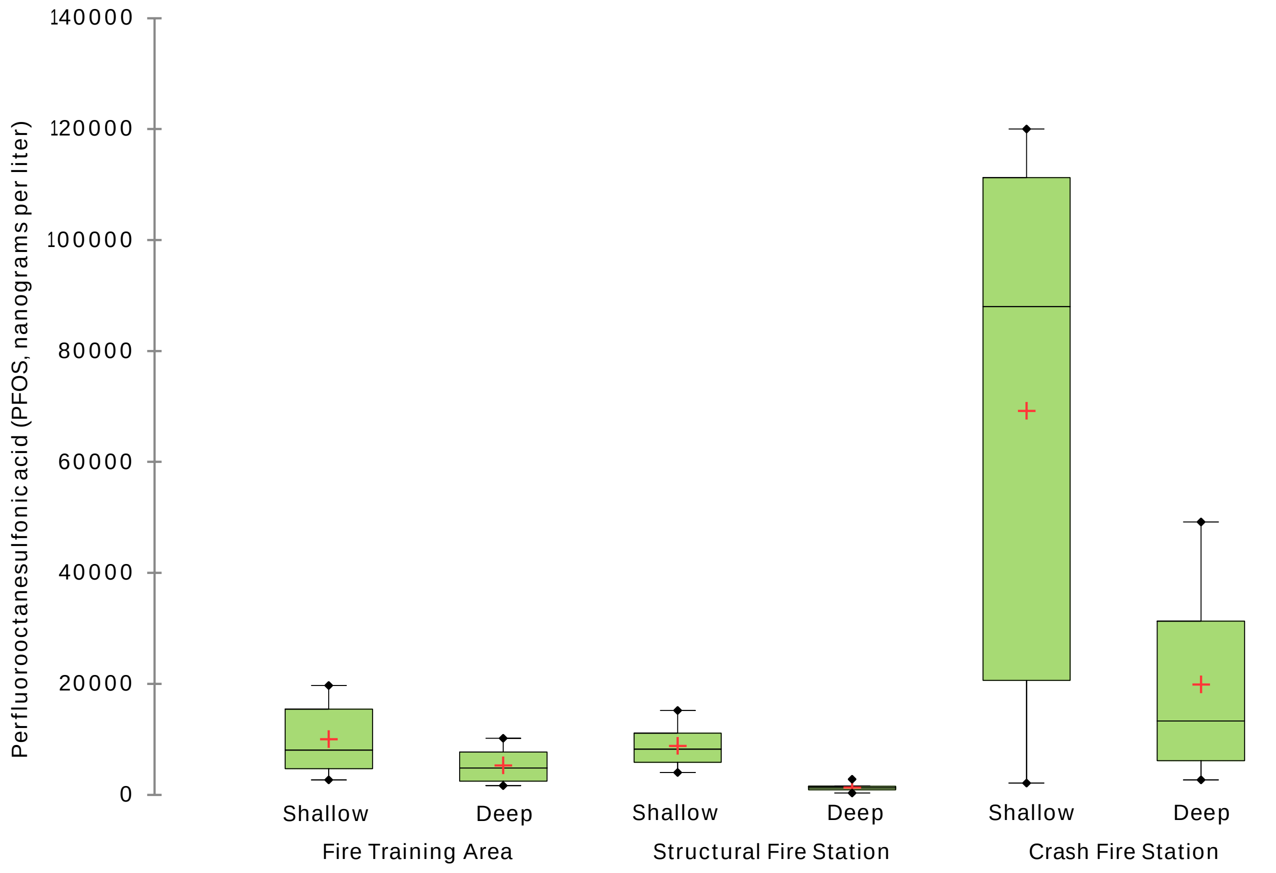

Figure N-30
Batch Sorption Testing PFOA Adsorbed versus Aqueous Concentration

Groundwater Model Development Report
Former Loring Air Force Base, Limestone, Maine

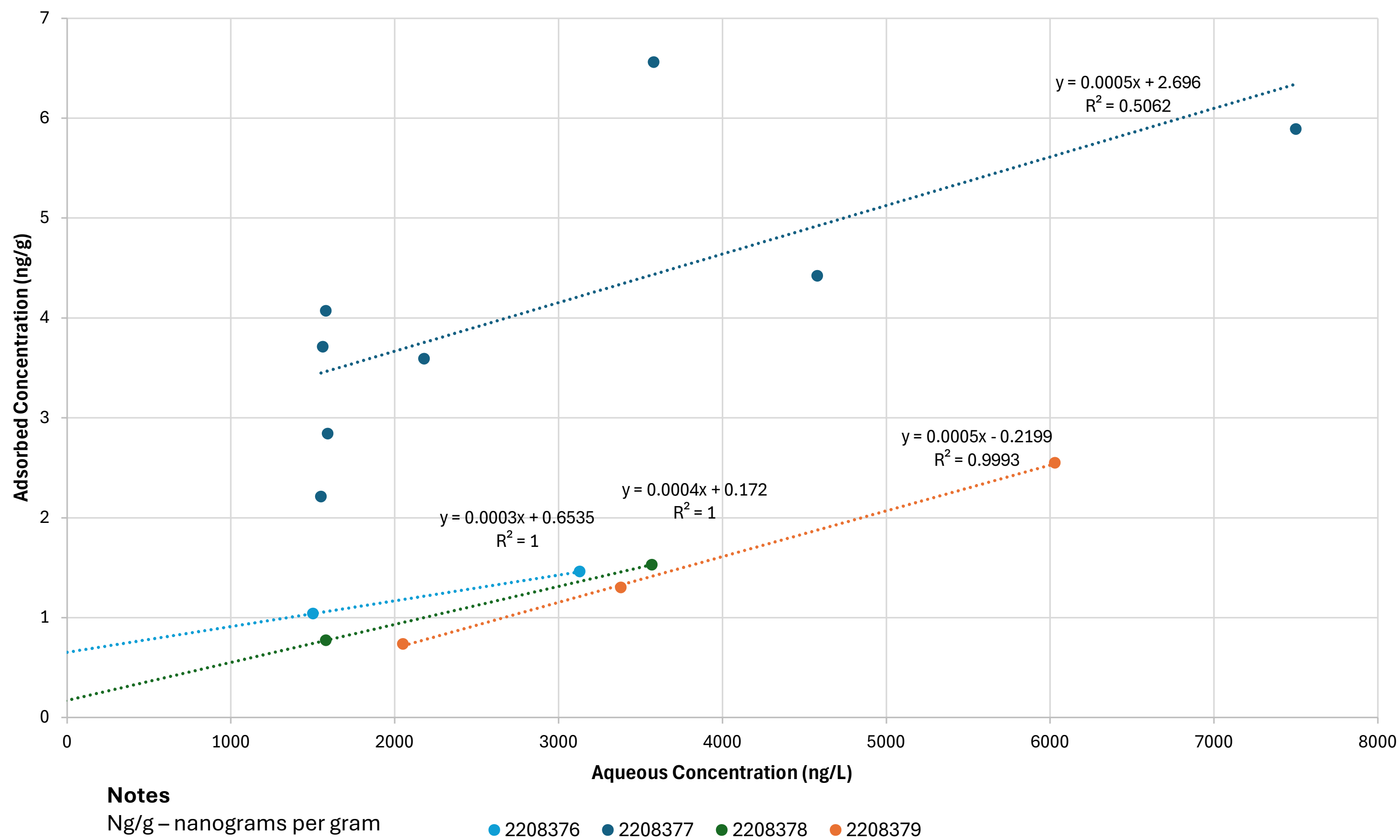

Notes
Ng/g – nanograms per gram
Ng/L – nanograms per liter

Figure N-31
Batch Sorption Testing PFOS Adsorbed versus Aqueous Concentration

Groundwater Model Development Report
Former Loring Air Force Base, Limestone, Maine

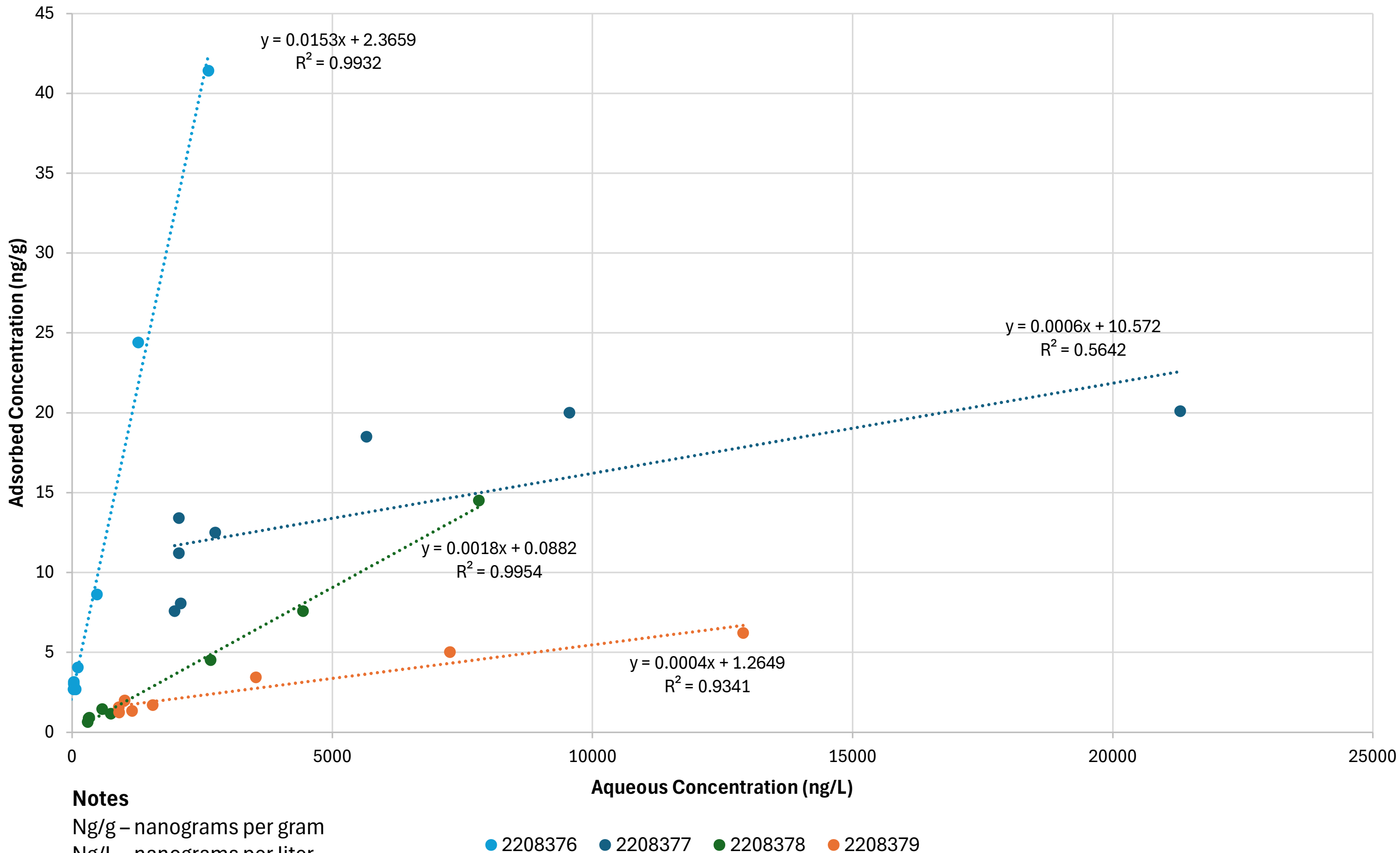

Notes
Ng/g – nanograms per gram
Ng/L – nanograms per liter

Figure N-32
Fire Training Area Shallow LEAF PFAS Concentrations versus Time

Groundwater Model Development Report
Former Loring Air Force Base, Limestone, Maine

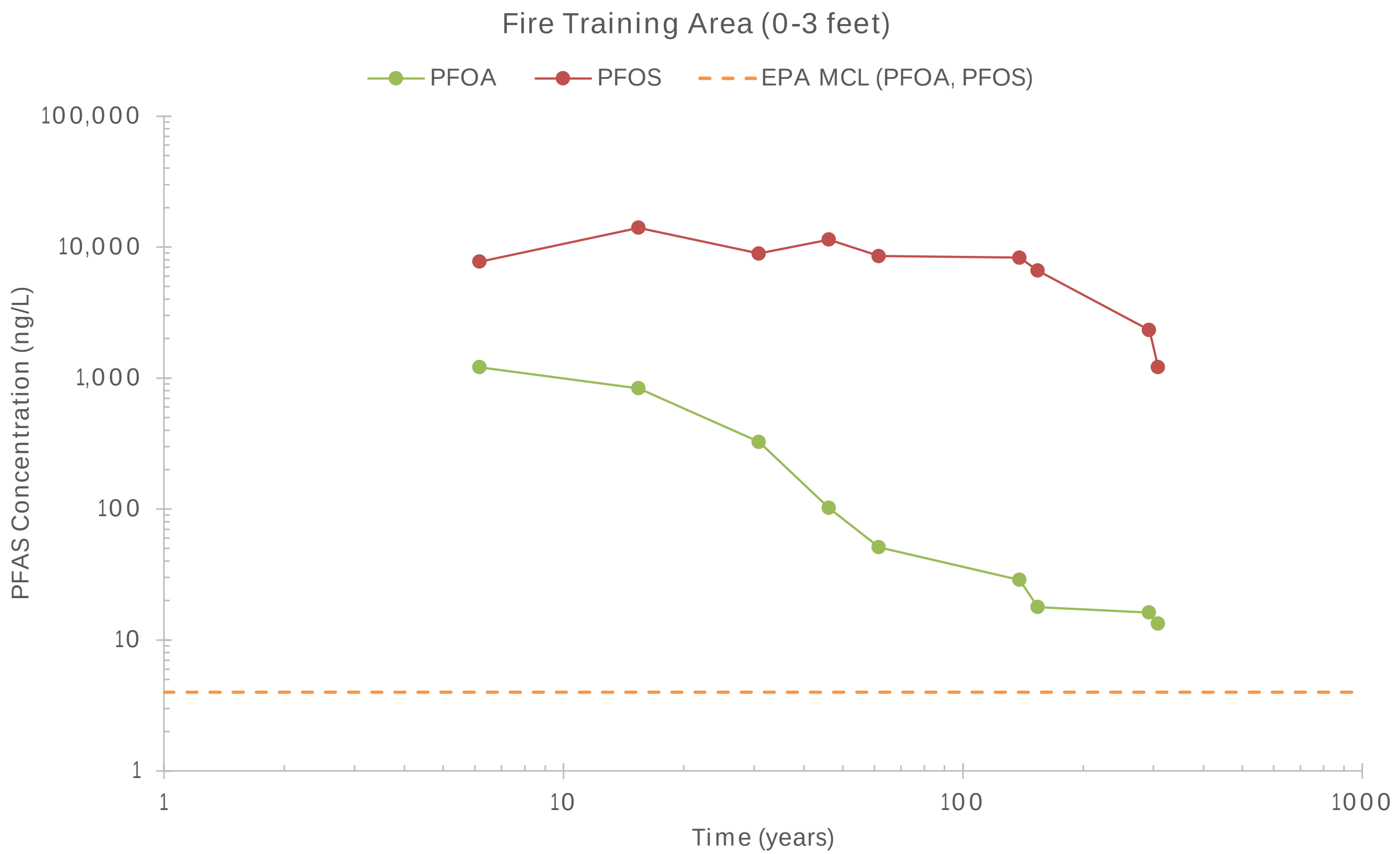

Notes
EPA MCL – Environmental Protection Agency Maximum Contaminant Level
ng/L – nanograms per liter
PFAS – per- and polyfluoroalkyl substances
PFOA – perfluorooctanoic acid
PFOS – perfluorooctanesulfonic acid

Figure N-33
Fire Training Area Deep LEAF PFAS Concentrations versus Time with Median Lysimeter Concentrations

Groundwater Model Development Report
Former Loring Air Force Base, Limestone, Maine

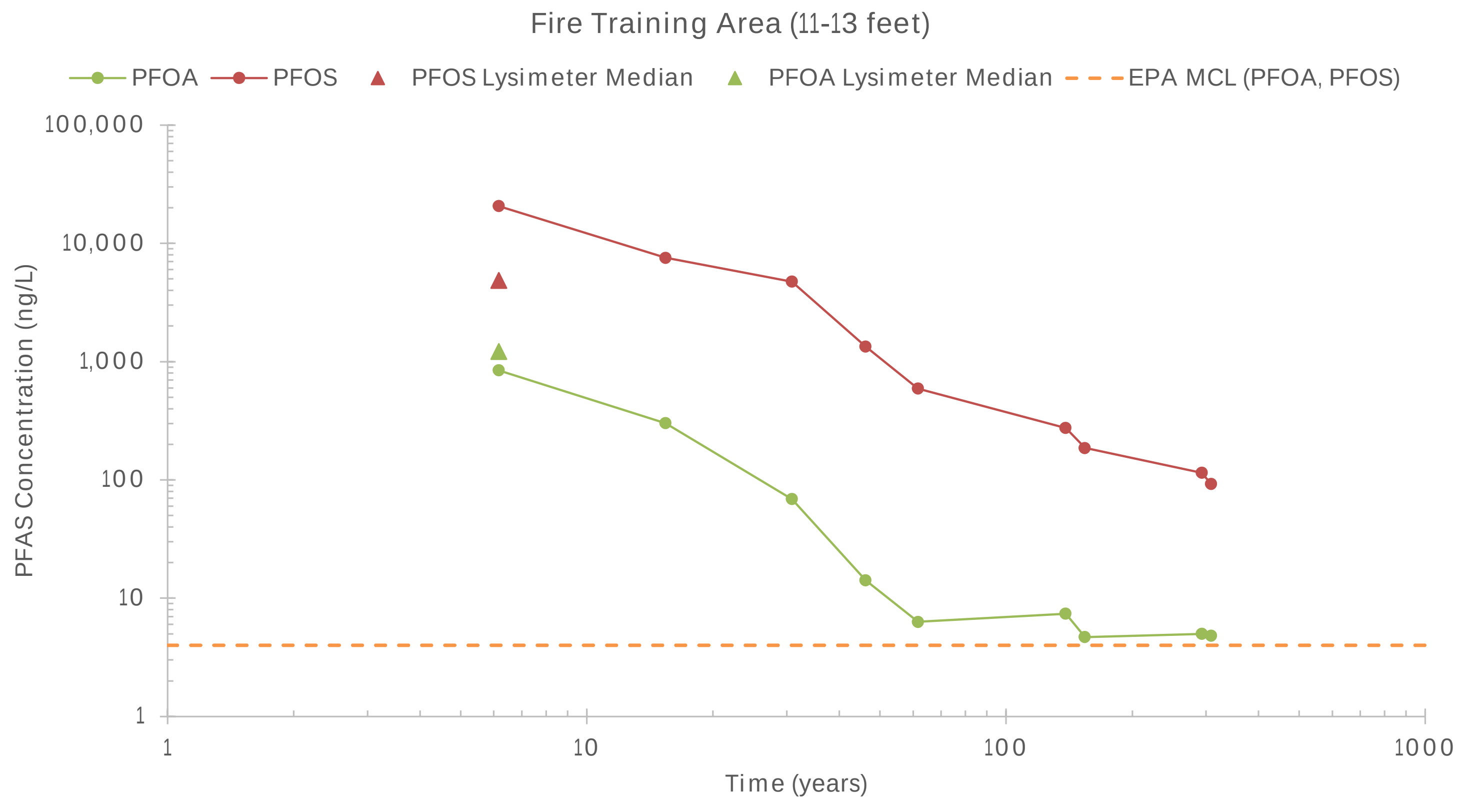

Notes
EPA MCL – Environmental Protection Agency Maximum Contaminant Level
ng/L – nanograms per liter
PFAS – per- and polyfluoroalkyl substances
PFOA – perfluorooctanoic acid
PFOS – perfluorooctanesulfonic acid

Figure N-34
Structural Fire Station Shallow LEAF PFAS Concentrations versus Time with Median Lysimeter Concentrations

Groundwater Model Development Report
Former Loring Air Force Base, Limestone, Maine

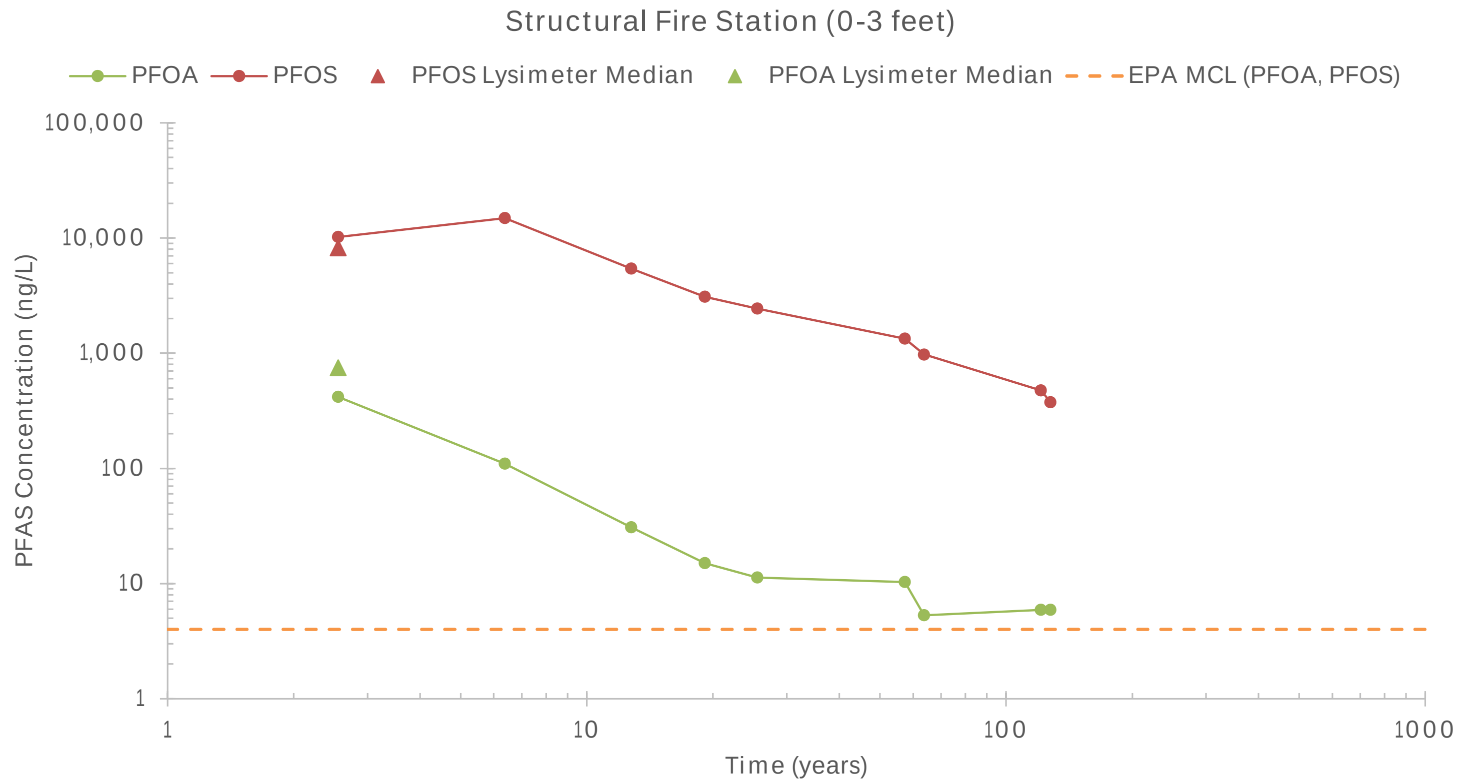

Notes
EPA MCL – Environmental Protection Agency Maximum Contaminant Level
ng/L – nanograms per liter
PFAS – per- and polyfluoroalkyl substances
PFOA – perfluorooctanoic acid
PFOS – perfluorooctanesulfonic acid

Figure N-35
Crash Fire Station Shallow LEAF PFAS Concentrations versus Time with Median Lysimeter Concentrations

Groundwater Model Development Report
Former Loring Air Force Base, Limestone, Maine

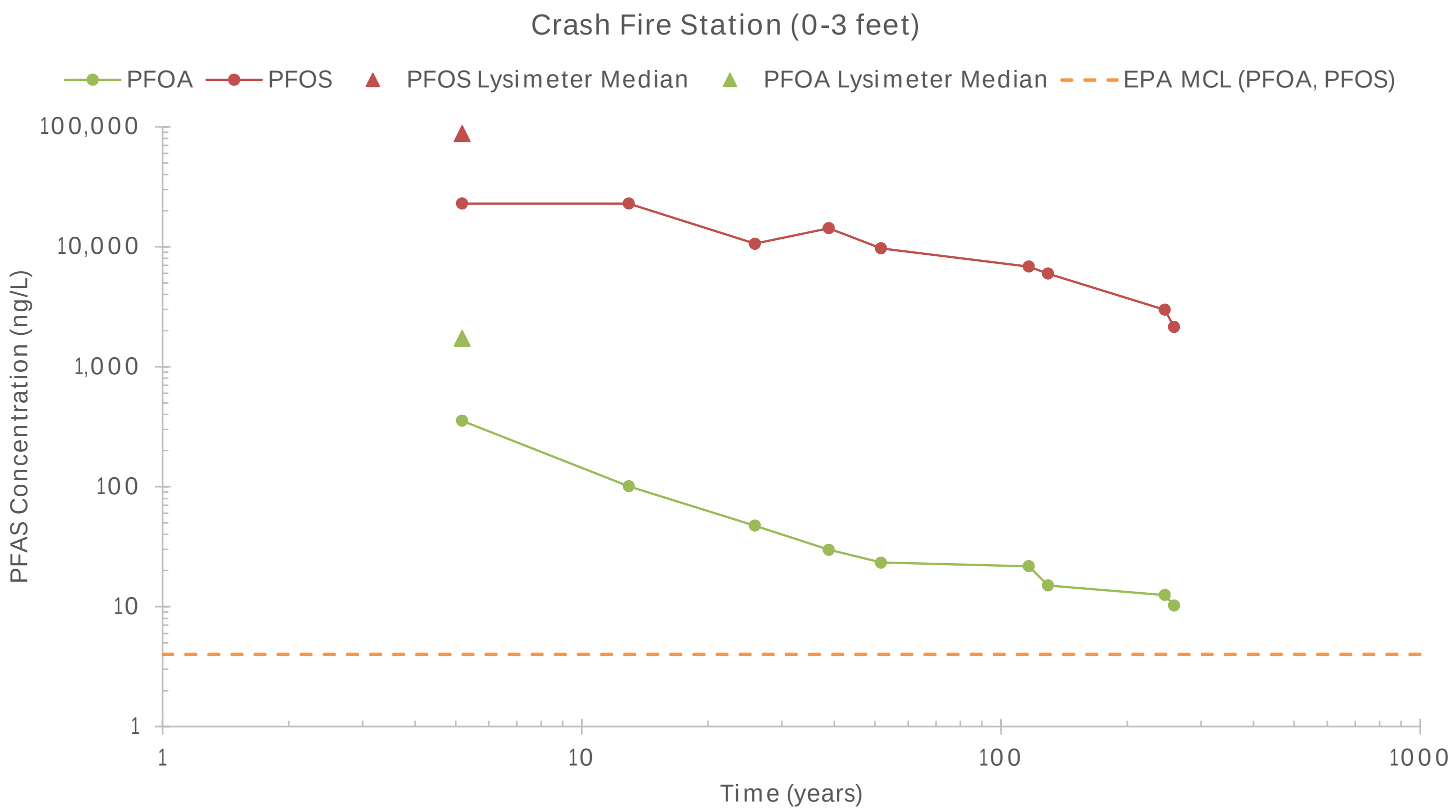

Notes
EPA MCL – Environmental Protection Agency Maximum Contaminant Level
ng/L – nanograms per liter
PFAS – per- and polyfluoroalkyl substances
PFOA – perfluorooctanoic acid
PFOS – perfluorooctanesulfonic acid

Figure N-36
Crash Fire Station Deep LEAF PFAS Concentrations versus Time with Median Lysimeter Concentrations

Groundwater Model Development Report
Former Loring Air Force Base, Limestone, Maine

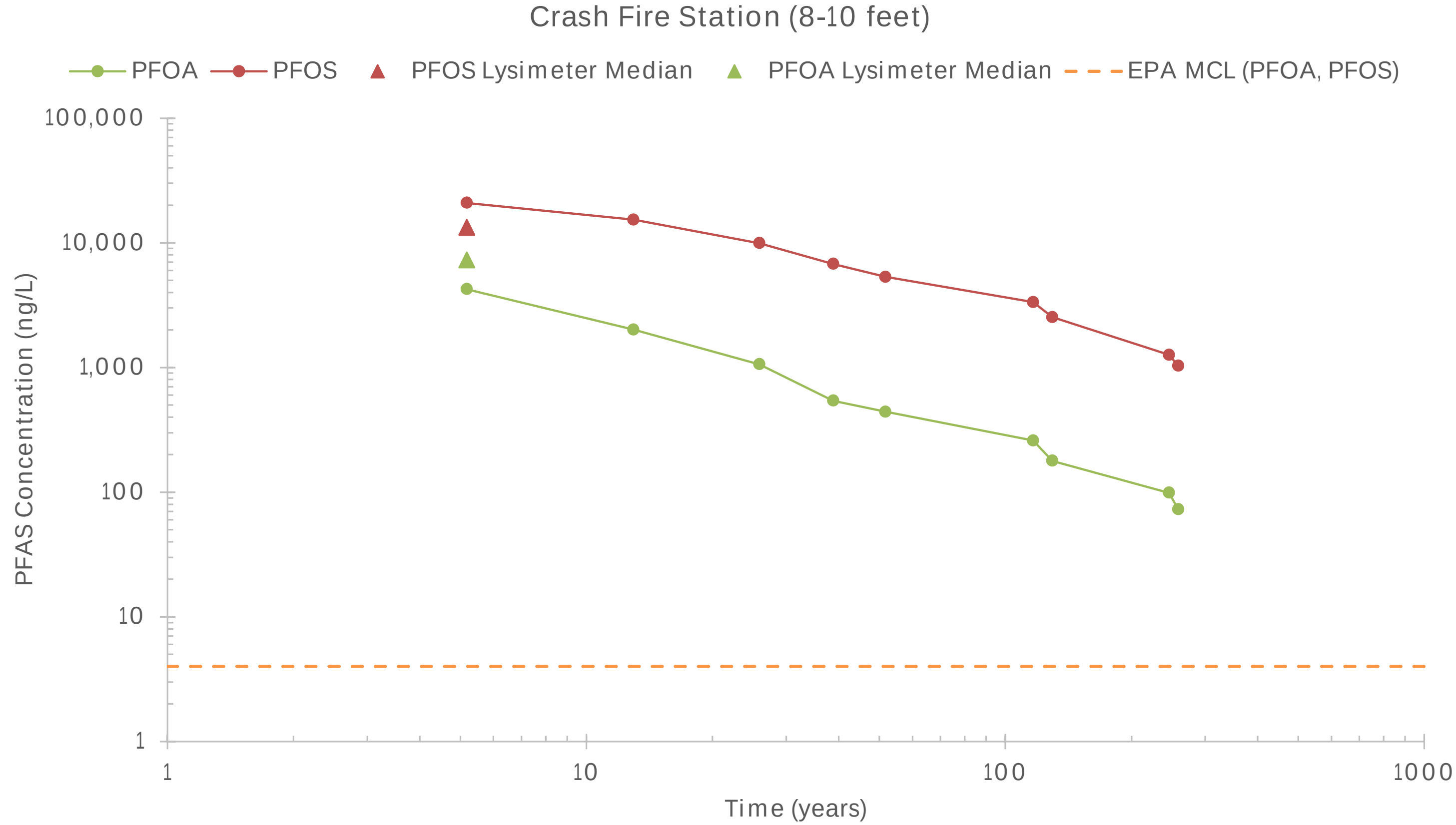

Notes
EPA MCL – Environmental Protection Agency Maximum Contaminant Level
ng/L – nanograms per liter
PFAS – per- and polyfluoroalkyl substances
PFOA – perfluorooctanoic acid
PFOS – perfluorooctanesulfonic acid

Figure N-37
Nose Dock Area Shallow LEAF PFAS Concentrations versus Time

Groundwater Model Development Report
Former Loring Air Force Base, Limestone, Maine

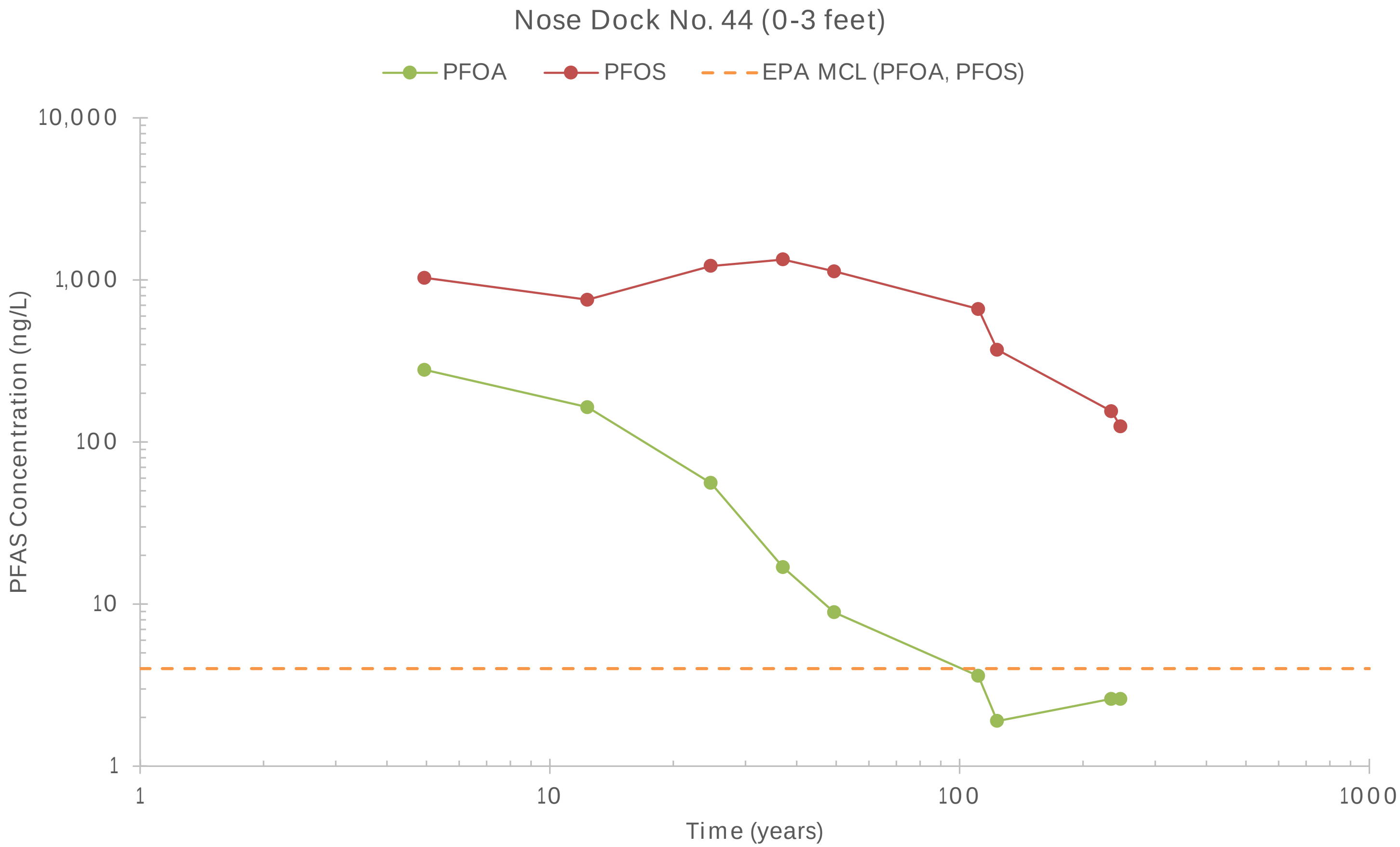

Notes
EPA MCL – Environmental Protection Agency Maximum Contaminant Level
ng/L – nanograms per liter
PFAS – per- and polyfluoroalkyl substances
PFOA – perfluorooctanoic acid
PFOS – perfluorooctanesulfonic acid

Figure N-38
2024 Fire Training Area Shallow LEAF PFAS Concentrations versus Time

Groundwater Model Development Report
Former Loring Air Force Base, Limestone, Maine

Notes
EPA MCL – Environmental Protection Agency Maximum Contaminant Level
ng/L – nanograms per liter
PFAS – per- and polyfluoroalkyl substances
PFOA – perfluorooctanoic acid
PFOS – perfluorooctanesulfonic acid

Figure N-39
2024 Fire Training Area Deep LEAF PFAS Concentrations versus Time

Groundwater Model Development Report
Former Loring Air Force Base, Limestone, Maine

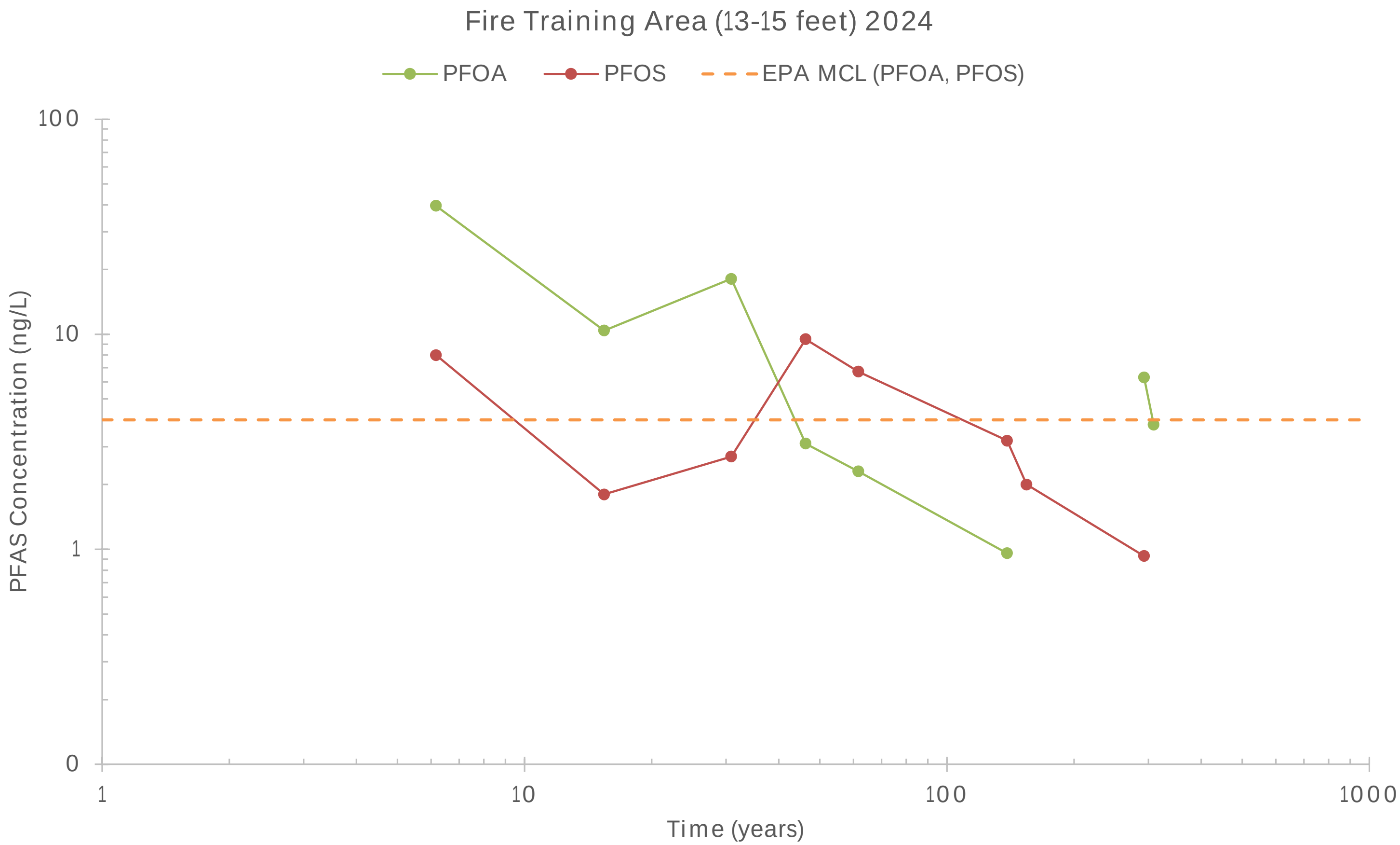

Notes
EPA MCL – Environmental Protection Agency Maximum Contaminant Level
ng/L – nanograms per liter
PFAS – per- and polyfluoroalkyl substances
PFOA – perfluorooctanoic acid
PFOS – perfluorooctanesulfonic acid

Figure N-40
2024 Structural Fire Station Shallow LEAF PFAS Concentrations versus Time

Groundwater Model Development Report
Former Loring Air Force Base, Limestone, Maine

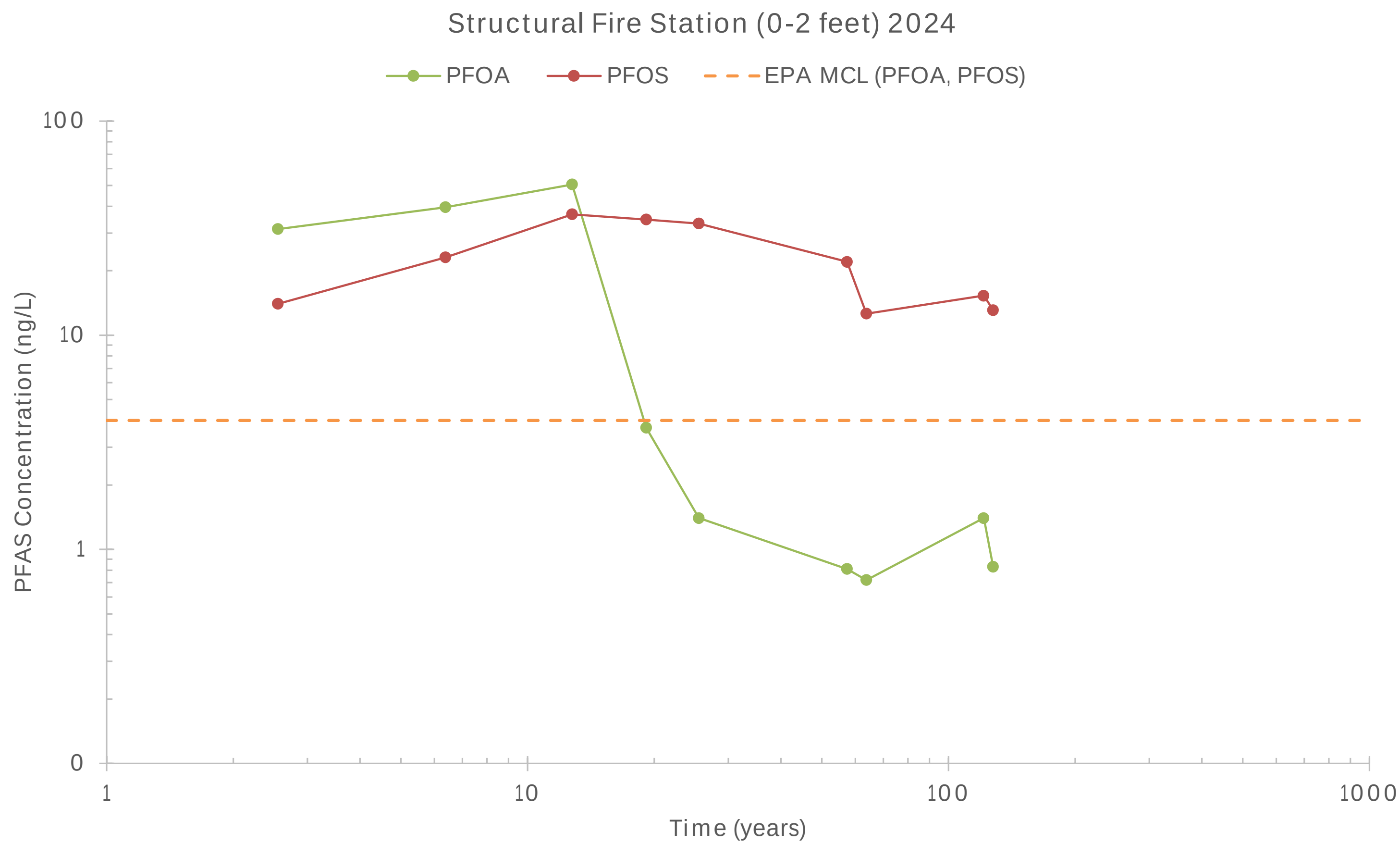

Notes
EPA MCL – Environmental Protection Agency Maximum Contaminant Level
ng/L – nanograms per liter
PFAS – per- and polyfluoroalkyl substances
PFOA – perfluorooctanoic acid
PFOS – perfluorooctanesulfonic acid

Figure N-41
2024 Structural Fire Station Deep LEAF PFAS Concentrations versus Time

Groundwater Model Development Report
Former Loring Air Force Base, Limestone, Maine

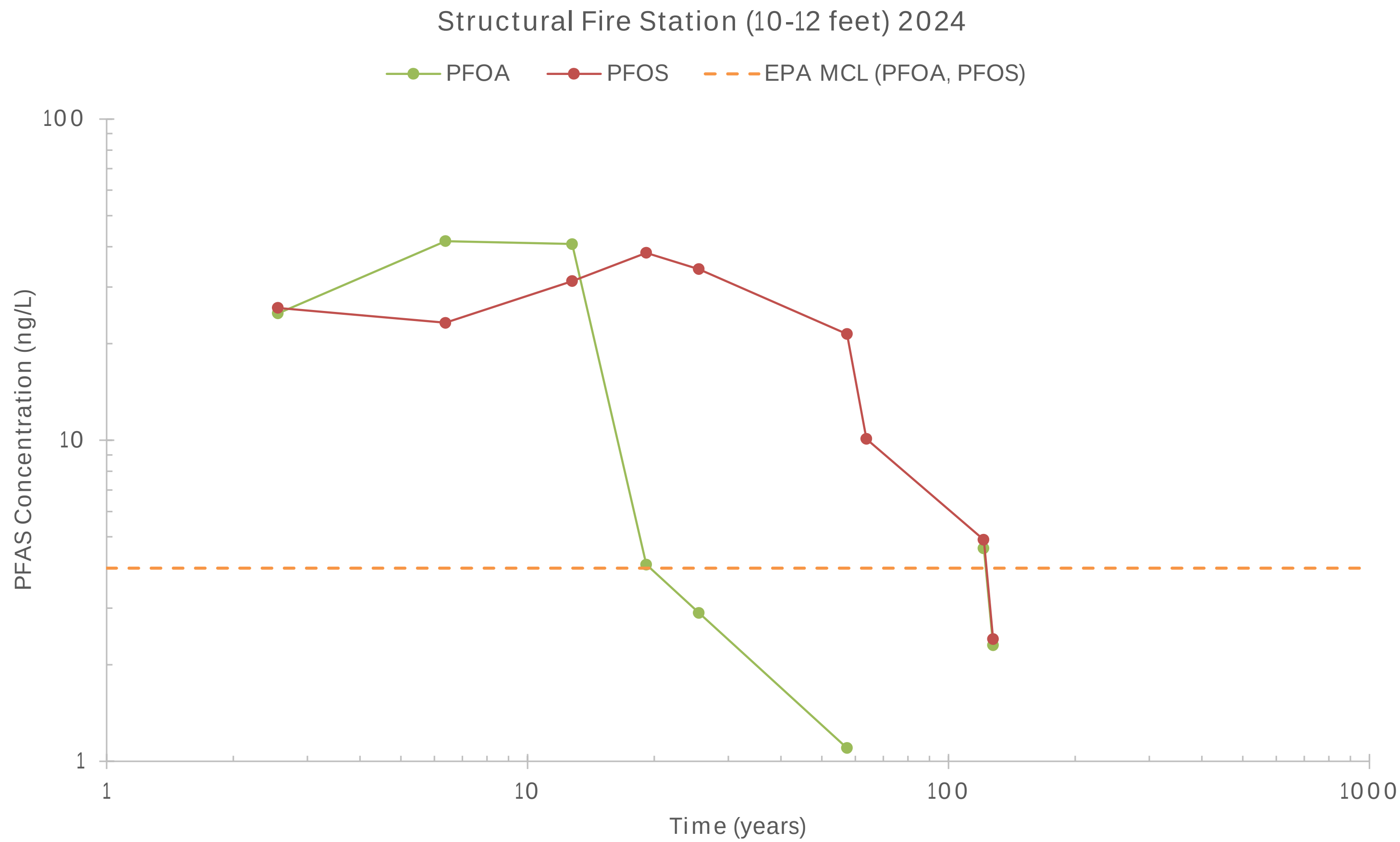

Notes
EPA MCL – Environmental Protection Agency Maximum Contaminant Level
ng/L – nanograms per liter
PFAS – per- and polyfluoroalkyl substances
PFOA – perfluorooctanoic acid
PFOS – perfluorooctanesulfonic acid

Figure N-42
2024 Crash Fire Station Shallow LEAF PFAS Concentrations versus Time

Groundwater Model Development Report
Former Loring Air Force Base, Limestone, Maine

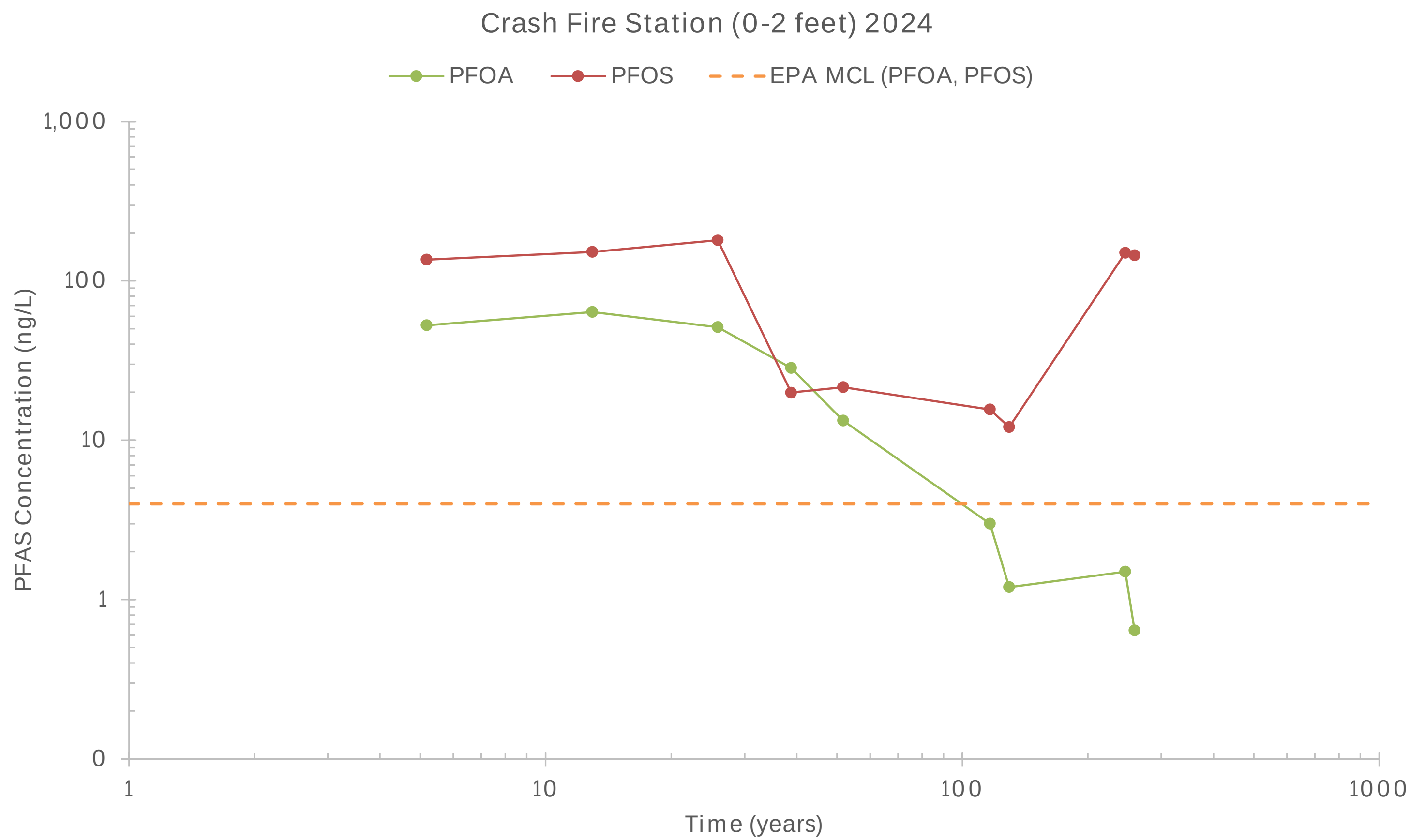

Notes
EPA MCL – Environmental Protection Agency Maximum Contaminant Level
ng/L – nanograms per liter
PFAS – per- and polyfluoroalkyl substances
PFOA – perfluorooctanoic acid
PFOS – perfluorooctanesulfonic acid

Figure N-43
2024 Crash Fire Station Deep LEAF PFAS Concentrations versus Time

Groundwater Model Development Report
Former Loring Air Force Base, Limestone, Maine

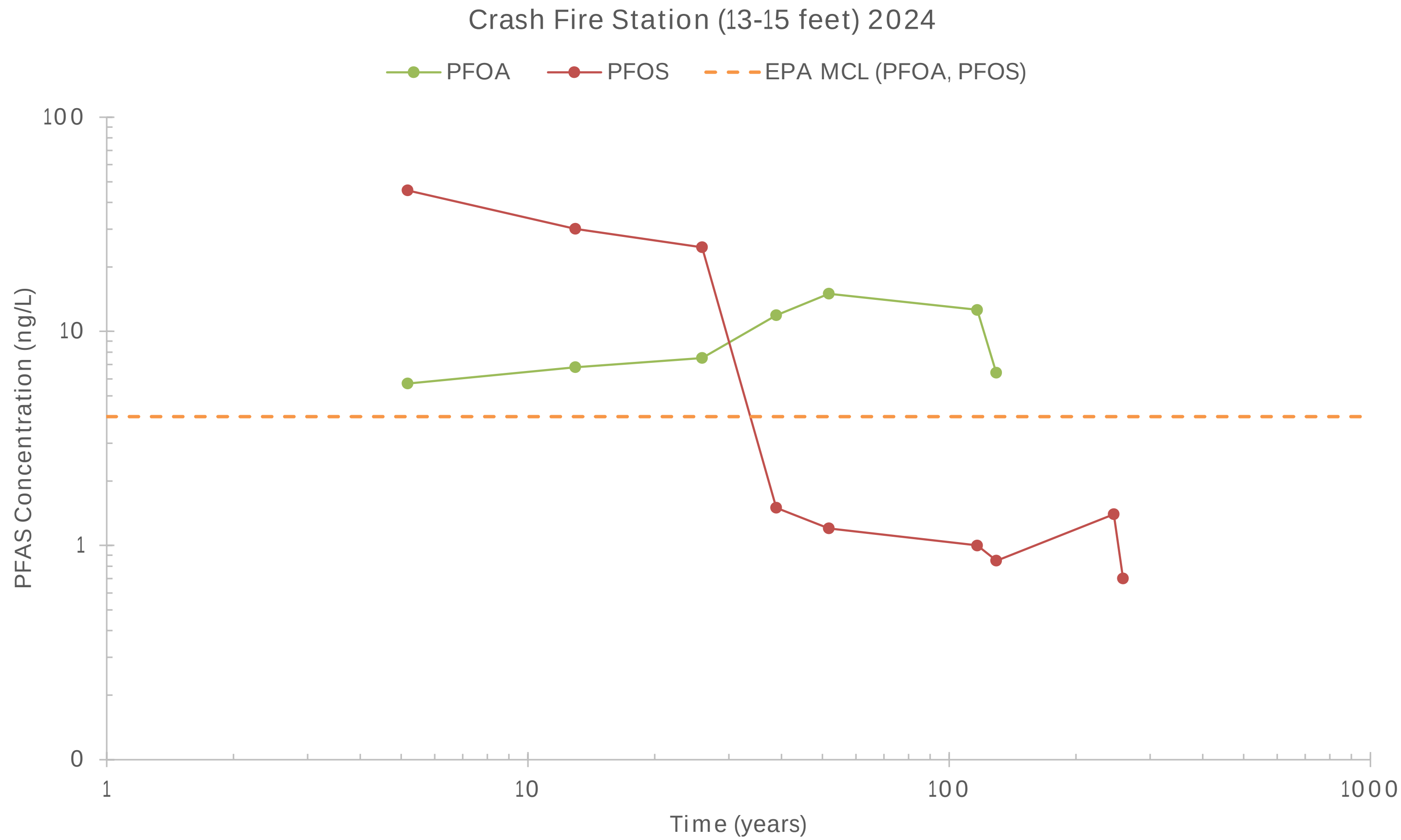

Notes
EPA MCL – Environmental Protection Agency Maximum Contaminant Level
ng/L – nanograms per liter
PFAS – per- and polyfluoroalkyl substances
PFOA – perfluorooctanoic acid
PFOS – perfluorooctanesulfonic acid

Figure N-44
2024 Nose Dock Area Shallow LEAF PFAS Concentrations versus Time

Groundwater Model Development Report
Former Loring Air Force Base, Limestone, Maine

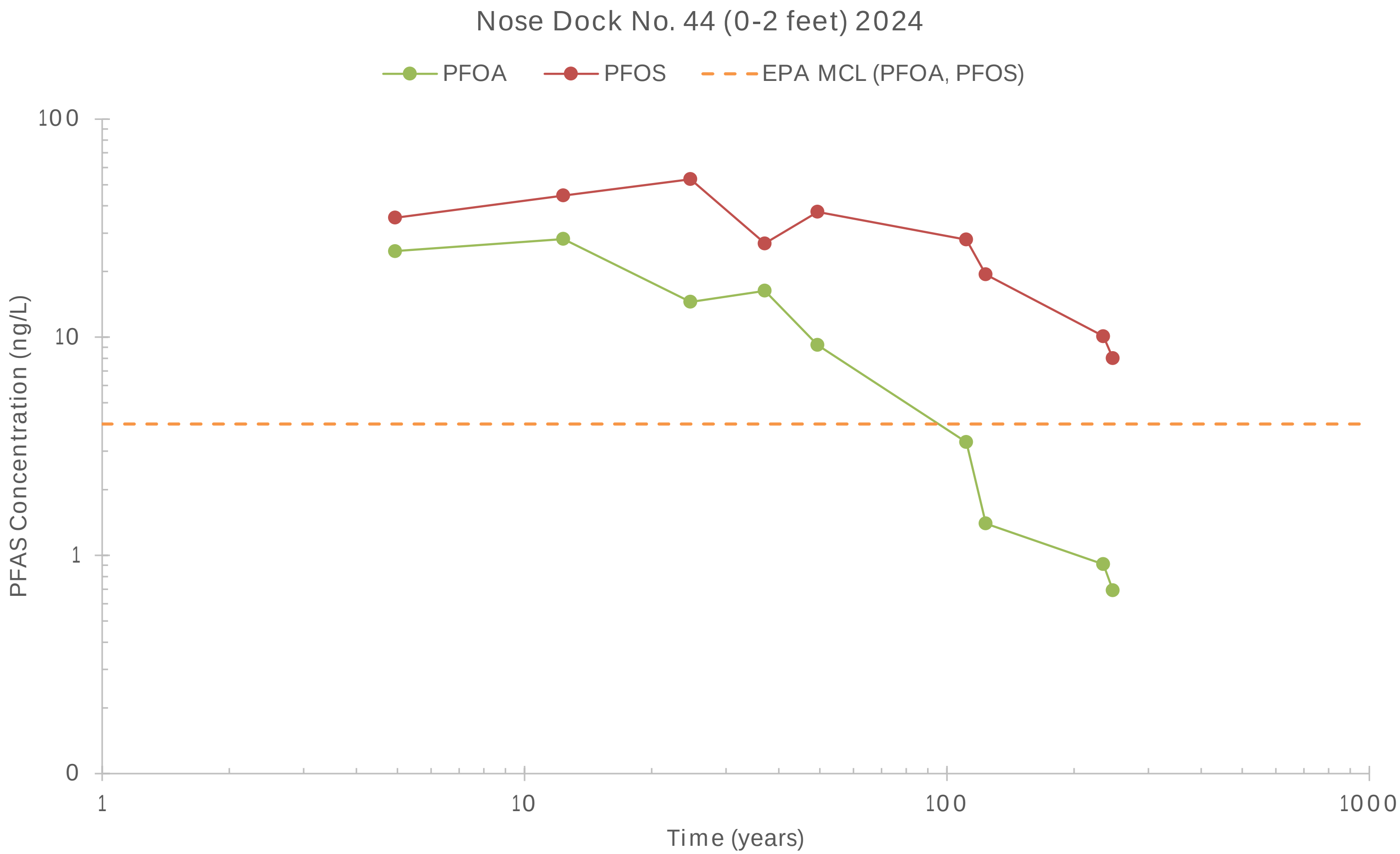

Notes
EPA MCL – Environmental Protection Agency Maximum Contaminant Level
ng/L – nanograms per liter
PFAS – per- and polyfluoroalkyl substances
PFOA – perfluorooctanoic acid
PFOS – perfluorooctanesulfonic acid

Figure N-45
2024 Nose Dock Area Deep LEAF PFAS Concentrations versus Time

Groundwater Model Development Report
Former Loring Air Force Base, Limestone, Maine

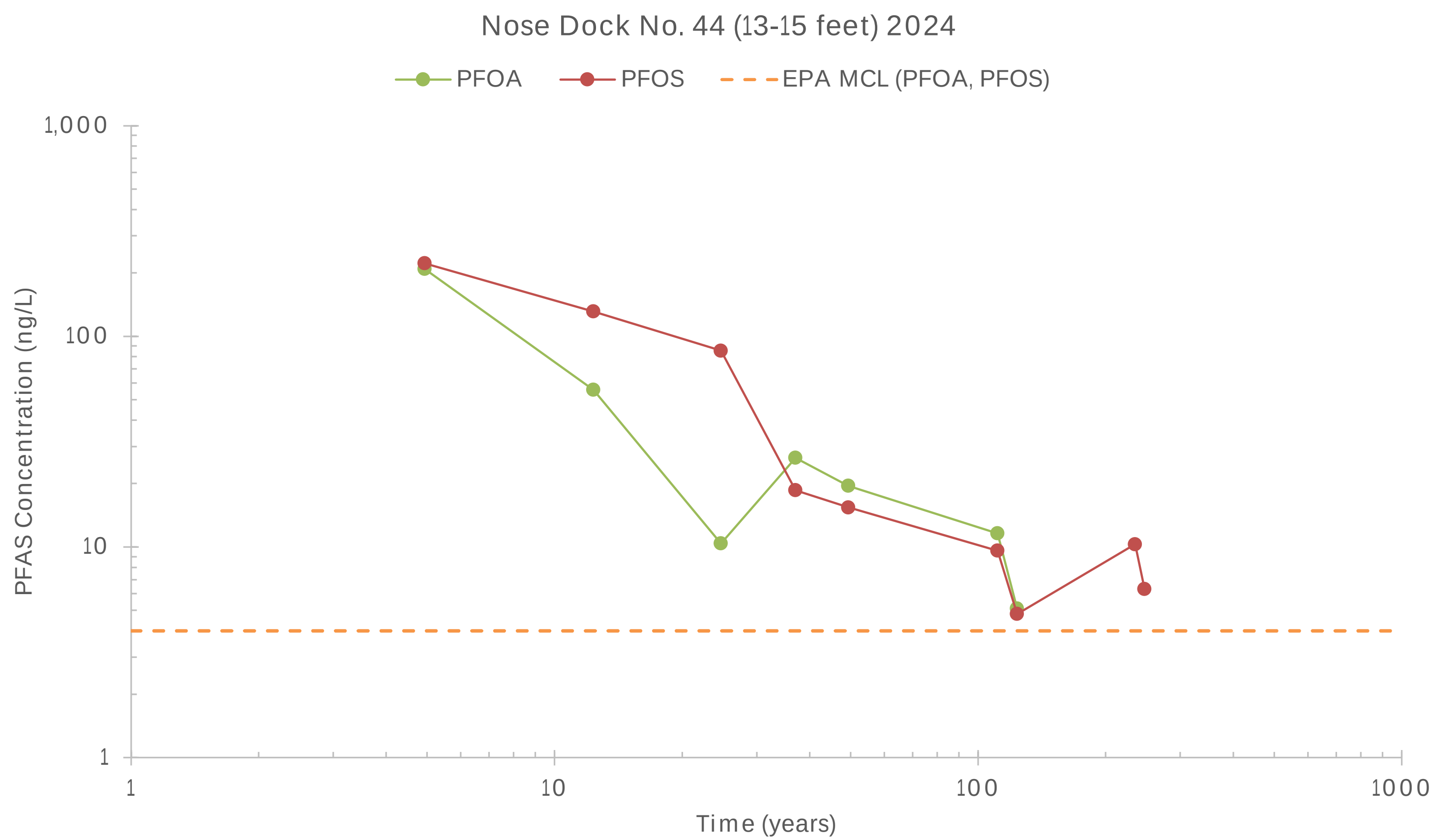

Notes
EPA MCL – Environmental Protection Agency Maximum Contaminant Level
ng/L – nanograms per liter
PFAS – per- and polyfluoroalkyl substances
PFOA – perfluorooctanoic acid
PFOS – perfluorooctanesulfonic acid

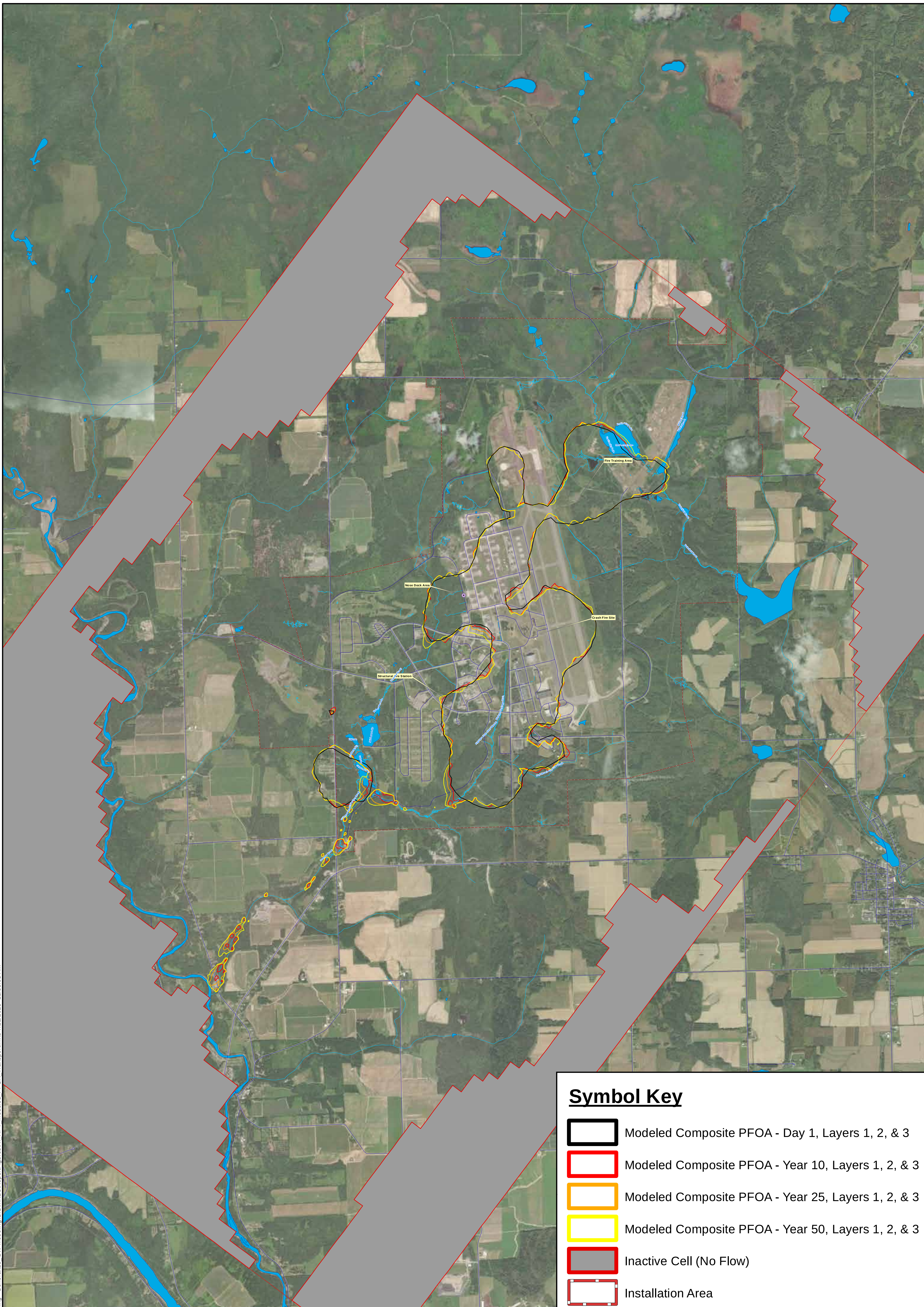

Air Force Civil Engineer Center
2261 Hughes Ave., Suite 163
JBSA Lackland, TX 78236

Figure N - 46
Model Predicted PFOA Extent - Composite of Layers 1, 2, & 3
Groundwater Model Development Report
Former Loring Air Force Base, Limestone, ME

0 500 1,000 2,000 3,000 4,000 Meters

0 1,000 2,000 4,000 6,000 8,000 10,000 Feet

N

NOTES:
-Aerial Imagery obtained from NAIP, USDA-FSA. Published September, 2021

Drawn: JL

Drawn Date: 07/22/2025

PROJ: 775361701

Document: C:\Users\USJL717025\WSP O365\WDS-Loring - General\15_GW Modeling\GIS\MXDs\ReportFigures\RI_RPT_Modeled_PFOA_Transport.mxd 7/22/2025 11:55:03 AM

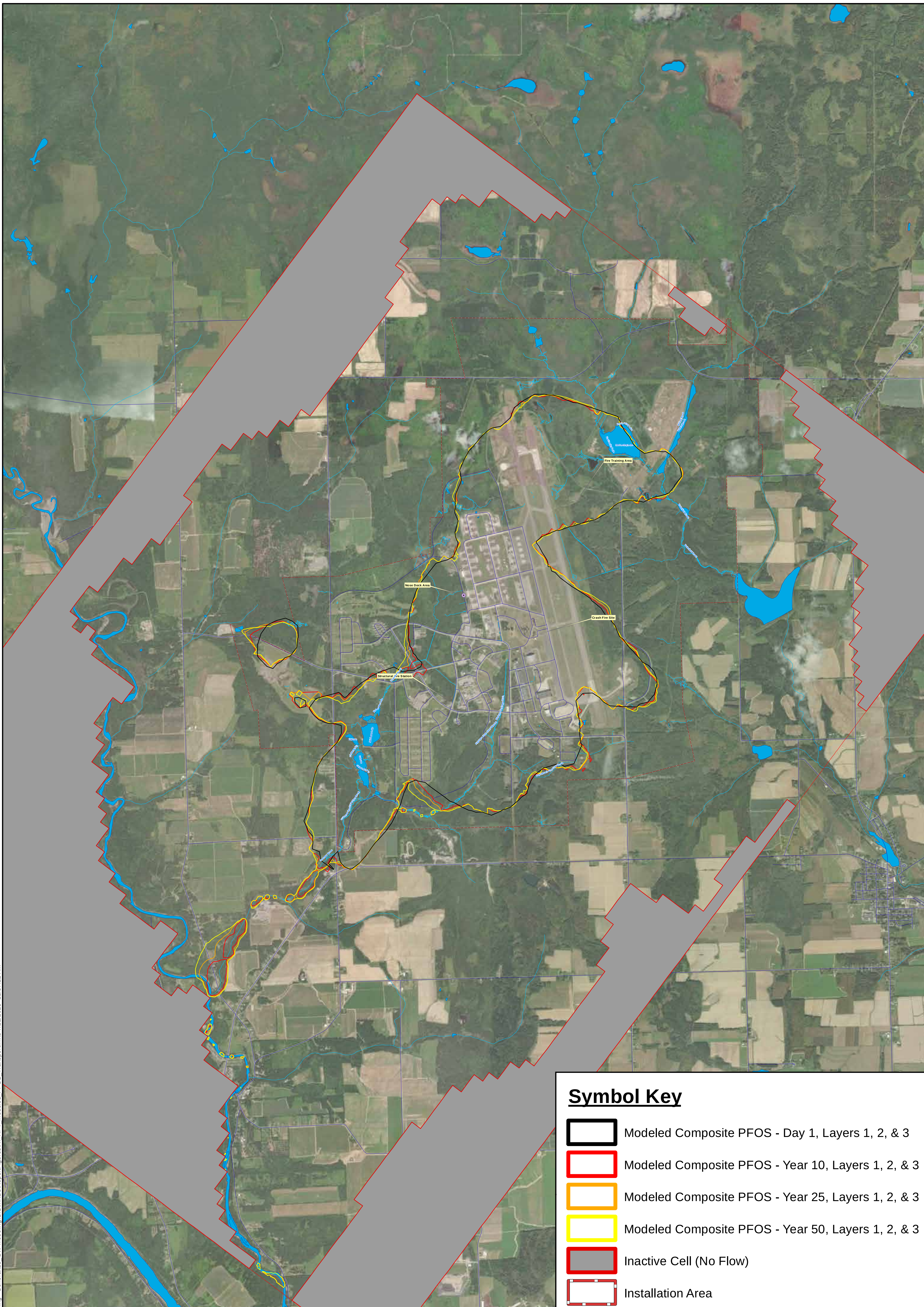

Air Force Civil Engineer Center
2261 Hughes Ave., Suite 163
JBSA Lackland, TX 78236

Figure N- 47
Model Predicted PFOS Extent - Composite of Layers 1, 2, & 3
Groundwater Model Development Report
Former Loring Air Force Base, Limestone, ME

0 500 1,000 2,000 3,000 4,000 Meters

0 1,000 2,000 4,000 6,000 8,000 10,000 Feet

N

NOTES:
-Aerial Imagery obtained from NAIP, USDA-FSA. Published September, 2021

Drawn: JL

Drawn Date: 07/22/2025

PROJ: 775361701

Document: C:\Users\USJL717025\WSP O365\WDS-Loring - General\15_GW Modeling\GIS\MXDs\ReportFigures\RI_RPT_Modeled_PFOS_Transport.mxd 7/22/2025 11:57:22 AM

TABLES

Table N-1
Model Construction Parameters

Groundwater Model Development Report
Former Loring Air Force Base, Limestone, Maine

Grid Information	
Number of Rows	97
Number of Columns	68
Parent Grid Cell Size	500 ft. x 500 ft.
Refined Grid Cell Size	31.25 ft. x 31.25 ft.
Number of Active Layers	3
Total Cells	279,756
Total Active Cells	269,736
Grid Rotation	Oriented to N36.78^{0} E
X-offset	1,101,824
Y-offset	1,181,418

Notes
^{0} - degrees
E - East
ft - Feet
N - north
NAD 1983 State Plane Maine East Feet

Table N-2
Slug Test Results

Groundwater Model Development Report
Former Loring Air Force Base, Limestone, ME

Well ID	X	Y	Zone	Average Hydraulic Conductivity (ft/day)
BW01005	1138298	1201437	Bedrock	0.90
BW01008	1140152.04	1202497.24	Bedrock	5.97
BW01009	1139561.33	1203247.29	Bedrock	2.26
BW05006	1132229.43	1191798.68	Bedrock	1.96
BW05009	1132590.58	1191565.4	Bedrock	1.40
BW06006	1134964.19	1188219.13	Bedrock	5.02
BW06008	1135400.03	1188078.39	Bedrock	7.80
BW07001	1136511.18	1195370.41	Bedrock	33.24
BW12006	1133030.34	1197014.03	Bedrock	2.59
JBW7326A	1134485.6	1189844.25	Bedrock	13.72
JBW7734	1133128.53	1196564.63	Bedrock	5.42
JBW7737A	1132521.65	1195846.67	Bedrock	43.50
JBW7737B	1132522.65	1195846.67	Bedrock	3.26
JBW7738A	1131802.03	1195404.64	Bedrock	5.29
JBW7738B	1131805.09	1195404.63	Bedrock	1.30
JBW8003B	1138914.62	1202108.63	Bedrock	3.31
JMW0683	1137343.17	1189272.09	Bedrock	2.35
JPZ0348	1134820.87	1191270	Bedrock	50.25
JPZ1780	1135289.97	1192032.61	Bedrock	29.00
AA20MW-02	1136371.55	1204702.57	Overburden	10.07
JPZ0686	1138219.87	1189641.94	Overburden	4.62
OW01004	1139579.31	1203226.16	Overburden	15.31
OW05003	1132330.14	1191919.17	Overburden	398.20
OW07001	1136516.9	1195364.51	Overburden	384.88
OW08001	1135625.16	1194148	Overburden	76.03
OW08002	1135375.98	1193499.68	Overburden	253.16
OW12002	1132986.28	1197199.4	Overburden	203.89
OW20001	1135911.89	1204788.54	Overburden	95.19
OW20003	1136629.5	1204822.38	Overburden	18.63
OW20005	1136760.5	1204366.24	Overburden	37.96
SB/OW12001	1133020.99	1197019.87	Overburden	207.45
SB/OW16001	1137654.97	1189376.51	Overburden	17.55

Notes

ID - Identification

ft/day - Feet per day

Table N-3
Well Construction Information and Water Levels

Groundwater Model Development Report
Former Loring Air Force Base, Limestone, Maine

					September 2022		October 2022		May 2023		October 2023	
	X	Y	Z (Ground)	BOW elev	Date	GW Elev	Date	GW Elev	Date	GW Elev	Date	GW Elev
Location_ID	m	m	ft amsl	ft amsl		ft amsl		ft amsl		ft amsl		ft amsl
043-MW03	1128625.91	1188010.68	598.26	573.31	9/15/2022	579.31	10/25/2022	579.46	5/2/2023	579.47	10/2/2023	579.61
044-RW01	1138790.93	1200027.56	752.91	723.47	9/15/2022	729.49	10/25/2022	730.46	5/3/2023	731.4	10/3/2023	730.53
051-MW03	1140546.74	1190335.81	706.69	702.39	9/15/2022	702.61	10/26/2022	703.44	5/2/2023	702.89	10/3/2023	702.94
056-MW02	1136146.11	1191699.8	700.24	676.94	9/16/2022	686.07	10/26/2022	684.89	5/2/2023	703.94	10/3/2023	686.53
056-MW03	1136194.5	1191503.77	699.84	685.6	9/16/2022	691.46	10/26/2022	692.36	5/2/2023	694.12	10/3/2023	693.35
056MW04	1136006.62	1191661.79	697	678.84	9/16/2022	685.68	10/26/2022	689.26	5/2/2023	690.47	10/3/2023	689.01
056MW06	1136060.74	1191491.03	694.9	646.87	9/16/2022	658.85	10/26/2022	664.02	5/2/2023	668.39	10/3/2023	667.09
059-MW03	1146002.49	1205475.13	756.72	730.52	Not Collected	Not Collected	10/26/2022	742.85	Not Collected	Not Collected	10/2/2023	745.54
AA07MW-01	1136564.15	1195074.81	720.44	700.92	9/15/2022	702.98	10/26/2022	703.17	5/2/2023	708.05	10/3/2023	706.88
AA18MW-01	1137614.12	1195186.69	729.2	671.52	9/15/2022	700.06	10/27/2022	700.96	5/1/2023	707.96	10/3/2023	706.37
AA18MW-02	1137671.36	1197490.62	739.81	688.36	9/15/2022	707.12	10/26/2022	707.27	5/2/2023	712.72	10/3/2023	711.39
AA19MW-01	1139589.47	1190472.62	707	687.35	9/16/2022	697.08	10/26/2022	700.97	5/2/2023	701.73	10/3/2023	701.18
AA19MW-02	1139346.38	1190362.15	706.32	687.24	9/17/2022	695.29	10/26/2022	703.94	5/2/2023	702.41	10/3/2023	700.97
AR25	1135037.39	1191021.85	672.17	515.19	9/16/2022	652.31	10/25/2022	653.74	5/2/2023	656.88	10/3/2023	656.13
ASMW101	1137076.297	1191243.63	724.6313	693.8613	9/16/2022	698.94	10/27/2022	700.68	5/2/2023	701.0613	10/3/2023	700.37
ASMW301	1136642.79	1194797.76	718.72	695.34	9/15/2022	698.60	10/26/2022	700.30	5/2/2023	705.76	10/3/2023	704.48
BB_BW001	1141889.361	1202159.997	654.8112	584.8112	9/16/2022	650.04	10/25/2022	646.25	5/3/2023	649.5112	10/2/2023	647.46
BB_BW002	1145613.906	1197508.076	625.7414	556.4214	9/16/2022	624.75	10/26/2022	626.27	5/3/2023	629.1714	10/3/2023	629.17
BB_OW001	1141886.292	1202156.849	654.7256	609.6756	9/16/2022	644.91	10/25/2022	645.95	5/3/2023	649.4056	10/2/2023	647.48
BB_OW002	1145616.164	1197505.971	625.4866	605.4166	9/16/2022	620.41	10/26/2022	620.79	5/3/2023	621.9866	10/3/2023	621.32
BMW712	1132437.07	1194902.84	701.91	681.55	9/16/2022	688.07	10/27/2022	689.38	5/3/2023	689.13	10/2/2023	688.64
BMW715	1132482.7	1194761.51	701.97	656.68	9/16/2022	686.26	10/27/2022	689.16	5/3/2023	690.56	10/2/2023	690.25
BMW717	1132650.51	1194809.56	703.71	667.91	9/16/2022	689.07	10/27/2022	692.92	5/3/2023	694.6	10/2/2023	694.12
BW01006	1138191.153	1202300.012	714.217	650.207	9/16/2022	696.64	10/25/2022	698.95	5/3/2023	704.327	10/3/2023	700.59
BW01008	1140152.035	1202497.242	689.7242	614.7342	9/16/2022	658.43	10/25/2022	660.09	5/5/2023	667.0842	10/2/2023	664.26
BW01009	1139561.328	1203247.29	674.1526	602.1526	9/16/2022	656.70	10/25/2022	657.50	5/3/2023	659.7626	10/2/2023	658.78
BW02001	1122723.666	1194679.199	575.5914	495.5914	9/15/2022	537.24	10/24/2022	538.41	5/2/2023	545.9814	10/2/2023	541.63
BW02002	1122855.159	1195124.299	574.067	464.077	9/15/2022	535.93	10/24/2022	536.61	5/2/2023	544.967	10/2/2023	539.77
BW03001	1126099.627	1190875.429	662.4509	597.9709	9/16/2022	608.77	10/24/2022	621.50	5/2/2023	628.5509	10/3/2023	621.23
BW03002	1124622.104	1192503.328	612.7567	552.7467	9/16/2022	609.96	10/25/2022	610.98	5/2/2023	613.5067	10/3/2023	613.85
BW05008	1132656.556	1191999.764	672.325	587.325	9/15/2022	660.19	10/24/2022	662.46	5/2/2023	664.235	10/3/2023	662.71
BW05009	1132590.578	1191565.4	674.518	590.408	9/15/2022	659.79	10/24/2022	661.93	5/3/2023	663.698	10/3/2023	662.24
BW05010	1131821.664	1191011.966	680.1348	590.4648	9/15/2022	659.18	10/24/2022	662.78	5/3/2023	663.8148	10/2/2023	662.23
BW05011D	1130563.542	1188588.148	641.681	362.691	9/16/2022	603.94	10/24/2022	612.39	5/2/2023	611.841	10/2/2023	609.93
BW06005	1134959.2	1188108.7	668.47	564	9/15/2022	645.93	10/26/2022	648.77	5/1/2023	654.96	10/3/2023	652.22
BW06006	1134964.19	1188219.132	665.7799	595.7699	9/15/2022	634.54	10/26/2022	636.37	5/1/2023	643.9399	10/3/2023	640.64
BW06007	1134972.94	1188004.736	669.0974	595.0774	9/15/2022	645.87	10/26/2022	648.73	5/1/2023	654.8874	10/3/2023	652.22
BW06008	1135400.027	1188078.387	662.4476	602.9676	9/15/2022	651.77	10/26/2022	653.52	5/2/2023	658.6776	10/3/2023	656.98
BW07001	1136511.176	1195370.412	719.6177	664.4977	9/15/2022	698.19	10/26/2022	699.81	5/2/2023	705.4977	10/3/2023	704.20
BW07002	1136596.162	1195093.802	718.0649	664.4649	9/15/2022	698.23	10/26/2022	699.90	5/2/2023	705.5449	10/3/2023	704.21
BW07003	1136175.058	1194962.571	707.3769	657.6769	9/15/2022	698.21	10/26/2022	699.85	5/2/2023	705.4169	10/3/2023	704.13
BW08003	1136490.992	1194107.462	720.8084	616.2084	9/15/2022	692.21	10/26/2022	693.14	5/2/2023	702.3284	10/3/2023	700.41
BW10006	1135688.52	1198565.12	735.26	637.34	9/15/2022	715.02	10/25/2022	715.43	5/2/2023	721.92	10/3/2023	720.28
BW10007	1136268.235	1199053.293	735.5791	650.5091	9/15/2022	717.84	10/25/2022	718.15	5/1/2023	726.3391	10/3/2023	724.11
BW12005	1133063.048	1196841.719	718.22	660.99	9/15/2022	706.99	10/26/2022	708.40	5/3/2023	712.5	10/2/2023	711.59
BW12006	1133030.341	1197014.026	719.3843	654.8443	9/15/2022	707.19	10/26/2022	708.72	5/3/2023	712.7843	10/2/2023	711.95
BW13002	1132830.986	1198392.394	754.0023	693.9923	9/15/2022	741.56	10/26/2022	745.99	5/3/2023	745.8423	10/2/2023	743.76
BW14005	1135493.27	1199409.38	739.2	660.75	9/15/2022	718.59	10/25/2022	719.11	5/2/2023	727.5	10/3/2023	725.29
BW16001	1138831.25	1189595.522	698.2277	593.7177	9/16/2022	679.08	10/26/2022	678.44	5/1/2023	686.2277	10/2/2023	684.47
BW16002	1135310.904	1189058.165	646.3581	546.3281	9/15/2022	634.03	10/26/2022	634.03	5/2/2023	643.1081	10/3/2023	641.58
BW17004	1135216.56	1200020.87	742.38	677.09	9/15/2022	718.64	10/25/2022	720.00	5/2/2023	727.6	10/3/2023	725.40
BW17005	1135934.493	1200777.28	741.1892	681.0692	9/15/2022	718.45	10/25/2022	718.75	5/1/2023	727.6192	10/3/2023	725.29
BW17006	1135389.238	1200842.176	752.5489	682.5589	9/15/2022	718.77	10/25/2022	719.08	5/1/2023	727.9389	10/3/2023	725.50
BW18003	1137326.043	1202714.059	725.4564	689.6164	9/15/2022	701.46	10/25/2022	703.66	5/3/2023	711.1464	10/3/2023	708.65
BW18004	1138150.635	1200006.045	748.4496	598.4896	9/15/2022	715.68	10/25/2022	716.36	5/2/2023	722.4696	10/3/2023	720.65
BW18006	1138170.487	1197499.7	732.8254	673.6654	9/15/2022	706.76	10/26/2022	706.88	5/1/2023	712.7354	10/3/2023	711.20
BW18007	1140520.874	1194864.072	734.6432	655.6332	9/15/2022	703.85	10/26/2022	706.92	5/3/2023	718.5432	10/3/2023	713.08
BW18008	1140428.358	1192378.903	734.6482	678.8782	9/15/2022	698.79	10/26/2022	701.82	5/3/2023	705.6282	10/3/2023	703.96
BW18009	1139657.77	1191749.012	738.8147	683.7647	9/15/2022	715.94	10/26/2022	719.14	5/3/2023	721.2447	10/3/2023	719.77
BW18010	1138175.204	1191826.244	737.7521	673.7421	9/15/2022	704.24	10/27/2022	710.40	5/3/2023	712.5821	10/3/2023	706.30
BW20001	1138969.899	1203913.859	683.0483	612.9983	9/16/2022	657.61	10/25/2022	648.32	5/3/2023	661.8483	10/3/2023	660.09
BW20002	1139196.916	1204209.203	684.6468	614.6668	9/16/2022	657.03	10/25/2022	657.86	5/3/2023	661.5168	10/3/2023	659.80
BW22001	1127472.398	1185389.333	542.9267	458.9267	9/15/2022	539.45	10/25/2022	540.38	5/2/2023	542.1767	10/2/2023	541.18
CMW2014	1138040.94	1201222.66	740.4	704.43	9/15/2022	717.06	10/25/2022	717.86	5/3/2023	724.07	10/3/2023	722.16
EBGB_BW001	1127875.362	1186703.975	572.5019	487.8819	9/15/2022	553.70	10/25/2022	513.79	5/2/2023	556.2819	10/2/2023	554.74
EBGB_BW002	1127098.709	1184867.399	559.1927	454.5827	9/15/2022	526.10	10/25/2022	490.13	5/2/2023	528.4027	10/2/2023	527.49
EBGB_OW002	1127098.82	1184863.443	559.4624	504.8124	9/15/2022	535.17	10/25/2022	536.54	5/2/2023	537.3524	10/2/2023	536.62
FMW3410	1135496.01	1201644.06	757.6	694.01	9/15/2022	714.61	10/25/2022	714.97	5/2/2023	723.98	10/3/2023	721.57
GC_BW001	1129541.886	1197222.27	724.1078	609.3078	9/16/2022	702.98	10/26/2022	702.86	5/3/2023	702.3578	10/3/2023	707.87
GC_BW002D	1129487.196	1195246.799	684.0377	489.0577	9/15/2022	670.39	10/26/2022	671.14	5/3/2023	674.3677	10/3/2023	673.30
GC_BW002S	1129487.196	1195246.799	684.0377	542.0577	9/15/2022	671.25	10/26/2022	672.44	5/3/2023	676.1877	10/3/2023	674.96
JBW7101	1134758.23	1188878.64	649.36	556.93	9/15/2022	631.72	10/26/2022	631.76	5/2/2023	635.67	10/3/2023	634.74
JBW7102	1135937.99	1188017.45	663.78	626.4	9/16/2022	655.23	10/26/2022	655.14	5/2/2023	659.73	10/3/2023	659.27
JBW7106B	1132631.83	1186997.03	615.84	550.28	9/15/2022	604.45	10/25/2022	603.45	5/2/2023	609.65	10/3/2023	607.76
JBW7107	1131579.183	1187073.18	601.4830614	553.4330614	Not Collected	Not Collected	Not Collected	Not Collected	5/2/2023	598.9430614	10/2/2023	597.58
JBW7203B	1134816.96	1189526.35	641.53	588.2	9/15/2022	633.67	10/26/2022	633.68	5/1/2023	639.43	10/3/2023	638.41
JBW7212A	1135955.25	1189775.6	666.36	471.74	9/17/2022	637.64	10/27/2022	644.50	5/2/2023	651.1	10/3/2023	645.71
JBW7215B	1136031.02	1190714.98	688.76	610.55	9/16/2022	643.67	10/27/2022	650.47	5/2/2023	651.22	10/3/2023	649.58
JBW7304	1135551.825	1190954.031	682	558.87	9/16/2022	644.05	10/27/2022	645.63	5/2/2023	654.03	10/3/2023	651.17
JBW7305	1134311.238	1192810.219	681.1183236	554.3183236	Not Collected	Not Collected	Not Collected	Not Collected	5/1/2023	668.7983236	10/3/2023	668.18
JBW7314	1134088.356	1194288.761	712	591.1	9/16/2022	689.92	10/25/2022	694.22	5/1/2023	694.74	10/3/2023	693.18
JBW7316	1137526.21	1193724.613	732	611.23	9/16/2022	704.30	10/26/2022	709.10	5/1/2023	713.07	10/3/2023	710.42

Table N-3
Well Construction Information and Water Levels

Groundwater Model Development Report
Former Loring Air Force Base, Limestone, Maine

	X	Y	Z (Ground)	BOW elev	September 2022		October 2022		May 2023		October 2023	
Location_ID	m	m	ft amsl	ft amsl	Date	GW Elev ft amsl	Date	GW Elev ft amsl	Date	GW Elev ft amsl	Date	GW Elev ft amsl
JBW7317	1137269.97	1194756.07	728.74	691.71	9/15/2022	693.39	10/26/2022	694.24	5/1/2023	702.23	10/3/2023	700.07
JBW7327	1135480.642	1192710.493	693.182229	182.482229	Not Collected	Not Collected	Not Collected	Not Collected	5/1/2023	668.392229	10/3/2023	668.11
JBW7328	1135956.71	1194208.45	721.78	682.08	9/15/2022	693.75	10/26/2022	694.30	5/2/2023	698.11	10/3/2023	696.81
JBW7338A	1136225.889	1192476.32	710	514.2	9/16/2022	672.56	10/26/2022	674.90	5/2/2023	681.08	10/3/2023	678.94
JBW7339A	1136008.63	1193911.74	723.68	555.08	9/15/2022	691.19	10/26/2022	692.38	5/2/2023	699.53	10/3/2023	697.16
JBW7340B	1136014.75	1192606.77	706.68	656.53	9/16/2022	678.02	10/26/2022	679.83	5/2/2023	684.47	10/3/2023	683.31
JBW7341A	1136234.69	1193792.71	722.71	595.96	9/15/2022	692.60	10/26/2022	693.47	5/2/2023	702.42	10/3/2023	700.61
JBW7344	1136525.66	1193154.82	722.55	682.26	9/16/2022	682.26	10/26/2022	696.34	5/1/2023	699.91	10/3/2023	698.74
JBW7345A	1136061.24	1193231.5	712.39	619.61	9/16/2022	685.32	10/26/2022	689.28	5/2/2023	692.32	10/3/2023	691.09
JBW7347B	1135775.91	1194004.09	712.24	679.15	9/15/2022	687.98	10/26/2022	681.87	5/1/2023	694.82	10/3/2023	693.30
JBW7348	1136264.089	1193446.678	721.6448	670.1348	9/16/2022	685.37	10/26/2022	686.41	5/2/2023	693.6448	10/3/2023	692.06
JBW7350	1136765.97	1193766.85	725.44	672.16	9/16/2022	692.21	10/26/2022	693.36	5/1/2023	676.44	10/3/2023	701.26
JBW7403	1140669.506	1188899.794	724.55	643	9/15/2022	687.93	10/26/2022	689.57	5/2/2023	701.51	10/3/2023	696.87
JBW7607	1132235.11	1194189.54	674.27	631.36	9/15/2022	661.44	10/27/2022	663.13	5/3/2023	664.55	10/3/2023	663.34
JBW7613	1132992.05	1195581.04	716.61	615.76	9/15/2022	702.46	10/26/2022	704.77	5/2/2023	709.47	10/2/2023	708.14
JBW7614	1132805.915	1194122.398	690.27	626.33	9/15/2022	664.20	10/25/2022	666.96	5/2/2023	667.31	10/3/2023	665.84
JBW7617A	1132235.18	1194189.522	668.87	468.9	9/16/2022	659.36	10/27/2022	660.06	5/3/2023	661.74	10/3/2023	660.69
JBW7617B	1131648.04	1193943.03	668.87	612.7	9/16/2022	659.15	10/27/2022	659.90	5/3/2023	661.53	10/3/2023	660.41
JBW7710	1134921.86	1194865.85	707.89	652.58	9/16/2022	696.31	10/25/2022	697.38	5/3/2023	701.11	10/3/2023	699.77
JBW7711	1134106.69	1199744.11	749.71	654.06	9/15/2022	720.73	10/25/2022	721.27	5/3/2023	729.75	10/3/2023	727.66
JBW7714	1134396.936	1198555.912	744	651.01	9/15/2022	718.38	10/25/2022	719.84	5/3/2023	722.57	10/3/2023	722.34
JBW7725	1134303.37	1196818.92	728.48	697.54	9/16/2022	710.09	10/26/2022	711.27	5/3/2023	714.76	10/3/2023	713.88
JBW7734	1133128.53	1196564.63	719.96	666.48	9/15/2022	705.71	10/26/2022	706.90	5/3/2023	710.49	10/2/2023	709.48
JBW7737A	1132521.65	1195846.67	701.02	497.97	9/15/2022	692.04	10/26/2022	694.19	5/2/2023	699.31	10/2/2023	698.61
JBW7738A	1131802.03	1195404.64	675.16	575.11	9/16/2022	670.62	10/26/2022	670.87	Not Collected	Not Collected	10/2/2023	673.29
JBW7738B	1131805.09	1195404.63	675.16	606.28	9/16/2022	670.42	10/26/2022	670.88	5/3/2023	673.53	10/2/2023	672.96
JBW7753A	1132983.27	1195789.59	721.29	686.32	9/15/2022	696.30	10/26/2022	699.61	5/2/2023	707.59	10/2/2023	706.39
JBW7806	1131713.19	1199095.21	716.26	683.9	9/16/2022	704.00	10/26/2022	704.83	5/3/2023	710.29	10/2/2023	708.73
JBW7816R	1132465.052	1199647.058	742	678.45	9/15/2022	730.80	10/26/2022	730.45	5/3/2023	731.32	10/3/2023	731.30
JBW7912	1134973.17	1201998.91	762.81	550.69	9/15/2022	720.46	10/25/2022	720.59	5/2/2023	729.87	10/3/2023	727.42
JBW8008	1139531.41	1201754.02	719.51	576.59	9/16/2022	702.87	10/25/2022	703.74	5/3/2023	706.46	10/3/2023	705.24
JBW8009	1137204.24	1200937.33	740.76	686.8	9/15/2022	719.17	10/25/2022	719.88	5/1/2023	726.6	10/3/2023	724.52
JEBS-5	1136248.34	1193023.26	719.87	665.74	9/16/2022	683.89	10/26/2022	681.39	5/2/2023	689.88	10/3/2023	687.83
JMW0201R	1132395.24	1199616.95	740.22	666.03	9/15/2022	705.13	10/26/2022	705.49	5/3/2023	705.98	10/3/2023	705.87
JMW-0406	1134603.96	1196636.07	723	706.33	9/16/2022	706.94	10/26/2022	714.53	5/3/2023	711.3	10/3/2023	710.33
JMW-0407	1135191.368	1198252.707	734.5	708.99	9/15/2022	715.37	10/25/2022	716.13	5/1/2023	730.97	10/3/2023	720.80
JMW-0416B	1135340.29	1196471.901	718	700.9	Not Collected	Not Collected	Not Collected	Not Collected	5/3/2023	711.61	10/3/2023	710.48
JMW0445	1135146.968	1197371.14	726.1216	703.5116	9/15/2022	709.85	10/25/2022	710.48	5/1/2023	715.7516	10/3/2023	714.40
JMW-0503	1136342.826	1194253.891	721	645.51	9/15/2022	694.71	10/26/2022	695.79	5/2/2023	702.03	10/3/2023	700.42
JMW-0505	1136431.493	1194156.069	720.2	690.41	9/15/2022	692.57	10/26/2022	693.43	5/2/2023	702.34	10/3/2023	700.39
JMW0542	1135204.73	1191610.33	677.26	658.55	9/16/2022	662.36	10/25/2022	663.26	5/2/2023	664.81	10/3/2023	663.96
JMW-0603	1137429.789	1188951.588	678.8	632.35	9/17/2022	678.91	10/26/2022	674.12	5/1/2023	679.65	10/2/2023	679.65
JMW-0604	1138270.487	1188791.209	693.6	604.55	9/16/2022	680.96	10/26/2022	679.20	5/1/2023	681.65	10/2/2023	683.16
JMW-0605	1137693.155	1189801.755	698	675.7	9/17/2022	675.90	10/26/2022	675.62	5/1/2023	695.36	10/2/2023	681.40
JMW-0606	1137277.292	1189538.816	685.4	664.76	9/17/2022	666.94	Not Collected	Not Collected	5/1/2023	675.53	10/2/2023	674.83
JMW0640	1137158.47	1189718.78	692.5	655.35	9/17/2022	663.98	10/26/2022	662.73	5/2/2023	671.35	10/2/2023	670.33
JMW0682	1137520.535	1190181.189	702	600.89	9/17/2022	670.81	Not Collected	Not Collected	5/1/2023	678.2	10/2/2023	676.09
JMW0683	1137343.166	1189272.091	682.91	639.36	9/17/2022	666.61	10/26/2022	665.21	5/1/2023	673.67	10/2/2023	676.98
JMW0685	1137508.99	1189719.92	697.07	653.89	9/17/2022	676.34	10/26/2022	673.23	5/1/2023	681.37	10/2/2023	679.47
JMW-0701	1132393.395	1194976.28	698	669.73	9/16/2022	686.02	10/26/2022	685.65	5/3/2023	686.62	10/2/2023	686.30
JMW-0804	1123999.415	1194678.803	602.9	583.95	9/15/2022	583.95	10/24/2022	584.51	5/2/2023	585.267	10/2/2023	583.95
JMW-0806	1123801.831	1194358.368	607.7	543.54	9/15/2022	552.91	10/24/2022	553.85	5/2/2023	559.5	10/2/2023	556.41
JMW0880	1124499.67	1193821.05	632.45	585	9/15/2022	588.01	10/25/2022	589.86	5/2/2023	595.53	10/2/2023	593.12
JMW0882	1124470.61	1194192.68	606.09	555.04	9/15/2022	561.11	10/25/2022	560.60	5/2/2023	565.7	10/2/2023	564.62
JMW0891	1123555.31	1195068.04	589.96	539.34	9/15/2022	539.34	10/24/2022	539.34	5/2/2023	545.58	10/2/2023	539.34
JMW-0903	1126492.1	1193111.1	644.3	624.8	9/16/2022	624.80	10/26/2022	625.81	5/2/2023	633.27	10/3/2023	627.97
JMW0941	1125106.02	1191554.92	644.1	593.19	9/16/2022	602.72	10/24/2022	603.18	5/2/2023	608.66	10/3/2023	606.49
JMW0960	1125733.35	1192154.27	617.8	597.61	9/15/2022	602.66	10/25/2022	605.03	5/2/2023	606.22	10/3/2023	603.26
JMW0961	1125422.53	1192449.4	611.49	596.94	9/15/2022	604.50	10/25/2022	605.04	5/2/2023	608.91	10/3/2023	607.51
JMW0980	1125542.32	1191784.64	658	596.13	9/16/2022	603.45	10/24/2022	603.17	5/2/2023	609.08	10/3/2023	607.44
JMW0982	1125043.01	1192445.85	631.25	601.31	9/15/2022	601.78	10/25/2022	603.12	5/2/2023	607.28	10/3/2023	606.97
JMW0991	1126845.3	1191182.93	638.32	583.05	9/15/2022	599.60	10/24/2022	599.65	5/2/2023	602.19	10/2/2023	601.33
JMW1103D	1138461.72	1201681.33	729.94	684.82	9/16/2022	710.03	10/25/2022	711.63	5/3/2023	714.46	10/3/2023	713.41
JMW1380	1140554.03	1202758.68	677.21	620.2	9/16/2022	658.55	10/25/2022	659.80	5/3/2023	664.24	10/3/2023	662.53
JMW1564	1136531.65	1194553.18	717.92	684	9/15/2022	697.53	10/26/2022	698.54	5/2/2023	701.1	10/3/2023	700.44
JMW1565	1136727.78	1194585.04	722	677.54	9/15/2022	696.43	10/26/2022	698.44	5/2/2023	704.82	10/3/2023	702.52
JMW1665	1137012.972	1193418.117	730	692.22	9/16/2022	697.86	Not Collected	Not Collected	5/2/2023	706.78	10/3/2023	705.16
JMW1684	1136583.03	1193438.51	723.51	680.19	Not Collected	Not Collected	Not Collected	Not Collected	5/2/2023	701.86	10/3/2023	699.67
JMW1762	1135617.921	1191711.793	682	649.46	9/16/2022	659.54	10/26/2022	661.16	5/2/2023	665.17	10/3/2023	663.92
JMW1860	1135626.55	1188212.45	659.73	632.53	9/15/2022	653.91	10/26/2022	655.43	5/1/2023	660.17	10/3/2023	658.78
JMW1881	1135555.12	1188471.14	655.53	604.81	9/15/2022	650.39	10/26/2022	651.75	5/1/2023	656.85	10/3/2023	655.30
JMW1960	1135390	1189781.07	656.03	621.04	9/17/2022	635.73	10/27/2022	635.66	5/2/2023	645.24	10/3/2023	643.51
JMW1964	1135497.65	1190170.93	659.41	621.98	9/17/2022	636.19	10/27/2022	636.23	5/2/2023	645.81	10/3/2023	644.44
JMW1981	1135233.789	1190105.189	655	603.72	Not Collected	Not Collected	10/26/2022	634.25	5/1/2023	643.29	10/3/2023	642.10
JMW1982	1135222.269	1189412.66	647.8333	602.6433	9/15/2022	634.46	10/26/2022	634.26	5/1/2023	642.6133	10/3/2023	641.29
JMW2680	1141663.13	1203271.81	668.7	642.865	9/17/2022	651.13	10/25/2022	653.53	5/3/2023	654.245	10/3/2023	653.04
JMW3102	1134609.96	1191073.73	652.01	631.93	9/17/2022	647.16	10/25/2022	647.63	5/2/2023	648.34	10/3/2023	648.07
JMW3202	1136282.28	1192871.68	714.09	668.02	9/16/2022	681.21	10/26/2022	685.03	5/2/2023	690.53	10/3/2023	688.20
JMW3203	1136224.93	1192767.9	711.11	665.31	9/16/2022	678.43	10/26/2022	682.11	5/2/2023	687.5	10/3/2023	685.41
JMW3284	1136178.51	1192689.53	712.21	668.33	9/16/2022	679.99	10/26/2022	684.99	5/2/2023	689.97	10/3/2023	688.18
JMW3285	1136145.07	1192837.35	712.51	609.72	9/16/2022	678.18	10/26/2022	680.15	5/2/2023	686.01	10/3/2023	684.53
JMW3501	1136488.72	1190173.155	688	603.78	9/16/2022	658.23	10/26/2022	658.78	5/2/2023	660.98	10/2/2023	661.19
JMW35X2	1136531.4	1189497.31	673.59	636.675	9/16/2022	654.00	10/26/2022	652.61	5/2/2023	662.025	10/2/2023	660.17
JMW3601	1135824.01	1190571.97	676.12	628.3	9/16/2022	647.25	10/27/2022	644.17	5/2/2023	657.37	10/3/2023	648.74
JMW6105	1132920.64	1195946.69	717.77	698.86	9/15/2022	702.30	10/26/2022	702.98	5/2/2023	707.07	10/3/2023	706.14

Table N-3
Well Construction Information and Water Levels

Groundwater Model Development Report
Former Loring Air Force Base, Limestone, Maine

					September 2022		October 2022		May 2023		October 2023	
Location_ID	X m	Y m	Z (Ground) ft amsl	BOW elev ft amsl	Date	GW Elev ft amsl	Date	GW Elev ft amsl	Date	GW Elev ft amsl	Date	GW Elev ft amsl
JMW7113	1131175.25	1186718.04	594.01	581.47	9/15/2022	588.83	10/25/2022	581.47	5/2/2023	591.8	10/2/2023	589.84
JMW7322	1134058.66	1190590.94	647.11	630.9	9/15/2022	644.48	10/26/2022	644.93	5/2/2023	645.52	10/2/2023	645.35
JMW7611	1132117.92	1195281.82	688.66	655.93	9/16/2022	676.99	10/26/2022	677.98	5/3/2023	678.8	10/2/2023	680.63
JMW7612	1131968.67	1194958.99	673.29	656.87	9/16/2022	671.75	10/26/2022	671.80	5/3/2023	672.83	10/2/2023	672.21
JMW7913	1135696.66	1201505.704	748.5407	724.5707	9/15/2022	734.47	10/25/2022	738.05	5/2/2023	739.5107	10/3/2023	737.71
JMW8011	1139510.68	1202891.29	686.51	642.63	9/16/2022	661.54	10/25/2022	662.56	5/3/2023	666.4	10/3/2023	665.08
JPZ0341	1135063.4	1193102.11	672.63	663.49	9/15/2022	667.33	10/26/2022	667.56	5/2/2023	668.12	10/3/2023	667.93
JPZ0342	1134984.4	1193239.35	672.18	634.81	9/16/2022	671.87	10/26/2022	672.91	5/2/2023	672.69	10/3/2023	674.83
JPZ0348	1134820.87	1191270	666.6	617.09	9/17/2022	654.99	10/25/2022	656.35	5/2/2023	659.05	10/3/2023	658.20
JPZ0349	1134826.67	1191278	666.63	636.57	9/17/2022	653.80	10/25/2022	654.61	5/2/2023	655.92	10/3/2023	655.50
JPZ0606	1138419.9	1189324.8	694	686.62	9/16/2022	687.99	Not Collected	Not Collected	5/1/2023	686.62	10/2/2023	693.54
JPZ0680	1137801.66	1189451.26	690.73	681.5	9/17/2022	683.13	10/26/2022	686.69	5/1/2023	690.5	10/5/2023	688.50
JPZ0683	1137959.99	1189785.25	700.58	686.94	9/17/2022	694.26	10/26/2022	697.35	5/1/2023	698.04	10/2/2023	696.94
JPZ0685	1137472.07	1189130.06	683.48	674.1	9/17/2022	679.35	10/26/2022	679.65	5/1/2023	682.76	10/2/2023	682.48
JPZ0686	1138219.87	1189641.94	696.51	667.58	9/16/2022	679.19	10/26/2022	678.63	5/1/2023	686.61	10/2/2023	684.68
JPZ1184R	1138007.23	1201390.51	737.5	706.27	9/15/2022	717.97	10/25/2022	718.89	5/3/2023	724.23	10/3/2023	722.66
JPZ1187	1138855.24	1201798.1	733.87	696.5	9/16/2022	707.72	10/25/2022	708.38	5/3/2023	709.97	10/3/2023	708.94
JPZ1360	1139913.07	1202916.12	681.3	628.99	9/17/2022	659.42	10/25/2022	660.47	5/3/2023	663.35	10/3/2023	662.34
JPZ1382	1140146.39	1202958.91	684	653.7	9/17/2022	661.48	10/25/2022	661.69	5/3/2023	667.96	10/3/2023	665.93
JPZ1780	1135289.97	1192032.61	676.97	647.83	9/16/2022	660.35	10/26/2022	661.83	5/1/2023	666.05	10/3/2023	664.99
JPZ1781	1135691.35	1192117.34	694.33	654.06	Not Collected	Not Collected	10/26/2022	663.66	5/2/2023	668.44	10/3/2023	667.11
JPZ7208	1134560.07	1189198.56	632.52	619.53	9/15/2022	628.07	10/26/2022	628.16	5/2/2023	628.69	10/3/2023	628.41
JPZ7312	1134997.89	1194609.41	698.02	681.77	9/16/2022	691.28	10/26/2022	692.24	5/3/2023	694.06	10/3/2023	693.97
JPZ7601	1131742.58	1195131.61	677.75	662.55	9/16/2022	669.72	10/26/2022	670.63	5/3/2023	670.99	10/2/2023	670.24
JPZ7602	1131721.493	1195105.439	678.11	631.09	9/16/2022	661.97	10/26/2022	662.54	5/3/2023	663.64	10/2/2023	663.01
JPZ7603	1132555.08	1195109.92	699.21	663.04	9/16/2022	694.13	10/26/2022	697.37	5/3/2023	700.43	10/2/2023	699.92
JPZ7704	1135139.117	1195800.476	711.6522	501.9022	9/15/2022	706.55	10/26/2022	706.84	5/3/2023	710.5322	10/3/2023	709.52
JPZ7739	1131799.4	1195398.57	674.81	662.18	9/16/2022	672.29	10/26/2022	672.83	5/3/2023	673.12	10/2/2023	672.73
JPZ7808	1131552.258	1198976.157	704	689.45	9/16/2022	699.99	10/26/2022	701.03	5/3/2023	702.39	10/2/2023	702.34
JPZ7901	1135124.29	1202261.56	762.51	692.73	9/15/2022	719.37	10/25/2022	719.83	5/2/2023	728.68	10/3/2023	726.19
LF2MW2	1124917.91	1194064.72	626.74	576.05	9/15/2022	591.88	10/24/2022	593.73	5/2/2023	600.75	10/2/2023	597.48
LF2MW4	1123563.84	1194784.21	595.52	527.18	9/15/2022	537.93	10/24/2022	538.78	5/2/2023	549.15	10/2/2023	543.10
LF2MW6	1123771.19	1194660.51	611.3	525.45	9/15/2022	543.65	10/24/2022	546.11	5/2/2023	553.91	10/2/2023	548.26
LF3MW2	1124940.75	1192716.66	610.23	602.27	9/15/2022	604.97	10/25/2022	605.97	5/2/2023	608.2	10/3/2023	607.33
LF3MW3	1126473.84	1191354.96	628.76	561.26	Not Collected	Not Collected	Not Collected	Not Collected	5/2/2023	607.34	10/3/2023	606.13
MMW0002	1126939.605	1190857.492	638.4938	593.5838	9/15/2022	599.27	10/24/2022	599.19	5/2/2023	601.4138	10/2/2023	600.81
MMW0003	1131702.64	1193470.27	669.78	624.63	9/15/2022	659.52	10/25/2022	660.88	5/3/2023	661.95	10/3/2023	660.93
MMW0005	1136225.35	1194416.02	720.37	677.82	9/16/2022	695.84	10/26/2022	697.09	5/2/2023	691.98	10/3/2023	700.41
MMW0006	1131331.64	1193789.1	658.94	615.49	9/15/2022	658.91	10/25/2022	659.94	5/3/2023	659.94	10/3/2023	659.94
MMW0008	1132457.91	1187272.99	600	586.685	9/15/2022	601.06	10/25/2022	600.62	5/2/2023	602.845	10/2/2023	602.85
MMW0009	1131326.75	1198453.96	702.77	653.52	9/16/2022	703.25	10/26/2022	704.13	5/3/2023	705.52	10/2/2023	705.52
MMW0010	1133768.25	1188597.92	620.06	546.48	9/15/2022	620.52	10/25/2022	620.58	5/3/2023	620.58	10/2/2023	620.58
MMW0013	1134427.67	1189422.83	631.32	598.81	9/15/2022	631.73	10/25/2022	630.88	5/5/2023	633.73	10/3/2023	633.73
MMW0015	1126936.69	1190475.69	646.56	595.63	9/15/2022	607.02	10/24/2022	608.69	5/2/2023	611.57	10/2/2023	609.85
MMW0016	1134336.57	1188917.25	622.93	603.09	9/16/2022	625.11	10/27/2022	625.11	5/3/2023	624.92	10/3/2023	625.11
MMW0017	1133686.75	1188119.62	623.46	598.92	9/15/2022	626.17	10/25/2022	626.17	5/2/2023	626.17	10/3/2023	626.17
MMW0018A	1127389.85	1190616.21	637.16	542.6	9/15/2022	599.25	10/24/2022	599.51	5/2/2023	600.44	10/2/2023	600.65
MMW0019	1132519.23	1187069.28	603.92	593.28	9/15/2022	600.33	10/25/2022	599.83	5/2/2023	601.95	10/3/2023	600.97
MMW0020	1130585.499	1197734.531	714.7223534	559.7023534	Not Collected	Not Collected	Not Collected	Not Collected	5/3/2023	710.5723534	10/3/2023	707.93
MMW0124	1135615.29	1190389.26	667.7	626.39	9/16/2022	642.01	10/27/2022	642.52	5/2/2023	650.5	10/3/2023	647.81
MMW0125R	1135777.26	1190483.24	672.4	629.71	9/17/2022	642.94	10/27/2022	643.70	5/2/2023	650.27	10/3/2023	648.66
MMW0127	1132509	1187173.35	599	558.51	9/15/2022	601.51	Not Collected	Not Collected	5/2/2023	601.51	10/3/2023	601.51
MMW0128	1135907.9	1191539.45	689.8	680.97	9/16/2022	682.52	10/26/2022	684.81	5/2/2023	685.12	10/3/2023	684.59
MMW0326	1131175.02	1193877	657.4	599.35	9/15/2022	659.56	10/25/2022	660.55	5/3/2023	661.35	10/3/2023	660.55
MMW0422	1131297.25	1197781.31	702	635.3	9/16/2022	703.36	10/26/2022	704.30	5/3/2023	705.1	10/3/2023	705.10
MMW0531	1135597.27	1201948.1	752.9	593.09	9/15/2022	719.86	10/25/2022	720.37	5/2/2023	728.87	10/3/2023	726.64
MMW1560	1136543.97	1194698.62	716.99	695.73	9/15/2022	697.13	10/26/2022	696.81	5/2/2023	701.89	10/3/2023	702.61
MMW3414	1135021.3	1202100.3	762.4	712.11	9/15/2022	720.12	10/25/2022	720.45	5/2/2023	729.45	10/3/2023	727.16
MMW7330	1135672.72	1192334.15	697.2	572.35	9/16/2022	662.86	10/26/2022	665.67	5/2/2023	669.33	10/3/2023	667.83
NP_BW001S	1146091.315	1190109.497	608.3013	476.2813	9/16/2022	599.67	10/26/2022	599.10	5/3/2023	605.6913	10/3/2023	604.45
OW01002	1138674.627	1201916.801	724.4584	699.4784	9/16/2022	704.45	10/25/2022	705.20	5/3/2023	705.6384	10/3/2023	705.47
OW01003	1139915.878	1203056.337	676.247	649.947	9/17/2022	660.29	10/25/2022	659.02	5/3/2023	664.397	10/3/2023	662.78
OW01004	1139579.309	1203226.164	674.3221	631.2821	9/16/2022	656.95	10/25/2022	657.28	5/3/2023	659.7821	10/2/2023	658.95
OW02001	1122715.378	1194675.011	575.4857	545.4757	9/15/2022	545.48	10/24/2022	546.70	5/2/2023	551.1957	10/2/2023	549.55
OW02002	1122874.082	1195133.559	574.4512	534.3642	9/15/2022	535.88	10/24/2022	536.57	5/2/2023	545.1142	10/2/2023	539.95
OW05004	1132204.939	1191737.876	677.797	657.907	9/15/2022	660.31	10/24/2022	662.95	5/3/2023	664.467	10/3/2023	662.98
OW07001	1136516.9	1195364.514	719.581	695.031	9/15/2022	698.26	10/26/2022	699.79	5/2/2023	705.571	10/3/2023	704.21
OW07002	1136278.261	1195332.474	718.443	692.463	9/15/2022	698.33	10/26/2022	700.01	5/2/2023	705.553	10/3/2023	704.27
OW07003	1136174.327	1194971.728	707.8419	682.8219	9/15/2022	698.02	10/26/2022	700.15	5/2/2023	704.6919	10/3/2023	703.55
OW08001	1135625.164	1194148.002	704.1301	684.0401	9/15/2022	690.72	10/26/2022	692.17	5/1/2023	694.2601	10/3/2023	693.71
OW08002	1135375.976	1193499.677	693.8533	667.8633	9/15/2022	678.44	10/26/2022	679.42	5/1/2023	682.8333	10/3/2023	681.04
OW10005	1135687.51	1198570.65	735.27	710.13	9/15/2022	728.97	10/25/2022	728.94	5/2/2023	729.63	10/3/2023	729.28
OW10007	1136269.564	1199045.384	735.5996	705.2596	9/15/2022	717.71	10/25/2022	718.05	5/1/2023	726.2396	10/3/2023	724.21
OW12002	1132986.278	1197199.398	720.1836	699.6036	9/15/2022	707.33	10/26/2022	708.74	5/3/2023	713.0336	10/2/2023	712.26
OW14004	1135491.98	1199414.15	739.45	714.65	9/15/2022	730.87	10/25/2022	732.10	5/2/2023	731.33	10/3/2023	732.21
OW16002	1135311.004	1189060.901	646.3416	601.2916	9/15/2022	632.49	10/26/2022	633.21	5/2/2023	640.4416	10/3/2023	639.10
OW17002	1135934.798	1200728.336	741.4448	713.2248	9/15/2022	718.45	10/25/2022	719.14	5/1/2023	727.1948	10/3/2023	724.69
OW17003	1135390.391	1200805.948	752.333	718.903	9/15/2022	726.13	10/25/2022	721.62	5/1/2023	733.553	10/3/2023	727.07
OW19009	1139125.47	1190351.15	703.56	681.86	9/16/2022	684.52	10/26/2022	684.72	5/2/2023	686.52	10/3/2023	686.29
OW19010	1139240.83	1190484.54	705.8	681.03	9/17/2022	700.08	10/27/2022	702.93	5/2/2023	704.44	10/3/2023	703.79
OW20002	1136337.648	1204490.437	731.9858	696.8158	9/15/2022	704.38	10/25/2022	709.39	5/3/2023	719.5458	10/3/2023	712.95
OW20003	1136629.498	1204822.383	723.7707	690.7907	9/15/2022	704.18	10/25/2022	709.17	5/3/2023	716.9807	10/3/2023	712.93
OW20005	1136760.498	1204366.238	719.0466	686.0066	9/15/2022	702.43	10/25/2022	705.17	5/3/2023	708.0566	10/3/2023	707.95
OW20006	1138973.908	1203922.563	683.1416	653.1016	9/16/2022	657.16	10/25/2022	658.02	5/3/2023	661.8216	10/3/2023	659.92
OW20007	1139201.092	1204216.945	684.4562	645.4562	9/16/2022	656.99	10/25/2022	657.80	5/3/2023	661.4262	10/3/2023	659.67

Table **N**-3
Well Construction Information and Water Levels

Groundwater Model Development Report
Former Loring Air Force Base, Limestone, Maine

					September 2022		October 2022		May 2023		October 2023	
	X	Y	Z (Ground)	BOW elev	Date	GW Elev	Date	GW Elev	Date	GW Elev	Date	GW Elev
Location_ID	m	m	ft amsl	ft amsl		ft amsl		ft amsl		ft amsl		ft amsl
OW21005	1134432.84	1191010.03	648.9	635.24	9/17/2022	644.88	10/25/2022	645.41	5/2/2023	645.99	10/3/2023	645.53
OW22003	1127436.781	1185182.429	540.2751	525.2051	9/15/2022	538.90	10/25/2022	538.65	5/2/2023	539.1151	10/2/2023	538.55
OW23001	1134757.264	1189534.763	641.4394	611.4294	9/15/2022	633.01	10/26/2022	633.02	5/1/2023	638.4694	10/3/2023	637.50
OW24001	1134737.259	1201803.63	757.41	719.38	9/15/2022	719.38	10/25/2022	719.63	5/2/2023	728.73	10/3/2023	726.28
RFW0413	1132816.4	1199598.26	781.28	678.78	9/16/2022	743.48	10/26/2022	743.57	5/4/2023	744.25	10/2/2023	743.67
RFW1144	1138287.33	1201531.83	736.56	656.77	9/16/2022	715.96	10/25/2022	717.27	5/3/2023	721.62	10/3/2023	720.15
RFW-3	1124455.796	1194471.222	609.7	518.94	9/15/2022	563.93	10/24/2022	563.64	5/2/2023	570.38	10/2/2023	568.34
RFW-38	1124964.811	1193495.537	606.41	469.66	9/16/2022	593.76	10/25/2022	596.12	5/2/2023	600.35	10/2/2023	599.59
RFW-5	1126607.094	1191026.51	626.8	547.54	9/15/2022	599.26	10/24/2022	600.57	5/2/2023	603.24	10/3/2023	601.95
RFW-8	1124594.084	1192263.432	616.8	608.81	9/16/2022	609.83	10/25/2022	611.26	5/2/2023	614.98	10/3/2023	614.07
SB/OW16001	1137654.97	1189376.51	688.24	673.35	9/17/2022	678.60	10/26/2022	678.07	5/1/2023	685.94	10/2/2023	684.27
SB/OW17001	1135640.43	1200145.53	740.54	711.73	9/15/2022	718.73	10/25/2022	719.05	5/1/2023	727.81	10/3/2023	725.37
UNK-033	1137087.494	1192707.879	729.5	672.44	9/16/2022	691.94	10/26/2022	701.24	5/1/2023	703.18	10/3/2023	699.72
UNK-034	1129711.305	1192558.777	654.5718345	373.6518345	Not Collected	Not Collected	Not Collected	Not Collected	5/2/2023	632.3818345	10/3/2023	631.05
UNK-042	1133741.581	1190194.784	649.9955493	585.8255493	Not Collected	Not Collected	Not Collected	Not Collected	5/2/2023	650.0955493	10/2/2023	649.72
UNK-044	1137033.695	1189328.637	679	655.9	9/16/2022	663.54	10/26/2022	662.10	5/2/2023	670.92	10/2/2023	669.90
UNK-23001	1140253.657	1188583.339	717	704.45	Not Collected	Not Collected	Not Collected	Not Collected	Not Collected	Not Collected	10/3/2023	711.41
UNK-TC01	1137925.759	1191565.441	735	689.51	Not Collected	Not Collected	Not Collected	Not Collected	Not Collected	Not Collected	10/4/2023	707.12
USMW004	1127949.682	1195684.54	678.5684838	651.1884838	Not Collected	Not Collected	Not Collected	Not Collected	5/2/2023	664.7984838	10/3/2023	660.76
USMW005	1127355.25	1195038.56	668.01	651.4	9/16/2022	652.51	10/26/2022	659.24	5/2/2023	660.16	10/3/2023	658.81
USMW006	1127417.154	1195709.27	674.092422	648.812422	Not Collected	Not Collected	Not Collected	Not Collected	5/2/2023	661.332422	10/3/2023	658.25
USMW012	1127002.17	1194062.33	671.27	641.46	9/16/2022	645.80	10/26/2022	651.82	5/2/2023	654.03	10/3/2023	651.02
USMW014	1127151.775	1195623.387	667.6510902	645.4310902	Not Collected	Not Collected	Not Collected	Not Collected	5/2/2023	657.2410902	10/3/2023	654.92
USMW019	1128143.49	1194179.22	673.1470078	632.0070078	Not Collected	Not Collected	Not Collected	Not Collected	5/2/2023	651.7770078	10/3/2023	645.75
USMW024	1126963.086	1195210.131	661.8465926	635.6365926	Not Collected	Not Collected	Not Collected	Not Collected	5/2/2023	653.2365926	10/3/2023	651.58
USMW101	1131419.09	1188551.77	649.05	622.35	9/15/2022	632.94	10/25/2022	637.10	5/2/2023	641.66	10/2/2023	640.15
USMW103	1130536.29	1189032.58	652.44	631.85	9/15/2022	637.36	10/25/2022	641.27	5/2/2023	642.4	10/2/2023	642.16
USMW115	1130156.85	1188690.69	633.5	605.18	9/16/2022	620.50	10/25/2022	621.30	5/2/2023	621.5	10/2/2023	621.27
USMW210	1141684.92	1202507.53	656.1	643.25	9/16/2022	653.29	10/25/2022	654.16	5/5/2023	654.67	10/3/2023	654.46
USMW214	1141039.47	1202082.96	653.5	635.5	9/16/2022	638.99	10/25/2022	641.30	5/3/2023	648.29	10/3/2023	644.02
WBGB_BW001	1129725.741	1192645.758	653.6966	563.6766	9/15/2022	629.36	10/25/2022	631.62	5/3/2023	633.1366	10/3/2023	631.72
WBGB_OW001	1129719.111	1192606.287	653.6966	633.6966	9/15/2022	634.53	10/25/2022	634.59	5/3/2023	634.9366	10/3/2023	634.84

Notes
Elev - Elevation
ft amsl - Feet above mean sea level
GW - Groundwater
ID - Identification
m - Meters

Table **N**-4
Model Calibration Water Level Targets

Groundwater Model Development Report
Former Loring Air Force Base, Limestone, Maine

	X	Y	Z (Ground)	BOW elev	Model Layer	Target elev
Location ID	m	m	ft amsl	ft amsl		ft amsl
043-MW03	1128625.91	1188010.68	598.26	573.31	1	730.470
044-RW01	1138790.93	1200027.56	752.91	723.47	2	688.605
051-MW03	1140546.74	1190335.81	706.69	702.39	1	664.588
056-MW02	1136146.11	1191699.8	700.24	676.94	2	744.195
056-MW03	1136194.5	1191503.77	699.84	685.6	2	703.838
056MW04	1136006.62	1191661.79	697	678.84	3	709.625
056MW06	1136060.74	1191491.03	694.9	646.87	2	654.765
059-MW03	1146002.49	1205475.13	756.72	730.52	3	700.264
AA07MW-01	1136564.15	1195074.81	720.44	700.92	1	648.316
AA18MW-01	1137614.12	1195186.69	729.2	671.52	2	627.341
AA18MW-02	1137671.36	1197490.62	739.81	688.36	2	689.058
AA19MW-01	1139589.47	1190472.62	707	687.35	1	692.678
AA19MW-02	1139346.38	1190362.15	706.32	687.24	1	700.125
AR25	1135037.39	1191021.85	672.17	515.19	3	662.469
ASMW101	1137076.297	1191243.63	724.6313	693.8613	3	658.188
ASMW301	1136642.79	1194797.76	718.72	695.34	1	540.817
BB_BW001	1141889.361	1202159.997	654.8112	584.8112	2	539.317
BB_BW002	1145613.906	1197508.076	625.7414	556.4214	3	620.014
BB_OW001	1141886.292	1202156.849	654.7256	609.6756	1	612.072
BB_OW002	1145616.164	1197505.971	625.4866	605.4166	1	662.395
BMW712	1132437.07	1194902.84	701.91	681.55	1	661.913
BMW715	1132482.7	1194761.51	701.97	656.68	3	662.005
BMW717	1132650.51	1194809.56	703.71	667.91	3	609.526
BW01006	1138191.153	1202300.012	714.217	650.207	2	650.470
BW01008	1140152.035	1202497.242	689.7242	614.7342	2	638.873
BW01009	1139561.328	1203247.29	674.1526	602.1526	3	650.425
BW02001	1122723.666	1194679.199	575.5914	495.5914	2	655.235
BW02002	1122855.159	1195124.299	574.067	464.077	2	701.923
BW03001	1126099.627	1190875.429	662.4509	597.9709	2	701.975
BW03002	1124622.104	1192503.328	612.7567	552.7467	2	701.899
BW05008	1132656.556	1191999.764	672.325	587.325	2	697.021
BW05009	1132590.578	1191565.4	674.518	590.408	2	718.163
BW05010	1131821.664	1191011.966	680.1348	590.4648	2	721.609
BW05011D	1130563.542	1188588.148	641.681	362.691	2	709.870
BW06005	1134959.2	1188108.7	668.47	564	2	710.164
BW06006	1134964.19	1188219.132	665.7799	595.7699	2	744.290
BW06007	1134972.94	1188004.736	669.0974	595.0774	2	722.623
BW06008	1135400.027	1188078.387	662.4476	602.9676	2	682.053
BW07001	1136511.176	1195370.412	719.6177	664.4977	2	638.186
BW07002	1136596.162	1195093.802	718.0649	664.4649	2	722.910
BW07003	1136175.058	1194962.571	707.3769	657.6769	2	722.527

Table **N**-4
Model Calibration Water Level Targets

Groundwater Model Development Report
Former Loring Air Force Base, Limestone, Maine

Location ID	X m	Y m	Z (Ground) ft amsl	BOW elev ft amsl	Model Layer	Target elev ft amsl
BW08003	1136490.992	1194107.462	720.8084	616.2084	3	722.821
BW10006	1135688.52	1198565.12	735.26	637.34	2	706.226
BW10007	1136268.235	1199053.293	735.5791	650.5091	2	718.790
BW12005	1133063.048	1196841.719	718.22	660.99	2	709.390
BW12006	1133030.341	1197014.026	719.3843	654.8443	2	710.601
BW13002	1132830.986	1198392.394	754.0023	693.9923	2	702.548
BW14005	1135493.27	1199409.38	739.2	660.75	2	719.027
BW16001	1138831.25	1189595.522	698.2277	593.7177	2	708.382
BW16002	1135310.904	1189058.165	646.3581	546.3281	3	656.966
BW17004	1135216.56	1200020.87	742.38	677.09	2	659.049
BW17005	1135934.493	1200777.28	741.1892	681.0692	2	540.794
BW17006	1135389.238	1200842.176	752.5489	682.5589	2	720.288
BW18003	1137326.043	1202714.059	725.4564	689.6164	2	544.629
BW18004	1138150.635	1200006.045	748.4496	598.4896	3	518.033
BW18006	1138170.487	1197499.7	732.8254	673.6654	2	718.783
BW18007	1140520.874	1194864.072	734.6432	655.6332	2	704.015
BW18008	1140428.358	1192378.903	734.6482	678.8782	2	672.298
BW18009	1139657.77	1191749.012	738.8147	683.7647	2	673.708
BW18010	1138175.204	1191826.244	737.7521	673.7421	2	633.473
BW20001	1138969.899	1203913.859	683.0483	612.9983	2	657.343
BW20002	1139196.916	1204209.203	684.6468	614.6668	3	606.328
BW22001	1127472.398	1185389.333	542.9267	458.9267	2	598.263
CMW2014	1138040.94	1201222.66	740.4	704.43	2	636.298
EBGB_BW001	1127875.362	1186703.975	572.5019	487.8819	2	644.738
EBGB_BW002	1127098.709	1184867.399	559.1927	454.5827	2	648.735
EBGB_OW002	1127098.82	1184863.443	559.4624	504.8124	1	648.720
FMW3410	1135496.01	1201644.06	757.6	694.01	3	693.015
GC_BW001	1129541.886	1197222.27	724.1078	609.3078	2	709.223
GC_BW002D	1129487.196	1195246.799	684.0377	489.0577	2	697.483
GC_BW002S	1129487.196	1195246.799	684.0377	542.0577	2	695.743
JBW7101	1134758.23	1188878.64	649.36	556.93	3	676.870
JBW7102	1135937.99	1188017.45	663.78	626.4	3	695.065
JBW7106B	1132631.83	1186997.03	615.84	550.28	3	681.408
JBW7107	1131579.183	1187073.18	601.4830614	553.4330614	3	697.275
JBW7203B	1134816.96	1189526.35	641.53	588.2	2	694.313
JBW7212A	1135955.25	1189775.6	666.36	471.74	3	689.503
JBW7215B	1136031.02	1190714.98	688.76	610.55	2	689.493
JBW7304	1135551.825	1190954.031	682	558.87	2	689.375
JBW7305	1134311.238	1192810.219	681.1183236	554.3183236	3	690.818
JBW7314	1134088.356	1194288.761	712	591.1	2	693.970
JBW7316	1137526.21	1193724.613	732	611.23	3	663.115
JBW7317	1137269.97	1194756.07	728.74	691.71	3	706.210
JBW7327	1135480.642	1192710.493	693.182229	182.482229	3	666.078

Table **N**-4
Model Calibration Water Level Targets

Groundwater Model Development Report
Former Loring Air Force Base, Limestone, Maine

	X	Y	Z (Ground)	BOW elev	Model Layer	Target elev
Location ID	m	m	ft amsl	ft amsl		ft amsl
JBW7328	1135956.71	1194208.45	721.78	682.08	2	660.463
JBW7338A	1136225.889	1192476.32	710	514.2	2	660.248
JBW7339A	1136008.63	1193911.74	723.68	555.08	2	698.643
JBW7340B	1136014.75	1192606.77	706.68	656.53	2	724.853
JBW7341A	1136234.69	1193792.71	722.71	595.96	2	720.783
JBW7344	1136525.66	1193154.82	722.55	682.26	2	712.500
JBW7345A	1136061.24	1193231.5	712.39	619.61	2	708.145
JBW7347B	1135775.91	1194004.09	712.24	679.15	2	696.038
JBW7348	1136264.089	1193446.678	721.6448	670.1348	2	671.593
JBW7350	1136765.97	1193766.85	725.44	672.16	2	671.948
JBW7403	1140669.506	1188899.794	724.55	643	2	702.473
JBW7607	1132235.11	1194189.54	674.27	631.36	2	706.963
JBW7613	1132992.05	1195581.04	716.61	615.76	2	730.968
JBW7614	1132805.915	1194122.398	690.27	626.33	2	724.585
JBW7617A	1132235.18	1194189.522	668.87	468.9	3	704.578
JBW7617B	1131648.04	1193943.03	668.87	612.7	3	722.543
JBW7710	1134921.86	1194865.85	707.89	652.58	2	685.748
JBW7711	1134106.69	1199744.11	749.71	654.06	2	705.618
JBW7714	1134396.936	1198555.912	744	651.01	2	698.238
JBW7725	1134303.37	1196818.92	728.48	697.54	2	697.183
JBW7734	1133128.53	1196564.63	719.96	666.48	2	678.083
JBW7737A	1132521.65	1195846.67	701.02	497.97	3	681.243
JBW7738A	1131802.03	1195404.64	675.16	575.11	3	682.070
JBW7738B	1131805.09	1195404.63	675.16	606.28	3	672.433
JBW7753A	1132983.27	1195789.59	721.29	686.32	2	667.098
JBW7806	1131713.19	1199095.21	716.26	683.9	3	675.033
JBW7816R	1132465.052	1199647.058	742	678.45	3	670.618
JBW7912	1134973.17	1201998.91	762.81	550.69	2	677.603
JBW8008	1139531.41	1201754.02	719.51	576.59	2	540.900
JBW8009	1137204.24	1200937.33	740.76	686.8	2	605.263
JEBS-5	1136248.34	1193023.26	719.87	665.74	2	604.293
JMW0201R	1132395.24	1199616.95	740.22	666.03	3	712.383
JMW-0406	1134603.96	1196636.07	723	706.33	2	661.280
JMW-0407	1135191.368	1198252.707	734.5	708.99	1	699.403
JMW-0416B	1135340.29	1196471.901	718	700.9	1	700.553
JMW0445	1135146.968	1197371.14	726.1216	703.5116	1	703.267
JMW-0503	1136342.826	1194253.891	721	645.51	3	700.765
JMW-0505	1136431.493	1194156.069	720.2	690.41	2	662.448
JMW0542	1135204.73	1191610.33	677.26	658.55	1	657.073
JMW-0603	1137429.789	1188951.588	678.8	632.35	2	653.573
JMW-0604	1138270.487	1188791.209	693.6	604.55	2	640.035
JMW-0605	1137693.155	1189801.755	698	675.7	2	640.668
JMW-0606	1137277.292	1189538.816	685.4	664.76	2	639.880

Table **N**-4
Model Calibration Water Level Targets

Groundwater Model Development Report
Former Loring Air Force Base, Limestone, Maine

	X	Y	Z (Ground)	BOW elev	Model Layer	Target elev
Location ID	m	m	ft amsl	ft amsl		ft amsl
JMW0640	1137158.47	1189718.78	692.5	655.35	2	638.158
JMW0682	1137520.535	1190181.189	702	600.89	3	652.983
JMW0683	1137343.166	1189272.091	682.91	639.36	3	686.243
JMW0685	1137508.99	1189719.92	697.07	653.89	2	683.363
JMW-0701	1132393.395	1194976.28	698	669.73	1	685.783
JMW-0804	1123999.415	1194678.803	602.9	583.95	1	682.218
JMW-0806	1123801.831	1194358.368	607.7	543.54	1	659.795
JMW0880	1124499.67	1193821.05	632.45	585	1	657.198
JMW0882	1124470.61	1194192.68	606.09	555.04	1	649.383
JMW0891	1123555.31	1195068.04	589.96	539.34	3	704.623
JMW-0903	1126492.1	1193111.1	644.3	624.8	2	673.075
JMW0941	1125106.02	1191554.92	644.1	593.19	2	657.148
JMW0960	1125733.35	1192154.27	617.8	597.61	2	720.938
JMW0961	1125422.53	1192449.4	611.49	596.94	1	708.753
JMW0980	1125542.32	1191784.64	658	596.13	1	661.395
JMW0982	1125043.01	1192445.85	631.25	601.31	1	663.305
JMW0991	1126845.3	1191182.93	638.32	583.05	1	666.403
JMW1103D	1138461.72	1201681.33	729.94	684.82	3	662.790
JMW1380	1140554.03	1202758.68	677.21	620.2	3	697.963
JMW1564	1136531.65	1194553.18	717.92	684	3	708.362
JMW1565	1136727.78	1194585.04	722	677.54	2	723.518
JMW1665	1137012.972	1193418.117	730	692.22	2	547.983
JMW1684	1136583.03	1193438.51	723.51	680.19	2	606.735
JMW1762	1135617.921	1191711.793	682	649.46	2	660.820
JMW1860	1135626.55	1188212.45	659.73	632.53	3	659.683
JMW1881	1135555.12	1188471.14	655.53	604.81	2	704.605
JMW1960	1135390	1189781.07	656.03	621.04	2	620.565
JMW1964	1135497.65	1190170.93	659.41	621.98	2	609.283
JMW1981	1135233.789	1190105.189	655	603.72	2	599.963
JMW1982	1135222.269	1189412.66	647.8333	602.6433	2	645.710
JMW2680	1141663.13	1203271.81	668.7	642.865	2	646.393
JMW3102	1134609.96	1191073.73	652.01	631.93	1	601.510
JMW3202	1136282.28	1192871.68	714.09	668.02	2	660.503
JMW3203	1136224.93	1192767.9	711.11	665.31	2	704.465
JMW3284	1136178.51	1192689.53	712.21	668.33	2	723.935
JMW3285	1136145.07	1192837.35	712.51	609.72	2	699.610
JMW3501	1136488.72	1190173.155	688	603.78	2	724.295
JMW35X2	1136531.4	1189497.31	673.59	636.675	2	666.423
JMW3601	1135824.01	1190571.97	676.12	628.3	2	602.229
JMW6105	1132920.64	1195946.69	717.77	698.86	2	705.188
JMW7113	1131175.25	1186718.04	594.01	581.47	1	662.675
JMW7322	1134058.66	1190590.94	647.11	630.9	1	710.344
JMW7611	1132117.92	1195281.82	688.66	655.93	1	636.312

Table **N**-4
Model Calibration Water Level Targets

Groundwater Model Development Report
Former Loring Air Force Base, Limestone, Maine

Location ID	X m	Y m	Z (Ground) ft amsl	BOW elev ft amsl	Model Layer	Target elev ft amsl
JMW7612	1131968.67	1194958.99	673.29	656.87	1	711.563
JMW7913	1135696.66	1201505.704	748.5407	724.5707	1	705.899
JMW8011	1139510.68	1202891.29	686.51	642.63	1	635.499
JPZ0341	1135063.4	1193102.11	672.63	663.49	1	743.743
JPZ0342	1134984.4	1193239.35	672.18	634.81	2	718.750
JPZ0348	1134820.87	1191270	666.6	617.09	2	566.573
JPZ0349	1134826.67	1191278	666.63	636.57	1	597.455
JPZ0606	1138419.9	1189324.8	694	686.62	1	601.255
JPZ0680	1137801.66	1189451.26	690.73	681.5	1	699.020
JPZ0683	1137959.99	1189785.25	700.58	686.94	1	649.906
JPZ0685	1137472.07	1189130.06	683.48	674.1	1	707.120
JPZ0686	1138219.87	1189641.94	696.51	667.58	1	662.778
JPZ1184R	1138007.23	1201390.51	737.5	706.27	2	657.680
JPZ1187	1138855.24	1201798.1	733.87	696.5	2	659.792
JPZ1360	1139913.07	1202916.12	681.3	628.99	3	650.668
JPZ1382	1140146.39	1202958.91	684	653.7	1	656.081
JPZ1780	1135289.97	1192032.61	676.97	647.83	2	648.762
JPZ1781	1135691.35	1192117.34	694.33	654.06	2	652.407
JPZ7208	1134560.07	1189198.56	632.52	619.53	1	637.963
JPZ7312	1134997.89	1194609.41	698.02	681.77	1	640.798
JPZ7601	1131742.58	1195131.61	677.75	662.55	1	621.143
JPZ7602	1131721.493	1195105.439	678.11	631.09	2	631.457
JPZ7603	1132555.08	1195109.92	699.21	663.04	2	668.488
JPZ7704	1135139.117	1195800.476	711.6522	501.9022	2	668.252
JPZ7739	1131799.4	1195398.57	674.81	662.18	1	631.717
JPZ7808	1131552.258	1198976.157	704	689.45	1	709.252
JPZ7901	1135124.29	1202261.56	762.51	692.73	3	579.463
LF2MW2	1124917.91	1194064.72	626.74	576.05	1	702.970
LF2MW4	1123563.84	1194784.21	595.52	527.18	1	690.358
LF2MW6	1123771.19	1194660.51	611.3	525.45	2	692.823
LF3MW2	1124940.75	1192716.66	610.23	602.27	1	705.270
LF3MW3	1126473.84	1191354.96	628.76	561.26	3	700.240
MMW0002	1126939.605	1190857.492	638.4938	593.5838	1	700.653
MMW0003	1131702.64	1193470.27	669.78	624.63	2	702.285
MMW0005	1136225.35	1194416.02	720.37	677.82	1	646.933
MMW0006	1131331.64	1193789.1	658.94	615.49	2	621.124
MMW0008	1132457.91	1187272.99	600	586.685	1	688.805
MMW0009	1131326.75	1198453.96	702.77	653.52	2	536.422
MMW0010	1133768.25	1188597.92	620.06	546.48	2	710.775
MMW0013	1134427.67	1189422.83	631.32	598.81	1	720.818
MMW0015	1126936.69	1190475.69	646.56	595.63	3	711.045
MMW0016	1134336.57	1188917.25	622.93	603.09	1	712.622
MMW0017	1133686.75	1188119.62	623.46	598.92	1	663.598

Table **N**-4
Model Calibration Water Level Targets

Groundwater Model Development Report
Former Loring Air Force Base, Limestone, Maine

Location ID	X m	Y m	Z (Ground) ft amsl	BOW elev ft amsl	Model Layer	Target elev ft amsl
MMW0018A	1127389.85	1190616.21	637.16	542.6	3	686.148
MMW0019	1132519.23	1187069.28	603.92	593.28	1	584.419
MMW0020	1130585.499	1197734.531	714.7223534	559.7023534	3	555.668
MMW0124	1135615.29	1190389.26	667.7	626.39	3	591.630
MMW0125R	1135777.26	1190483.24	672.4	629.71	3	563.008
MMW0127	1132509	1187173.35	599	558.51	3	627.963
MMW0128	1135907.9	1191539.45	689.8	680.97	2	606.490
MMW0326	1131175.02	1193877	657.4	599.35	2	605.785
MMW0422	1131297.25	1197781.31	702	635.3	3	604.788
MMW0531	1135597.27	1201948.1	752.9	593.09	2	600.693
MMW1560	1136543.97	1194698.62	716.99	695.73	2	647.800
MMW3414	1135021.3	1202100.3	762.4	712.11	3	587.985
MMW7330	1135672.72	1192334.15	697.2	572.35	2	645.070
NP_BW001S	1146091.315	1190109.497	608.3013	476.2813	2	678.600
OW01002	1138674.627	1201916.801	724.4584	699.4784	2	672.148
OW01003	1139915.878	1203056.337	676.247	649.947	1	737.436
OW01004	1139579.309	1203226.164	674.3221	631.2821	1	663.895
OW02001	1122715.378	1194675.011	575.4857	545.4757	1	667.735
OW02002	1122874.082	1195133.559	574.4512	534.3642	1	654.958
OW05004	1132204.939	1191737.876	677.797	657.907	2	689.383
OW07001	1136516.9	1195364.514	719.581	695.031	1	687.205
OW07002	1136278.261	1195332.474	718.443	692.463	1	696.648
OW07003	1136174.327	1194971.728	707.8419	682.8219	1	681.060
OW08001	1135625.164	1194148.002	704.1301	684.0401	1	682.278
OW08002	1135375.976	1193499.677	693.8533	667.8633	1	664.265
OW10005	1135687.51	1198570.65	735.27	710.13	1	628.333
OW10007	1136269.564	1199045.384	735.5996	705.2596	1	692.888
OW12002	1132986.278	1197199.398	720.1836	699.6036	2	670.395
OW14004	1135491.98	1199414.15	739.45	714.65	1	672.743
OW16002	1135311.004	1189060.901	646.3416	601.2916	2	701.438
OW17002	1135934.798	1200728.336	741.4448	713.2248	1	595.960
OW17003	1135390.391	1200805.948	752.333	718.903	1	542.240
OW19009	1139125.47	1190351.15	703.56	681.86	1	606.618
OW19010	1139240.83	1190484.54	705.8	681.03	1	600.174
OW20002	1136337.648	1204490.437	731.9858	696.8158	2	696.330
OW20003	1136629.498	1204822.383	723.7707	690.7907	1	601.840
OW20005	1136760.498	1204366.238	719.0466	686.0066	2	632.518
OW20006	1138973.908	1203922.563	683.1416	653.1016	1	625.063
OW20007	1139201.092	1204216.945	684.4562	645.4562	1	626.170
OW21005	1134432.84	1191010.03	648.9	635.24	1	600.770
OW22003	1127436.781	1185182.429	540.2751	525.2051	1	684.260
OW23001	1134757.264	1189534.763	641.4394	611.4294	2	661.620
OW24001	1134737.259	1201803.63	757.41	719.38	1	658.242

Table **N**-4
Model Calibration Water Level Targets

Groundwater Model Development Report
Former Loring Air Force Base, Limestone, Maine

	X	Y	Z (Ground)	BOW elev	Model Layer	Target elev
Location ID	m	m	ft amsl	ft amsl		ft amsl
RFW0413	1132816.4	1199598.26	781.28	678.78	2	548.228
RFW1144	1138287.33	1201531.83	736.56	656.77	2	539.382
RFW-3	1124455.796	1194471.222	609.7	518.94	3	701.959
RFW-38	1124964.811	1193495.537	606.41	469.66	2	702.043
RFW-5	1126607.094	1191026.51	626.8	547.54	3	701.604
RFW-8	1124594.084	1192263.432	616.8	608.81	1	692.715
SB/OW16001	1137654.97	1189376.51	688.24	673.35	1	680.436
SB/OW17001	1135640.43	1200145.53	740.54	711.73	1	729.205
UNK-033	1137087.494	1192707.879	729.5	672.44	3	721.552
UNK-034	1129711.305	1192558.777	654.5718345	373.6518345	3	731.628
UNK-042	1133741.581	1190194.784	649.9955493	585.8255493	3	722.372
UNK-044	1137033.695	1189328.637	679	655.9	1	727.096
UNK-23001	1140253.657	1188583.339	717	704.45	1	685.513
UNK-TC01	1137925.759	1191565.441	735	689.51	2	702.810
USMW004	1127949.682	1195684.54	678.5684838	651.1884838	2	710.816
USMW005	1127355.25	1195038.56	668.01	651.4	2	659.232
USMW006	1127417.154	1195709.27	674.092422	648.812422	3	658.969
USMW012	1127002.17	1194062.33	671.27	641.46	2	645.453
USMW014	1127151.775	1195623.387	667.6510902	645.4310902	3	538.800
USMW019	1128143.49	1194179.22	673.1470078	632.0070078	2	723.505
USMW024	1126963.086	1195210.131	661.8465926	635.6365926	2	612.535
USMW101	1131419.09	1188551.77	649.05	622.35	3	681.720
USMW103	1130536.29	1189032.58	652.44	631.85	3	722.740
USMW115	1130156.85	1188690.69	633.5	605.18	3	666.615
USMW210	1141684.92	1202507.53	656.1	643.25	1	711.410
USMW214	1141039.47	1202082.96	653.5	635.5	1	654.145
WBGB_BW001	1129725.741	1192645.758	653.6966	563.6766	2	643.150
WBGB_OW001	1129719.111	1192606.287	653.6966	633.6966	1	634.722

Notes
BOW - Bottom of well
Elev - Elevation
ft asml - Feet above mean sea level
ID - Identification
m - Meters

Table N-5
Model Calibration Statistics

Groundwater Model Development Report
Former Loring Air Force Base, Limestone, Maine

Name	X	Y	Layer	Group	Observed	Computed	Residual	Weight
043-MW03	1128625.91	1188010.68	1	1	730.47	714.05	16.42	1
044-RW01	1138790.93	1200027.56	2	1	688.61	664.20	24.41	1
051-MW03	1140546.74	1190335.81	1	1	664.59	663.43	1.15	1
056-MW02	1136146.11	1191699.8	2	1	744.20	725.16	19.04	1
056-MW03	1136194.5	1191503.77	2	1	703.84	707.48	-3.64	1
056MW04	1136006.62	1191661.79	3	1	709.63	713.84	-4.22	1
056MW06	1136060.74	1191491.03	2	1	654.77	652.38	2.38	1
059-MW03	1146002.49	1205475.13	3	1	700.26	681.09	19.17	1
AA07MW-01	1136564.15	1195074.81	1	1	648.32	650.28	-1.96	1
AA18MW-01	1137614.12	1195186.69	2	1	627.34	623.20	4.14	1
AA18MW-02	1137671.36	1197490.62	2	1	689.06	674.39	14.67	1
AA19MW-01	1139589.47	1190472.62	1	1	692.68	676.77	15.91	1
AA19MW-02	1139346.38	1190362.15	1	1	700.12	700.32	-0.19	1
AR25	1135037.39	1191021.85	3	1	662.47	664.88	-2.41	1
ASMW101	1137076.297	1191243.63	3	1	658.19	666.17	-7.98	1
ASMW301	1136642.79	1194797.76	1	1	540.82	547.71	-6.89	1
BB_BW001	1141889.361	1202159.997	2	1	539.32	546.11	-6.79	1
BB_BW002	1145613.906	1197508.076	3	1	620.01	617.07	2.94	1
BB_OW001	1141886.292	1202156.849	1	1	612.07	603.63	8.44	1
BB_OW002	1145616.164	1197505.971	1	1	662.40	665.97	-3.57	1
BMW712	1132437.07	1194902.84	1	1	661.91	662.62	-0.70	1
BMW715	1132482.7	1194761.51	3	1	662.00	660.28	1.73	1
BMW717	1132650.51	1194809.56	3	1	609.53	613.06	-3.54	1
BW01006	1138191.153	1202300.012	2	1	650.47	642.20	8.27	1
BW01008	1140152.035	1202497.242	2	1	638.87	641.12	-2.24	1
BW01009	1139561.328	1203247.29	3	1	650.42	640.96	9.46	1
BW02001	1122723.666	1194679.199	2	1	655.24	647.90	7.33	1
BW02002	1122855.159	1195124.299	2	1	701.92	701.76	0.16	1
BW03001	1126099.627	1190875.429	2	1	701.97	700.55	1.42	1
BW03002	1124622.104	1192503.328	2	1	701.90	696.81	5.09	1
BW05008	1132656.556	1191999.764	2	1	697.02	695.37	1.65	1
BW05009	1132590.578	1191565.4	2	1	718.16	720.71	-2.55	1
BW05010	1131821.664	1191011.966	2	1	721.61	720.46	1.15	1
BW05011D	1130563.542	1188588.148	2	1	709.87	702.10	7.77	1
BW06005	1134959.2	1188108.7	2	1	710.16	703.95	6.22	1
BW06006	1134964.19	1188219.132	2	1	744.29	725.34	18.94	1
BW06007	1134972.94	1188004.736	2	1	722.62	723.73	-1.10	1
BW06008	1135400.027	1188078.387	2	1	682.05	687.90	-5.85	1
BW07001	1136511.176	1195370.412	2	1	638.19	641.26	-3.08	1
BW07002	1136596.162	1195093.802	2	1	722.91	725.32	-2.41	1
BW07003	1136175.058	1194962.571	2	1	722.53	723.17	-0.64	1
BW08003	1136490.992	1194107.462	3	1	722.82	723.78	-0.96	1
BW10006	1135688.52	1198565.12	2	1	706.23	704.12	2.11	1
BW10007	1136268.235	1199053.293	2	1	718.79	717.54	1.25	1
BW12005	1133063.048	1196841.719	2	1	709.39	713.63	-4.24	1
BW12006	1133030.341	1197014.026	2	1	710.60	712.92	-2.32	1

Table N-5
Model Calibration Statistics

Groundwater Model Development Report
Former Loring Air Force Base, Limestone, Maine

Name	X	Y	Layer	Group	Observed	Computed	Residual	Weight
BW13002	1132830.986	1198392.394	2	1	702.55	711.10	-8.56	1
BW14005	1135493.27	1199409.38	2	1	719.03	712.86	6.17	1
BW16001	1138831.25	1189595.522	2	1	708.38	705.23	3.15	1
BW16002	1135310.904	1189058.165	3	1	656.97	667.79	-10.83	1
BW17004	1135216.56	1200020.87	2	1	659.05	663.49	-4.44	1
BW17005	1135934.493	1200777.28	2	1	540.79	549.59	-8.79	1
BW17006	1135389.238	1200842.176	2	1	720.29	714.48	5.81	1
BW18003	1137326.043	1202714.059	2	1	544.63	560.58	-15.95	1
BW18004	1138150.635	1200006.045	3	1	518.03	543.90	-25.87	1
BW18006	1138170.487	1197499.7	2	1	718.78	723.02	-4.24	1
BW18007	1140520.874	1194864.072	2	1	704.02	683.06	20.95	1
BW18008	1140428.358	1192378.903	2	1	672.30	660.07	12.23	1
BW18009	1139657.77	1191749.012	2	1	673.71	660.07	13.64	1
BW18010	1138175.204	1191826.244	2	1	633.47	631.83	1.65	1
BW20001	1138969.899	1203913.859	2	1	657.34	653.20	4.14	1
BW20002	1139196.916	1204209.203	3	1	606.33	602.70	3.63	1
BW22001	1127472.398	1185389.333	2	1	598.26	592.53	5.73	1
CMW2014	1138040.94	1201222.66	2	1	636.30	635.31	0.99	1
EBGB_BW001	1127875.362	1186703.975	2	1	644.74	652.76	-8.02	1
EBGB_BW002	1127098.709	1184867.399	2	1	648.74	656.31	-7.58	1
EBGB_OW002	1127098.82	1184863.443	1	1	648.72	654.69	-5.97	1
FMW3410	1135496.01	1201644.06	3	1	693.02	686.98	6.04	1
GC_BW001	1129541.886	1197222.27	2	1	709.22	704.17	5.05	1
GC_BW002D	1129487.196	1195246.799	2	1	697.48	704.83	-7.35	1
GC_BW002S	1129487.196	1195246.799	2	1	695.74	691.76	3.98	1
JBW7101	1134758.23	1188878.64	3	1	676.87	675.09	1.78	1
JBW7102	1135937.99	1188017.45	3	1	695.07	688.50	6.57	1
JBW7106B	1132631.83	1186997.03	3	1	681.41	673.04	8.37	1
JBW7107	1131579.183	1187073.18	3	1	697.28	689.73	7.55	1
JBW7203B	1134816.96	1189526.35	2	1	694.31	689.08	5.23	1
JBW7212A	1135955.25	1189775.6	3	1	689.50	680.90	8.60	1
JBW7215B	1136031.02	1190714.98	2	1	689.49	688.61	0.89	1
JBW7304	1135551.825	1190954.031	2	1	689.37	687.05	2.32	1
JBW7305	1134311.238	1192810.219	3	1	690.82	696.97	-6.16	1
JBW7314	1134088.356	1194288.761	2	1	693.97	687.60	6.37	1
JBW7316	1137526.21	1193724.613	3	1	663.12	671.50	-8.39	1
JBW7317	1137269.97	1194756.07	3	1	706.21	687.23	18.98	1
JBW7327	1135480.642	1192710.493	3	1	666.08	677.70	-11.62	1
JBW7328	1135956.71	1194208.45	2	1	660.46	670.84	-10.38	1
JBW7338A	1136225.889	1192476.32	2	1	660.25	662.77	-2.52	1
JBW7339A	1136008.63	1193911.74	2	1	698.64	692.91	5.73	1
JBW7340B	1136014.75	1192606.77	2	1	724.85	729.01	-4.16	1
JBW7341A	1136234.69	1193792.71	2	1	720.78	725.03	-4.24	1
JBW7344	1136525.66	1193154.82	2	1	712.50	707.19	5.31	1
JBW7345A	1136061.24	1193231.5	2	1	708.15	699.31	8.83	1
JBW7347B	1135775.91	1194004.09	2	1	696.04	680.75	15.29	1

Table N-5
Model Calibration Statistics

Groundwater Model Development Report
Former Loring Air Force Base, Limestone, Maine

Name	X	Y	Layer	Group	Observed	Computed	Residual	Weight
JBW7348	1136264.089	1193446.678	2	1	671.59	670.75	0.84	1
JBW7350	1136765.97	1193766.85	2	1	671.95	670.75	1.20	1
JBW7403	1140669.506	1188899.794	2	1	702.47	688.92	13.55	1
JBW7607	1132235.11	1194189.54	2	1	706.96	705.34	1.63	1
JBW7613	1132992.05	1195581.04	2	1	730.97	731.47	-0.51	1
JBW7614	1132805.915	1194122.398	2	1	724.59	723.25	1.33	1
JBW7617A	1132235.18	1194189.522	3	1	704.58	685.15	19.43	1
JBW7617B	1131648.04	1193943.03	3	1	722.54	719.35	3.19	1
JBW7710	1134921.86	1194865.85	2	1	685.75	682.21	3.54	1
JBW7711	1134106.69	1199744.11	2	1	705.62	728.13	-22.51	1
JBW7714	1134396.936	1198555.912	2	1	698.24	695.07	3.17	1
JBW7725	1134303.37	1196818.92	2	1	697.18	695.18	2.00	1
JBW7734	1133128.53	1196564.63	2	1	678.08	667.24	10.84	1
JBW7737A	1132521.65	1195846.67	3	1	681.24	680.31	0.94	1
JBW7738A	1131802.03	1195404.64	3	1	682.07	677.38	4.69	1
JBW7738B	1131805.09	1195404.63	3	1	672.43	662.66	9.78	1
JBW7753A	1132983.27	1195789.59	2	1	667.10	661.97	5.13	1
JBW7806	1131713.19	1199095.21	3	1	675.03	674.48	0.55	1
JBW7816R	1132465.052	1199647.058	3	1	670.62	664.37	6.25	1
JBW7912	1134973.17	1201998.91	2	1	677.60	671.71	5.89	1
JBW8008	1139531.41	1201754.02	2	1	540.90	554.13	-13.23	1
JBW8009	1137204.24	1200937.33	2	1	605.26	611.78	-6.51	1
JEBS-5	1136248.34	1193023.26	2	1	604.29	612.09	-7.80	1
JMW0201R	1132395.24	1199616.95	3	1	712.38	701.14	11.24	1
JMW-0406	1134603.96	1196636.07	2	1	661.28	660.99	0.29	1
JMW-0407	1135191.368	1198252.707	1	1	699.40	697.55	1.85	1
JMW-0416B	1135340.29	1196471.901	1	1	700.55	699.88	0.67	1
JMW0445	1135146.968	1197371.14	1	1	703.27	698.58	4.68	1
JMW-0503	1136342.826	1194253.891	3	1	700.77	693.16	7.61	1
JMW-0505	1136431.493	1194156.069	2	1	662.45	661.10	1.35	1
JMW0542	1135204.73	1191610.33	1	1	657.07	649.99	7.08	1
JMW-0603	1137429.789	1188951.588	2	1	653.57	647.07	6.51	1
JMW-0604	1138270.487	1188791.209	2	1	640.04	645.65	-5.62	1
JMW-0605	1137693.155	1189801.755	2	1	640.67	649.22	-8.55	1
JMW-0606	1137277.292	1189538.816	2	1	639.88	645.95	-6.07	1
JMW0640	1137158.47	1189718.78	2	1	638.16	640.21	-2.05	1
JMW0682	1137520.535	1190181.189	3	1	652.98	654.08	-1.10	1
JMW0683	1137343.166	1189272.091	3	1	686.24	680.73	5.51	1
JMW0685	1137508.99	1189719.92	2	1	683.36	679.13	4.24	1
JMW-0701	1132393.395	1194976.28	1	1	685.78	677.11	8.68	1
JMW-0804	1123999.415	1194678.803	1	1	682.22	678.17	4.05	1
JMW-0806	1123801.831	1194358.368	1	1	659.80	658.42	1.37	1
JMW0880	1124499.67	1193821.05	1	1	657.20	657.42	-0.22	1
JMW0882	1124470.61	1194192.68	1	1	649.38	654.26	-4.88	1
JMW0891	1123555.31	1195068.04	3	1	704.62	689.75	14.87	1
JMW-0903	1126492.1	1193111.1	2	1	673.08	670.08	3.00	1

Table N-5
Model Calibration Statistics

Groundwater Model Development Report
Former Loring Air Force Base, Limestone, Maine

Name	X	Y	Layer	Group	Observed	Computed	Residual	Weight
JMW0941	1125106.02	1191554.92	2	1	657.15	653.72	3.42	1
JMW0960	1125733.35	1192154.27	2	1	720.94	712.81	8.13	1
JMW0961	1125422.53	1192449.4	1	1	708.75	698.23	10.52	1
JMW0980	1125542.32	1191784.64	1	1	661.40	663.87	-2.48	1
JMW0982	1125043.01	1192445.85	1	1	663.31	661.20	2.10	1
JMW0991	1126845.3	1191182.93	1	1	666.40	665.29	1.11	1
JMW1103D	1138461.72	1201681.33	3	1	662.79	668.59	-5.80	1
JMW1380	1140554.03	1202758.68	3	1	697.96	674.95	23.02	1
JMW1564	1136531.65	1194553.18	3	1	708.36	700.20	8.17	1
JMW1565	1136727.78	1194585.04	2	1	723.52	722.60	0.92	1
JMW1665	1137012.972	1193418.117	2	1	547.98	561.68	-13.69	1
JMW1684	1136583.03	1193438.51	2	1	606.74	616.25	-9.52	1
JMW1762	1135617.921	1191711.793	2	1	660.82	664.04	-3.22	1
JMW1860	1135626.55	1188212.45	3	1	659.68	658.81	0.87	1
JMW1881	1135555.12	1188471.14	2	1	704.61	689.36	15.25	1
JMW1960	1135390	1189781.07	2	1	620.57	616.88	3.69	1
JMW1964	1135497.65	1190170.93	2	1	609.28	612.47	-3.18	1
JMW1981	1135233.789	1190105.189	2	1	599.96	612.65	-12.69	1
JMW1982	1135222.269	1189412.66	2	1	645.71	651.51	-5.80	1
JMW2680	1141663.13	1203271.81	2	1	646.39	653.45	-7.06	1
JMW3102	1134609.96	1191073.73	1	1	601.51	601.75	-0.24	1
JMW3202	1136282.28	1192871.68	2	1	660.50	657.75	2.75	1
JMW3203	1136224.93	1192767.9	2	1	704.47	683.84	20.62	1
JMW3284	1136178.51	1192689.53	2	1	723.94	721.65	2.29	1
JMW3285	1136145.07	1192837.35	2	1	699.61	698.11	1.50	1
JMW3501	1136488.72	1190173.155	2	1	724.30	723.18	1.11	1
JMW35X2	1136531.4	1189497.31	2	1	666.42	666.87	-0.45	1
JMW3601	1135824.01	1190571.97	2	1	602.23	609.94	-7.71	1
JMW6105	1132920.64	1195946.69	2	1	705.19	698.70	6.49	1
JMW7113	1131175.25	1186718.04	1	1	662.67	664.28	-1.61	1
JMW7322	1134058.66	1190590.94	1	1	710.34	705.89	4.46	1
JMW7611	1132117.92	1195281.82	1	1	636.31	641.52	-5.20	1
JMW7612	1131968.67	1194958.99	1	1	711.56	702.86	8.70	1
JMW7913	1135696.66	1201505.704	1	1	705.90	699.00	6.90	1
JMW8011	1139510.68	1202891.29	1	1	635.50	634.90	0.60	1
JPZ0341	1135063.4	1193102.11	1	1	743.74	749.96	-6.22	1
JPZ0342	1134984.4	1193239.35	2	1	718.75	708.13	10.62	1
JPZ0348	1134820.87	1191270	2	1	566.57	578.31	-11.73	1
JPZ0349	1134826.67	1191278	1	1	597.46	594.33	3.13	1
JPZ0606	1138419.9	1189324.8	1	1	601.26	615.64	-14.38	1
JPZ0680	1137801.66	1189451.26	1	1	699.02	696.52	2.50	1
JPZ0683	1137959.99	1189785.25	1	1	649.91	637.42	12.48	1
JPZ0685	1137472.07	1189130.06	1	1	707.12	698.88	8.24	1
JPZ0686	1138219.87	1189641.94	1	1	662.78	650.10	12.67	1
JPZ1184R	1138007.23	1201390.51	2	1	657.68	640.45	17.23	1
JPZ1187	1138855.24	1201798.1	2	1	659.79	638.34	21.45	1

Table N-5
Model Calibration Statistics

Groundwater Model Development Report
Former Loring Air Force Base, Limestone, Maine

Name	X	Y	Layer	Group	Observed	Computed	Residual	Weight
JPZ1360	1139913.07	1202916.12	3	1	650.67	635.89	14.78	1
JPZ1382	1140146.39	1202958.91	1	1	656.08	638.34	17.74	1
JPZ1780	1135289.97	1192032.61	2	1	648.76	642.11	6.65	1
JPZ1781	1135691.35	1192117.34	2	1	652.41	633.94	18.47	1
JPZ7208	1134560.07	1189198.56	1	1	637.96	604.06	33.90	1
JPZ7312	1134997.89	1194609.41	1	1	640.80	610.63	30.17	1
JPZ7601	1131742.58	1195131.61	1	1	621.14	604.76	16.38	1
JPZ7602	1131721.493	1195105.439	2	1	631.46	636.12	-4.66	1
JPZ7603	1132555.08	1195109.92	2	1	668.49	669.38	-0.89	1
JPZ7704	1135139.117	1195800.476	2	1	668.25	669.08	-0.83	1
JPZ7739	1131799.4	1195398.57	1	1	631.72	634.56	-2.84	1
JPZ7808	1131552.258	1198976.157	1	1	709.25	682.34	26.91	1
JPZ7901	1135124.29	1202261.56	3	1	579.46	575.34	4.12	1
LF2MW2	1124917.91	1194064.72	1	1	702.97	688.49	14.48	1
LF2MW4	1123563.84	1194784.21	1	1	690.36	666.51	23.85	1
LF2MW6	1123771.19	1194660.51	2	1	692.82	665.32	27.50	1
LF3MW2	1124940.75	1192716.66	1	1	705.27	700.17	5.10	1
LF3MW3	1126473.84	1191354.96	3	1	700.24	694.45	5.79	1
MMW0002	1126939.605	1190857.492	1	1	700.65	693.79	6.86	1
MMW0003	1131702.64	1193470.27	2	1	702.29	699.46	2.82	1
MMW0005	1136225.35	1194416.02	1	1	646.93	650.32	-3.39	1
MMW0006	1131331.64	1193789.1	2	1	621.12	622.77	-1.65	1
MMW0008	1132457.91	1187272.99	1	1	688.81	673.63	15.18	1
MMW0009	1131326.75	1198453.96	2	1	536.42	543.67	-7.25	1
MMW0010	1133768.25	1188597.92	2	1	710.78	704.83	5.95	1
MMW0013	1134427.67	1189422.83	1	1	720.82	717.90	2.92	1
MMW0015	1126936.69	1190475.69	3	1	711.05	704.73	6.31	1
MMW0016	1134336.57	1188917.25	1	1	712.62	710.09	2.53	1
MMW0017	1133686.75	1188119.62	1	1	663.60	658.40	5.20	1
MMW0018A	1127389.85	1190616.21	3	1	686.15	672.96	13.19	1
MMW0019	1132519.23	1187069.28	1	1	584.42	561.58	22.84	1
MMW0020	1130585.499	1197734.531	3	1	555.67	561.58	-5.91	1
MMW0124	1135615.29	1190389.26	3	1	591.63	585.96	5.67	1
MMW0125R	1135777.26	1190483.24	3	1	563.01	574.27	-11.26	1
MMW0127	1132509	1187173.35	3	1	627.96	623.41	4.55	1
MMW0128	1135907.9	1191539.45	2	1	606.49	608.24	-1.75	1
MMW0326	1131175.02	1193877	2	1	605.79	612.14	-6.35	1
MMW0422	1131297.25	1197781.31	3	1	604.79	603.66	1.13	1
MMW0531	1135597.27	1201948.1	2	1	600.69	616.06	-15.37	1
MMW1560	1136543.97	1194698.62	2	1	647.80	650.08	-2.28	1
MMW3414	1135021.3	1202100.3	3	1	587.99	589.18	-1.19	1
MMW7330	1135672.72	1192334.15	2	1	645.07	643.11	1.96	1
NP_BW001S	1146091.315	1190109.497	2	1	678.60	671.10	7.50	1
OW01002	1138674.627	1201916.801	2	1	672.15	669.06	3.09	1
OW01003	1139915.878	1203056.337	1	1	737.44	722.75	14.69	1
OW01004	1139579.309	1203226.164	1	1	663.90	672.20	-8.30	1

Table N-5
Model Calibration Statistics

Groundwater Model Development Report
Former Loring Air Force Base, Limestone, Maine

Name	X	Y	Layer	Group	Observed	Computed	Residual	Weight
OW02001	1122715.378	1194675.011	1	1	667.74	669.43	-1.70	1
OW02002	1122874.082	1195133.559	1	1	654.96	654.21	0.74	1
OW05004	1132204.939	1191737.876	2	1	689.38	684.41	4.98	1
OW07001	1136516.9	1195364.514	1	1	687.21	677.81	9.39	1
OW07002	1136278.261	1195332.474	1	1	696.65	681.85	14.80	1
OW07003	1136174.327	1194971.728	1	1	681.06	668.09	12.97	1
OW08001	1135625.164	1194148.002	1	1	682.28	684.46	-2.18	1
OW08002	1135375.976	1193499.677	1	1	664.27	664.19	0.07	1
OW10005	1135687.51	1198570.65	1	1	628.33	626.14	2.19	1
OW10007	1136269.564	1199045.384	1	1	692.89	690.93	1.96	1
OW12002	1132986.278	1197199.398	2	1	670.40	668.80	1.59	1
OW14004	1135491.98	1199414.15	1	1	672.74	670.62	2.12	1
OW16002	1135311.004	1189060.901	2	1	701.44	699.99	1.45	1
OW17002	1135934.798	1200728.336	1	1	595.96	585.96	10.00	1
OW17003	1135390.391	1200805.948	1	1	542.24	553.74	-11.50	1
OW19009	1139125.47	1190351.15	1	1	606.62	603.66	2.96	1
OW19010	1139240.83	1190484.54	1	1	600.17	615.17	-15.00	1
OW20002	1136337.648	1204490.437	2	1	696.33	694.67	1.66	1
OW20003	1136629.498	1204822.383	1	1	601.84	601.95	-0.11	1
OW20005	1136760.498	1204366.238	2	1	632.52	627.48	5.04	1
OW20006	1138973.908	1203922.563	1	1	625.06	623.70	1.37	1
OW20007	1139201.092	1204216.945	1	1	626.17	616.90	9.27	1
OW21005	1134432.84	1191010.03	1	1	600.77	600.63	0.14	1
OW22003	1127436.781	1185182.429	1	1	684.26	662.07	22.19	1
OW23001	1134757.264	1189534.763	2	1	661.62	665.81	-4.19	1
OW24001	1134737.259	1201803.63	1	1	658.24	668.01	-9.77	1
RFW0413	1132816.4	1199598.26	2	1	548.23	547.77	0.45	1
RFW1144	1138287.33	1201531.83	2	1	539.38	546.08	-6.69	1
RFW-3	1124455.796	1194471.222	3	1	701.96	701.81	0.15	1
RFW-38	1124964.811	1193495.537	2	1	702.04	699.89	2.15	1
RFW-5	1126607.094	1191026.51	3	1	701.60	696.60	5.01	1
RFW-8	1124594.084	1192263.432	1	1	692.72	689.93	2.79	1
SB/OW16001	1137654.97	1189376.51	1	1	680.44	674.40	6.04	1
SB/OW17001	1135640.43	1200145.53	1	1	729.21	720.71	8.50	1
UNK-033	1137087.494	1192707.879	3	1	721.55	720.49	1.06	1
UNK-034	1129711.305	1192558.777	3	1	731.63	723.73	7.90	1
UNK-042	1133741.581	1190194.784	3	1	722.37	722.80	-0.43	1
UNK-044	1137033.695	1189328.637	1	1	727.10	723.83	3.27	1
UNK-23001	1140253.657	1188583.339	1	1	685.51	693.37	-7.86	1
UNK-TC01	1137925.759	1191565.441	2	1	702.81	694.67	8.14	1
USMW004	1127949.682	1195684.54	2	1	710.82	697.97	12.84	1
USMW005	1127355.25	1195038.56	2	1	659.23	667.83	-8.60	1
USMW006	1127417.154	1195709.27	3	1	658.97	662.10	-3.13	1
USMW012	1127002.17	1194062.33	2	1	645.45	649.24	-3.79	1
USMW014	1127151.775	1195623.387	3	1	538.80	546.62	-7.82	1
USMW019	1128143.49	1194179.22	2	1	723.51	723.30	0.20	1

Table N-5
Model Calibration Statistics

Groundwater Model Development Report
Former Loring Air Force Base, Limestone, Maine

Name	X	Y	Layer	Group	Observed	Computed	Residual	Weight
USMW024	1126963.086	1195210.131	2	1	612.54	604.89	7.65	1
USMW101	1131419.09	1188551.77	3	1	681.72	674.08	7.64	1
USMW103	1130536.29	1189032.58	3	1	722.74	724.17	-1.43	1
USMW115	1130156.85	1188690.69	3	1	666.62	660.72	5.89	1
USMW210	1141684.92	1202507.53	1	1	711.41	689.94	21.47	1
USMW214	1141039.47	1202082.96	1	1	654.15	651.82	2.32	1
WBGB_BW001	1129725.741	1192645.758	2	1	643.15	657.05	-13.90	1
WBGB_OW001	1129719.111	1192606.287	1	1	634.72	635.72	-0.99	1

Statistic	Value
Number of Targets	284
Range in Observed Values	226.26
Minimum Residual	-25.87
Maximum Residual	33.90
Sum of Squared Residuals	24520.41
Root Mean Square (RMS) Error	9.29
Residual Mean	2.77
Absolute Residual Mean	6.89
Standard Deviation	8.87
Scaled Residual Mean	0.01
Scaled Absolute Residual Mean	0.03
Scaled Standard Deviation	0.04
Scaled Root Mean Square (RMS) Error	0.04

Table N-6
Calibrated Surface Water Flows

Groundwater Model Development Report
Former Loring Air Force Base, Limestone, Maine

	Observed Flow (cfs)	Modeled Flow (cfs)
Butterfield Brook above Willard Brook	13.2	11.8
Butterfield Borro below Willard Brook	21.3	20.8
Butterfield Brook, upper	3.6	1.3
Flightline Drainage Ditch, lower	2.3	0.7
Flightline Drainage Ditch, upper	1.5	0.5
Greenlaw Brook, upper	2.2	0.6
Greenlaw Brook, lower above East Branch	2.9	4.1
Greenlaw Brook Lower below East Branch	6.0	5.8
Masters Brook	5.9	9.4
Noyes Brook	0.6	1.1
Swamp Brook Above Flightline Drainage Ditch	0.7	1.6
East Branch Greenlaw Brook	4.0	2.2

Notes

cfs - cubic feet per second

Table **N**-7
Calibrated Model Parameters

Groundwater Model Development Report
Former Loring Air Force Base, Limestone, Maine

Hydraulic Conductivity (feet/day)				
Model Layer	**Lithology**	**Kx**	**Ky**	**Kz**
1	Overburden	22.48	22.48	2.2
		15	15	1.5
	Alluvium	100	100	10
2	Fractured Bedrock	30	30	3
		50	50	5
		50	50	10
		7.5	7.5	0.7
		4	4	0.04
		10	10	0.7
		5	5	0.5
	Alluvium	100	100	10
3	Competent Bedrock	0.1	0.1	0.008

Table N-8
Calibrated Model Water Balance

Groundwater Model Development Report
Former Loring Air Force Base, Limestone, Maine

IN:	ft^3/day	OUT:	ft^3/day
CLN Constant Head	2,021,004.9	Constant Head	0.0
Drains	0.0	CLN Drains	4,200,353.3
Head Dependent Bounds	59,250.7	Head Dependent Bounds	675,602.4
Recharge	2,795,700.3	Recharge	0.0
Total	4,875,955.83		4,875,955.76
Percent Discrepancy	0.00		

Notes
CLN - Connected Linear Network
ft^3/day - cubic feet per day

Table N-9
Calculated PFOA and PFOS Source Areas

Groundwater Model Development Report
Former Loring Air Force Base, Limestone, Maine

Area	PFAS	
Fire Training Area	PFOA	PFOS
Area (sq ft)	1,445,327	3,204,068
Area (acres)	33	74
Structural Fire Station	PFOA	PFOS
Area (sq ft)	124,223	154,819
Area (acres)	2.9	3.6
Crash Fire Station	PFOA	PFOS
Area (sq ft)	535,425	914,995
Area (acres)	12	21
Nose Dock #44	PFOA	PFOS
Area (sq ft)	--	210,397
Area (acres)	--	4.8

Notes:

PFAS - per- and polyfluoroalkyl substances

PFOA - perfluorooctanoic acid

PFOS - perfluorooctane sulfonate
sq ft - square feet

Table N-10
PFOA and PFOS Lysimeter Porewater to Groundwater Flux Rates

Groundwater Model Development Report
Former Loring Air Force Base, Limestone, Maine

Source Area	Lysimeter Location	Parameter	PFOA	PFOS
Fire Training Area	LYS01007D	Recharge Rate (ft/yr)	*1.15*	
		Deep Median Concentration (ng/L)	*1220*	*4855*
		Mass Flux Rate (ng/yr/ft^2)	*39693*	*157961*
		Source Area (ft^2)	*1445327*	*3204068*
		Total Mass Flux Rate (g/yr)	*57*	*506*
Structural Fire Station	LYS05012D	Recharge Rate (ft/yr)	*1.89*	
		Deep Median Concentration (ng/L)	*1125*	*1250*
		Mass Flux Rate (ng/yr/ft^2)	*60267*	*66993*
		Source Area (ft^2)	*124223*	*154819*
		Total Mass Flux Rate (g/yr)	*7.5*	*10*
Crash Fire Station	LYS07007D	Recharge Rate (ft/yr)	*1.04*	
		Deep Median Concentration (ng/L)	*7260*	*13300*
		Mass Flux Rate (ng/yr/ft^2)	*214731*	*393377*
		Source Area (ft^2)	*535425*	*914995*
		Total Mass Flux Rate (g/yr)	*115*	*360*

Notes:

PFOA - perfluorooctanoic acid

PFOS - perfluorooctane sulfonate

ft/yr - Feet per year

ng/L - Nanograms per Liter

ng/yr/ft^2 - Nanograms per year per square feet

ft^2 - Square feet

g/yr - Gram per year

Table N-11
Fire Training Area Soil Screening Level Calculations

Groundwater Model Development Report
Former Loring Air Force Base, Limestone, Maine

Calculation	Parameter	Parameter Description	PFOA	PFOS
Main SSL Input Parameters	C_{gw} (ng/L)[a]	Target groundwater concentration	4	4
	K_d (L/kg)	Distribution coefficient	3.3	16
	K_{aw} (L^3/L^2)	Air-water interfacial adsorption coefficient	1.6E-02	1.1E-01
	a_{aw} (L^2/L^3)	Air-water interfacial area	400	
	H' at 20 degrees Celsius	Henry's constant	2.0E-02	4.5E-02
	Θ_a	Air filled porosity	0.28	
	Θ_w	Water filled porosity	0.13	
	ρb (kg/L)	Dry bulk density	1.58	

DAF Input Parameters	K (ft/yr)	Hydraulic conductivity	768	
	i (ft/ft)	Hydraulic gradient	0.017	
	d_a (ft)	Aquifer saturated thickness	60.0	
	I (ft/yr)	Infiltration rate	1.15	
	L (ft)	Length of source	1463	2970
	d_m (ft)	Mixing depth	60.0	60.0
	DAF	**Dilution Attenuation Factor**	1.5	1.2

C_{pw} (ng/L)	**Target Soil Porewater Concentration**	5.9E+00	4.9E+00
SSL (mg/kg)	**Soil Screening Level**	2.0E-05	8.1E-05
SSL^{Rev} (mg/kg)	**Soil Screening Level Revised**	4.4E-05	2.2E-04

Notes:

[a]USEPA Maximum Contaminant Levels (MCLs). Final PFAS National Primary Drinking Water Regulation. April 2024. [URL: https://www.epa.gov/sdwa/and-polyfluoroalkyl-substances-pfas]

$SSL = C_{gw}DAF[K_d+(\Theta_w + \Theta_a H')/\rho b]$ — U.S. EPA. 1996. Soil Screening Guidance: User's Guide. EPA/540/R-96/018. Office of Emergency and Remedial Response, Washington, DC. PB96-963505.

$SSL^{Rev} = C_{gw}DAF[K_d+(K_{aw}a_w + \Theta_w + \Theta_a H')/\rho b]$ — Brusseau, M. L., and Guo, B. 2023. Revising the EPA dilution-attenuation soil screening model for PFAS. Journal of Hazardous Materials Letters, vol. 4.

NA - not applicable due to soil concentrations below detection
ng/L - nanograms per liter
L/kg - liters per kilogram
kg/L - kilograms per liter
ft/yr - feet per year
ft/ft - feet per foot
ft - feet
mg/kg - milligram per kilogram
DAF - Dilution attenuation factor
PFOA - perfluorooctanoic acid
PFOS - perfluorooctanesulfonic acid
SSL - Soil screening levels

Table N-12

Structural Fire Station Soil Screening Level Calculations

Groundwater Model Development Report

Former Loring Air Force Base, Limestone, Maine

Calculation	Parameter	Parameter Description	PFOA	PFOS
Main SSL Input Parameters	C_{gw} (ng/L)[a]	Target groundwater concentration	4	4
	K_d (L/kg)	Distribution coefficient	1.7	18
	K_{aw} (L^3/L^2)	Air-water interfacial adsorption coefficient	1.6E-02	1.1E-01
	a_{aw} (L^2/L^3)	Air-water interfacial area	334	
	H' at 20 degrees Celsius	Henry's constant	2.0E-02	4.5E-02
	Θ_a	Air filled porosity	0.32	
	Θ_w	Water filled porosity	0.07	
	ρb (kg/L)	Dry bulk density	1.61	

DAF Input Parameters	K (ft/yr)	Hydraulic conductivity	140014	
	i (ft/ft)	Hydraulic gradient	0.005	
	d_a (ft)	Aquifer saturated thickness	5.4	
	I (ft/yr)	Infiltration rate	1.89	
	L (ft)	Length of source	635	620
	d_m (ft)	Mixing depth	5.4	5.4
	DAF	**Dilution Attenuation Factor**	4.1	4.2

C_{pw} (ng/L)	**Target Soil Porewater Concentration**	1.6E+01	1.7E+01
SSL (mg/kg)	**Soil Screening Level**	2.9E-05	3.0E-04
SSL^{Rev} (mg/kg)	**Soil Screening Level Revised**	8.3E-05	6.9E-04

Notes:

[a]USEPA Maximum Contaminant Levels (MCLs). Final PFAS National Primary Drinking Water Regulation. April 2024. [URL: https://www.epa.gov/sdwa/and-polyfluoroalkyl-substances-pfas]

$SSL = C_{gw}DAF[K_d+(\Theta_w + \Theta_a H')/\rho b]$

U.S. EPA. 1996. Soil Screening Guidance: User's Guide. EPA/540/R-96/018. Office of Emergency and Remedial Response, Washington, DC. PB96-963505.

$SSL^{Rev} = C_{gw}DAF[K_d+(K_{aw}a_w + \Theta_w + \Theta_a H')/\rho b]$

Brusseau, M. L., and Guo, B. 2023. Revising the EPA dilution-attenuation soil screening model for PFAS. Journal of Hazardous Materials Letters, vol. 4.

NA - not applicable due to soil concentrations below detection

ng/L - nanograms per liter

L/kg - liters per kilogram

kg/L - kilograms per liter

ft/yr - feet per year

ft/ft - feet per foot

ft - feet

mg/kg - milligram per kilogram

DAF - Dilution attenuation factor

PFOA - perfluorooctanoic acid

PFOS - perfluorooctanesulfonic acid

SSL - Soil screening levels

Table N-13
Crash Fire Station Soil Screening Level Calculations

Groundwater Model Development Report
Former Loring Air Force Base, Limestone, Maine

Calculation	Parameter	Parameter Description	PFOA	PFOS
Main SSL Input Parameters	C_{gw} (ng/L)[a]	Target groundwater concentration	4	4
	K_d (L/kg)	Distribution coefficient	4.0	14
	K_{aw} (L^3/L^2)	Air-water interfacial adsorption coefficient	1.6E-02	1.1E-01
	a_{aw} (L^2/L^3)	Air-water interfacial area	171	
	H' at 20 degrees Celsius	Henry's constant	2.0E-02	4.5E-02
	Θ_a	Air filled porosity	0.30	
	Θ_w	Water filled porosity	0.10	
	ρb (kg/L)	Dry bulk density	1.55	

DAF Input Parameters	K (ft/yr)	Hydraulic conductivity	117377	
	i (ft/ft)	Hydraulic gradient	0.007	
	d_a (ft)	Aquifer saturated thickness	2.0	
	I (ft/yr)	Infiltration rate	1.04	
	L (ft)	Length of source	1190	1680
	d_m (ft)	Mixing depth	2.0	2.0
	DAF	**Dilution Attenuation Factor**	2.3	2.0

C_{pw} (ng/L)	**Target Soil Porewater Concentration**	9.4E+00	7.8E+00
SSL (mg/kg)	**Soil Screening Level**	3.9E-05	1.1E-04
SSL^{Rev} (mg/kg)	**Soil Screening Level Revised**	5.5E-05	2.0E-04

Notes:

[a]USEPA Maximum Contaminant Levels (MCLs). Final PFAS National Primary Drinking Water Regulation. April 2024. [URL: https://www.epa.gov/sdwa/and-polyfluoroalkyl-substances-pfas]

$SSL = C_{gw}DAF[K_d+(\Theta_w + \Theta_a H')/\rho b]$

U.S. EPA. 1996. Soil Screening Guidance: User's Guide. EPA/540/R-96/018. Office of Emergency and Remedial Response, Washington, DC. PB96-963505.

$SSL^{Rev} = C_{gw}DAF[K_d+(K_{aw}a_w + \Theta_w + \Theta_a H')/\rho b]$

Brusseau, M. L., and Guo, B. 2023. Revising the EPA dilution-attenuation soil screening model for PFAS. Journal of Hazardous Materials Letters, vol. 4.

NA - not applicable due to soil concentrations below detection
ng/L - nanograms per liter
L/kg - liters per kilogram
kg/L - kilograms per liter
ft/yr - feet per year
ft/ft - feet per foot
ft - feet
mg/kg - milligram per kilogram
DAF - Dilution attenuation factor
PFOA - perfluorooctanoic acid
PFOS - perfluorooctanesulfonic acid
SSL - Soil screening levels

Table N-14

Nose Dock #44 Soil Screening Level Calculations

Groundwater Model Development Report

Former Loring Air Force Base, Limestone, Maine

Calculation	Parameter	Parameter Description	PFOA	PFOS
Main SSL Input Parameters	C_{gw} (ng/L)[a]	Target groundwater concentration	4	4
	K_d (L/kg)	Distribution coefficient	8.5	35
	K_{aw} (L^3/L^2)	Air-water interfacial adsorption coefficient	1.6E-02	1.1E-01
	a_{aw} (L^2/L^3)	Air-water interfacial area	177	
	H' at 20 degrees Celsius	Henry's constant	2.0E-02	4.5E-02
	Θ_a	Air filled porosity	0.29	
	Θ_w	Water filled porosity	0.11	
	ρb (kg/L)	Dry bulk density	1.60	
DAF Input Parameters	K (ft/yr)	Hydraulic conductivity	73599	
	i (ft/ft)	Hydraulic gradient	0.017	
	d_a (ft)	Aquifer saturated thickness	4.9	
	I (ft/yr)	Infiltration rate	0.72	
	L (ft)	Length of source	0	530
	d_m (ft)	Mixing depth	NA	4.9
	DAF	**Dilution Attenuation Factor**	NA	16.6
C_{pw} (ng/L)		**Target Soil Porewater Concentration**	NA	6.6E+01
SSL (mg/kg)		**Soil Screening Level**	NA	2.3E-03
SSL^{Rev} (mg/kg)		**Soil Screening Level Revised**	NA	3.1E-03

Notes:

[a]USEPA Maximum Contaminant Levels (MCLs). Final PFAS National Primary Drinking Water Regulation. April 2024. [URL: https://www.epa.gov/sdwa/and-polyfluoroalkyl-substances-pfas]

$SSL = C_{gw}DAF[K_d+(\Theta_w + \Theta_a H')/\rho b]$ — U.S. EPA. 1996. Soil Screening Guidance: User's Guide. EPA/540/R-96/018. Office of Emergency and Remedial Response, Washington, DC. PB96-963505.

$SSL^{Rev} = C_{gw}DAF[K_d+(K_{aw}a_w + \Theta_w + \Theta_a H')/\rho b]$ — Brusseau, M. L., and Guo, B. 2023. Revising the EPA dilution-attenuation soil screening model for PFAS. Journal of Hazardous Materials Letters, vol. 4.

NA - not applicable due to soil concentrations below detection

ng/L - nanograms per liter

L/kg - liters per kilogram

kg/L - kilograms per liter

ft/yr - feet per year

ft/ft - feet per foot

ft - feet

mg/kg - milligram per kilogram

DAF - Dilution attenuation factor

PFOA - perfluorooctanoic acid

PFOS - perfluorooctanesulfonic acid

SSL - Soil screening levels

Table N-15
Summary of Soil Screening Level Calculations

Groundwater Model Development Report
Former Loring Air Force Base, Limestone, Maine

SOURCE AREA	Analyte:	PFOA	PFOS
Fire Training Area	SSL (mg/kg)	2.0E-05	8.1E-05
	SSL^{Rev} (mg/kg)	4.4E-05	2.2E-04
	DAF	1.5	1.2
	C_{pw} (ng/L)	5.9	4.9
	C_{mpw} (ng/L)	1220	4855
Structural Fire Station	SSL (mg/kg)	2.9E-05	3.0E-04
	SSL^{Rev} (mg/kg)	8.3E-05	6.9E-04
	DAF	4.1	4.2
	C_{pw} (ng/L)	16	17
	C_{mpw} (ng/L)	1125	1250
Crash Fire Station	SSL (mg/kg)	3.9E-05	1.1E-04
	SSL^{Rev} (mg/kg)	5.5E-05	2.0E-04
	DAF	2.3	2.0
	C_{pw} (ng/L)	9.4	7.8
	C_{mpw} (ng/L)	7260	13300
Nose Dock #44	SSL (mg/kg)	NA	2.3E-03
	SSL^{Rev} (mg/kg)	NA	3.1E-03
	DAF	NA	66
	C_{pw} (ng/L)	NA	66
	C_{mpw} (ng/L)	NS	NS

Notes:

mg/kg - milligram per kilogram
ng/L - nanograms per liter
Pooled Method 1633 Detection Limit (mg/kg) 7.0E-05
Reported Method 1633 Detection Limit (mg/kg) 1.1E-03
Value is at or below Method 1633 detection limit

SSL - USEPA soil screening level
SSL^{Rev} - modified USEPA SSL by Brusseau and Gao (2023) taking into account attenuation at the air water interface
DAF - site specific calculated dilution attenuation factor
C_{pw} - target soil porewater concentration
C_{mpw} - soil porewater median concentration from deep lysimeter sampling
NA - not applicable due to soil concentrations below detection
NS - no samples were collected
mg/kg - milligram per kilogram
ng/L - nanograms per liter
PFOA - perfluorooctanoic acid
PFOS - perfluorooctane sulfonate

Table N-16
PFOA and PFOS Vadose Zone distribution Coefficients from Porewater Soil Pairs

Groundwater Model Development Report
Former Loring Air Force Base, Limestone, Maine

Source Area	Sample ID	Sample Type	Sample Depth (ft)	Units	PFOA	PFOS
Fire Training Area	LYS01007S	median porewater	3	ng/L	1050	8050
	SB01007	soil	0-1	mg/kg	0.0012	0.122
	LYS01007D	median porewater	12	ng/L	1220	4855
	SB01007	soil	8-10	mg/kg	<0.0011	0.022
	Median K_d			L/kg	1.1	9.8
Structural Fire Station	LYS05012S	median porewater	3	ng/L	746	8215
	SB05012	soil	0-1	mg/kg	<0.001	0.291
	LYS05012D	median porewater	10	ng/L	1124.5	1250
	SB05012	soil	8-10	mg/kg	0.00087	0.0186
	Median K_d			L/kg	0.77	25
Crash Fire Station	LYS07007S	median porewater	3	ng/L	1730	88000
	SB07007	soil	0-1	mg/kg	0.0015	0.223
	LYS07007D	median porewater	10	ng/L	7260	13300
	SB07007	soil	8-9	mg/kg	0.0235	<0.0012
	Median K_d			L/kg	2.1	2.5

Notes:

ft - feet

K_d - Distribution coefficient

L/kg - Liters per kilogram

mg/kg - milligram per kilogram

NA - Not aplicable due to either soil or porewater, or both, concentrations below detection limit

ng/L - nanograms per liter

PFOA - perfluorooctanoic acid

PFOS - perfluorooctane sulfonate

Table N-17

PFOA and PFOS Vadose Zone distribution Coefficients from Product of Koc and foc

Groundwater Model Development Report

Former Loring Air Force Base, Limestone, Maine

PFAS	log K_{oc} (-)	K_{oc} (-)	Fire Training Area	Structural Fire Station	Crash Fire Station	Nose Dock #44
			K_d (foc = 0.010)	K_d (foc = 0.005)	K_d (foc = 0.011)	K_d (foc = 0.015)
Median PFOA	2.7	546	5.55	2.70	6.02	8.46
Median PFOS	3.4	2239	22.7	11.1	24.7	34.7

Notes:

K_{oc} - Organic carbon-water partition coefficient

K_d - Distribution coefficient with values reported in liters per kilogram

foc - fraction of organic carbon taken as the median of from soil sample analyses

PFAS - per- and polyfluoroalkyl substance

PFOA - perfluorooctanoic acid

PFOS - perfluorooctane sulfonate

Table N-18
Summary of Calculated Vadose Zone Distribution Coefficients

Groundwater Model Development Report
Former Loring Air Force Base, Limestone, Maine

Source Area	Median K_d from K_{oc} x foc		Median K_d of lysimeter porewater and collocated soil		Combined Median K_d	
	PFOA	PFOS	PFOA	PFOS	PFOA	PFOS
Fire Training Area	5.55	22.7	1.14	9.84	3.34	16.28
Structural Fire Station	2.70	11.1	0.77	25.2	1.74	18.10
Crash Fire Station	6.02	24.7	2.05	2.53	4.04	13.60
Nose Dock #44	8.46	34.7	--	--	8.46	34.67

Notes:

K_{oc} - Organic carbon-water partition coefficient

K_d - Distribution coefficient with values reported in liters per kilogram

foc - fraction of organic carbon taken as the median of from soil sample analyses

PFOA - perfluorooctanoic acid

PFOS - perfluorooctane sulfonate

Table N-19
Soil Physical Properties Table

Groundwater Model Development Report
Former Loring Air Force Base, Limestone, Maine

Source Area	Sample Location	Sample ID	Depth Interval Top (ftbgs)	Depth Interval Bottom (ftbgs)	Bulk Density (g/cm3)	Moisture Content (%)	Effective Porosity, n_e	Total Porosity, n_T
Fire Training Area	LYS01007	LORNG_LYS01007_0-3_08042022_E	0	3	1.45	16.1	0.32	0.45
		LORNG_LYS01007_11-13_08042022E	11	13	1.70	8.95	0.11	0.36
	Median				1.58	12.5	0.22	0.41
Structural Fire Station	LYS05012	LORNG_LYS05012_0-3_08052022_E	0	3	1.64	5.54	0.31	0.38
		LORNG_LYS05012_8-10_08052022_E	8	10	1.57	8.71	0.14	0.41
		LORNG_LYS05012_18-20_08052022E	18	20	2.20	12.5	0.32	0.17
	Median				1.64	8.71	0.31	0.39
Crash Fire Station	LYS07007	LORNG_LYS07007_0-3_08052022_E	0	3	1.63	10.8	0.26	0.38
		LORNG_LYS07007_8-10_08052022_E	8	10	1.55	10.3	0.20	0.42
		LORNG_LYS07007_18-20_08052022E	18	20	1.55	9.29	0.18	0.42
	Median				1.55	10.3	0.20	0.42
Nose Dock #44	LYS12010	LORNG_LYS12010_0-3_08042022_E	0	3	1.37	10.7	0.32	0.48
		LORNG_LYS12010_6-8_08052022_E	6	8	1.82	10.9	0.18	0.31
	Median				1.58	10.3	0.22	0.40

Notes:

ftbgs - feet below ground surface

g/cm^3 - grams per cubic centimeter

n_e - effective porosity

n_T - total porosity

Table N-20
Air-Water Interfacial Area Calaculations Table

Groundwater Model Development Report
Former Loring Air Force Base, Limestone, Maine

Source Area	a_{aw}	GSA (L^2/L^3)	n (-)	D_{50} (um)*			Sw (-)
				Shallow	Intermediate	Deep	
Fire Training Area	400	579	0.41	3727	61	--	0.31
Structural Fire Station	300	417	0.39	5875	88	1482	0.28
Crash Fire Station	168	221	0.42	460	171	144	0.24
Nose Dock #44	177	243	0.40	1638	148	--	0.27

Notes:

a_w - air-water interfacial area

D_{50} - particle size where 50 percent of the total particles are smaller

GSA - geometric surface area of the medium

um - micro meter

Sw - volumetric water content divided by total porosity

* Shallow is 0-3 feet at all source areas, Intermediate is 6-8 feet at NDA, 8-10 feet at Structural Fire Station and Crash Fire Station, and 11-13 feet at FTA, and deep is 18-20 feet .

Table N-21

Summarized Grain Size Analysis and Calculated Effective Porosity Values from Shallow Soil Sample LYS01007

Groundwater Model Development Report

Former Loring Air Force Base, Limestone, Maine

LYS01007 0-3 ft							
Sample Fraction	Size (um)	Pan Tare (g)	Pan+Sample (g)	Sample (g)	%Finer	Classification	Subclass
3”	75000	0	0	0	100	Gravel	
2”	50000	0	0	0	100	Gravel	
1.5”	37500	0	0	0	100	Gravel	
1”	25000	0	0	0	100	Gravel	
3/4”	19000	0	0	0	100	Gravel	
1/4”	6300	403.7	460.4	56.7	55.67	Gravel	
#4	4750	405	408.6	3.6	52.85	Gravel	
#10	2000	368.3	378.1	9.8	45.19	Sand	Coarse
#20	850	303.7	313.9	10.2	37.21	Sand	Medium
#40	425	269.7	276.9	7.2	31.58	Sand	Medium
#60	250	245.6	250.6	5	27.67	Sand	Fine
#80	180	246.3	248.6	2.3	25.88	Sand	Fine
#100	150	234.5	235.7	1.2	24.94	Sand	Fine
#200	75	314.2	317.9	3.7	22.04	Sand	Fine

Mt (g)*	127.89

Pi	ln(di,g)	Piln(di,g)	Dlng (um)	effective porosity (n_e)
0.00	10.0	0.0	613.3	**0.321**
44.33	9.3	412.3		
2.81	8.6	24.2		
7.66	8.0	61.6		
7.98	7.2	57.2		
5.63	6.4	36.0		
3.91	5.8	22.6		
1.80	5.4	9.6		
0.94	5.1	4.8		
2.89	4.7	13.5		

Uniformity Coefficient (D_{60}/D_{10})
1073

Notes:

D_{10} - particle size where 10 percent of the total particles are smaller

D_{60} - particle size where 60 percent of the total particles are smaller

Dlng - the geometric particle size diameter

g - gram

ln(di,g) - natrual log of the geometric mean of the referential grain size

Mt - total mass of dry sample

Pi - percentile of the sieve residue mass in the total mass of the sample

um - micrometer

* Total sample mass is taken as the oven dried weight provided in the laboratory report

Table N-22

Summarized Grain Size Analysis and Calculated Effective Porosity Values from Intermediate Soil Sample LYS01007

Groundwater Model Development Report

Former Loring Air Force Base, Limestone, Maine

LYS01007 11-13 ft							
Sample Fraction	Size (um)	Pan Tare (g)	Pan+Sample (g)	Sample (g)	%Finer	Classification	Subclass
3”	75000	0	0	0	100	Gravel	
2”	50000	0	0	0	100	Gravel	
1.5”	37500	0	0	0	100	Gravel	
1”	25000	0	0	0	100	Gravel	
3/4”	19000	0	0	0	100	Gravel	
1/4”	6300	403.7	415.8	12.1	91.16	Gravel	
#4	4750	405	409.5	4.5	87.87	Gravel	
#10	2000	368.3	382.3	14	77.65	Sand	Coarse
#20	850	303.7	313.3	9.6	70.64	Sand	Medium
#40	425	269.7	276.3	6.6	65.81	Sand	Medium
#60	250	245.6	250.7	5.1	62.09	Sand	Fine
#80	180	246.3	249.3	3	59.9	Sand	Fine
#100	150	234.5	236.3	1.8	58.58	Sand	Fine
#200	75	314.2	320	5.8	54.35	Sand	Fine

Mt (g)*	136.9

Pi	ln(di,g)	Piln(di,g)	Dlng (um)	effective porosity (n_e)
0.00	10.0	0.0	28.1	**0.111**
8.84	9.3	82.2		
3.29	8.6	28.3		
10.23	8.0	82.2		
7.01	7.2	50.3		
4.82	6.4	30.8		
3.73	5.8	21.6		
2.19	5.4	11.7		
1.31	5.1	6.7		
4.24	4.7	19.8		

Uniformity Coefficient (D_{60}/D_{10})
143

Notes:

D_{10} - particle size where 10 percent of the total particles are smaller

D_{60} - particle size where 60 percent of the total particles are smaller

Dlng - the geometric particle size diameter

g - gram

ln(di,g) - natrual log of the geometric mean of the referential grain size

Mt - total mass of dry sample

Pi - percentile of the sieve residue mass in the total mass of the sample

um - micrometer

* Total sample mass is taken as the oven dried weight provided in the laboratory report

Table N-23

Summarized Grain Size Analysis and Calculated Effective Porosity Values from Shallow Soil Sample LYS05012

Groundwater Model Development Report

Former Loring Air Force Base, Limestone, Maine

LYS05012 0-3 feet							
Sample Fraction	Size (um)	Pan Tare (g)	Pan+Sample (g)	Sample (g)	%Finer	Classification	Subclass
3”	75000	0	0	0	100	Gravel	
2”	50000	0	0	0	100	Gravel	
1.5”	37500	0	0	0	100	Gravel	
1”	25000	0	0	0	100	Gravel	
3/4”	19000	0	0	0	100	Gravel	
1/4”	6300	403.7	468.9	65.2	54.38	Gravel	
#4	4750	405	413.2	8.2	48.64	Gravel	
#10	2000	368.3	383.9	15.6	37.72	Sand	Coarse
#20	850	303.7	316.3	12.6	28.91	Sand	Medium
#40	425	269.7	278.4	8.7	22.82	Sand	Medium
#60	250	245.6	251.1	5.5	18.97	Sand	Fine
#80	180	246.3	248.5	2.2	17.43	Sand	Fine
#100	150	234.5	235.4	0.9	16.8	Sand	Fine
#200	75	314.2	317.1	2.9	14.77	Sand	Fine

Mt (g)*	142.91

Pi	ln(di,g)	Piln(di,g)	Dlng (um)	effective porosity (n_e)
0.00	10.0	0.0	1173.5	**0.310**
45.62	9.3	424.3		
5.74	8.6	49.4		
10.92	8.0	87.7		
8.82	7.2	63.2		
6.09	6.4	39.0		
3.85	5.8	22.3		
1.54	5.4	8.2		
0.63	5.1	3.2		
2.03	4.7	9.5		

Uniformity Coefficient (D_{60}/D_{10})
272

Notes:

D_{10} - particle size where 10 percent of the total particles are smaller

D_{60} - particle size where 60 percent of the total particles are smaller

Dlng - the geometric particle size diameter

g - gram

ln(di,g) - natrual log of the geometric mean of the referential grain size

Mt - total mass of dry sample

Pi - percentile of the sieve residue mass in the total mass of the sample

um - micrometer

* Total sample mass is taken as the oven dried weight provided in the laboratory report

Table N-24

Summarized Grain Size Analysis and Calculated Effective Porosity Values from Intermediate Soil Sample LYS05012

Groundwater Model Development Report

Former Loring Air Force Base, Limestone, Maine

LYS05012 8-10 feet							
Sample Fraction	Size (um)	Pan Tare (g)	Pan+Sample (g)	Sample (g)	%Finer	Classification	Subclass
3”	75000	0	0	0	100	Gravel	
2”	50000	0	0	0	100	Gravel	
1.5”	37500	0	0	0	100	Gravel	
1”	25000	0	0	0	100	Gravel	
3/4”	19000	0	0	0	100	Gravel	
1/4”	6300	403.9	424.5	20.6	85.39	Gravel	
#4	4750	405	408.9	3.9	82.63	Gravel	
#10	2000	368.1	379.1	11	74.83	Sand	Coarse
#20	850	303.6	313.6	10	67.74	Sand	Medium
#40	425	269.9	276.6	6.7	62.98	Sand	Medium
#60	250	245.6	251.5	5.9	58.8	Sand	Fine
#80	180	246.3	250.1	3.8	56.11	Sand	Fine
#100	150	234.3	236.7	2.4	54.4	Sand	Fine
#200	75	314.1	321.6	7.5	49.09	Sand	Fine

Mt (g)*	141.02

Pi	ln(di,g)	Piln(di,g)	Dlng (um)	effective porosity (n_e)
0.00	10.0	0.0	42.8	**0.140**
14.61	9.3	135.9		
2.77	8.6	23.8		
7.80	8.0	62.7		
7.09	7.2	50.9		
4.75	6.4	30.4		
4.18	5.8	24.2		
2.69	5.4	14.4		
1.70	5.1	8.7		
5.32	4.7	24.8		

Uniformity Coefficient (D_{60}/D_{10})
191

Notes:

D_{10} - particle size where 10 percent of the total particles are smaller

D_{60} - particle size where 60 percent of the total particles are smaller

Dlng - the geometric particle size diameter

g - gram

ln(di,g) - natrual log of the geometric mean of the referential grain size

Mt - total mass of dry sample

Pi - percentile of the sieve residue mass in the total mass of the sample

um - micrometer

* Total sample mass is taken as the oven dried weight provided in the laboratory report

Table N-25

Summarized Grain Size Analysis and Calculated Effective Porosity Values from Deep Soil Sample LYS05012

Groundwater Model Development Report

Former Loring Air Force Base, Limestone, Maine

LYS05012 18-20 feet							
Sample Fraction	Size (um)	Pan Tare (g)	Pan+Sample (g)	Sample (g)	%Finer	Classification	Subclass
3”	75000	0	0	0	100	Gravel	
2”	50000	0	0	0	100	Gravel	
1.5”	37500	0	0	0	100	Gravel	
1”	25000	0	0	0	100	Gravel	
3/4”	19000	556.6	575.6	19	86.12	Gravel	
1/4”	6300	403.7	434.8	31.1	63.4	Gravel	
#4	4750	405	409.8	4.8	59.89	Gravel	
#10	2000	368.3	377.7	9.4	53.03	Sand	Coarse
#20	850	303.7	312.9	9.2	46.3	Sand	Medium
#40	425	269.7	277.6	7.9	40.53	Sand	Medium
#60	250	245.6	250.9	5.3	36.66	Sand	Fine
#80	180	246.3	248.8	2.5	34.83	Sand	Fine
#100	150	234.5	235.9	1.4	33.81	Sand	Fine
#200	75	314.2	317.9	3.7	31.11	Sand	Fine

Mt (g)*	136.88

Pi	ln(di,g)	Piln(di,g)	Dlng (um)	effective porosity (n_e)
13.88	10.0	138.7	300.3	**0.320**
22.72	9.3	211.3		
3.51	8.6	30.2		
6.87	8.0	55.2		
6.72	7.2	48.2		
5.77	6.4	36.9		
3.87	5.8	22.4		
1.83	5.4	9.8		
1.02	5.1	5.2		
2.70	4.7	12.6		

Uniformity Coefficient (D_{60}/D_{10})
1557

Notes:

D_{10} - particle size where 10 percent of the total particles are smaller

D_{60} - particle size where 60 percent of the total particles are smaller

Dlng - the geometric particle size diameter

g - gram

ln(di,g) - natrual log of the geometric mean of the referential grain size

Mt - total mass of dry sample

Pi - percentile of the sieve residue mass in the total mass of the sample

um - micrometer

* Total sample mass is taken as the oven dried weight provided in the laboratory report

Table N-26

Summarized Grain Size Analysis and Calculated Effective Porosity Values from Shallow Soil Sample LYS07007

Groundwater Model Development Report

Former Loring Air Force Base, Limestone, Maine

LYS07007 0-3 feet							
Sample Fraction	Size (um)	Pan Tare (g)	Pan+Sample (g)	Sample (g)	%Finer	Classification	Subclass
3”	75000	0	0	0	100	Gravel	
2”	50000	0	0	0	100	Gravel	
1.5”	37500	0	0	0	100	Gravel	
1”	25000	0	0	0	100	Gravel	
3/4”	19000	556.4	574	17.6	87.05	Gravel	
1/4”	6300	403.9	419.3	15.4	75.72	Gravel	
#4	4750	405	409.5	4.5	72.41	Gravel	
#10	2000	368.1	381	12.9	62.92	Sand	Coarse
#20	850	303.6	314.3	10.7	55.05	Sand	Medium
#40	425	269.9	277.4	7.5	49.54	Sand	Medium
#60	250	245.6	251.3	5.7	45.34	Sand	Fine
#80	180	246.3	249.4	3.1	43.06	Sand	Fine
#100	150	234.3	236.2	1.9	41.66	Sand	Fine
#200	75	314.1	319.6	5.5	37.62	Sand	Fine

Mt (g)*	135.94

Pi	ln(di,g)	Piln(di,g)	Dlng (um)	effective porosity (n_e)
12.95	10.0	129.3	139.3	**0.260**
11.33	9.3	105.4		
3.31	8.6	28.5		
9.49	8.0	76.2		
7.87	7.2	56.5		
5.52	6.4	35.3		
4.19	5.8	24.3		
2.28	5.4	12.2		
1.40	5.1	7.1		
4.05	4.7	18.9		

Uniformity Coefficient (D_{60}/D_{10})
275

Notes:

D_{10} - particle size where 10 percent of the total particles are smaller

D_{60} - particle size where 60 percent of the total particles are smaller

Dlng - the geometric particle size diameter

g - gram

ln(di,g) - natrual log of the geometric mean of the referential grain size

Mt - total mass of dry sample

Pi - percentile of the sieve residue mass in the total mass of the sample

um - micrometer

* Total sample mass is taken as the oven dried weight provided in the laboratory report

Table N-27

Summarized Grain Size Analysis and Calculated Effective Porosity Values from Intermediate Soil Sample LYS07007

Groundwater Model Development Report

Former Loring Air Force Base, Limestone, Maine

LYS07007 8-10 feet							
Sample Fraction	**Size (um)**	**Pan Tare (g)**	**Pan+Sample (g)**	**Sample (g)**	**%Finer**	**Classification**	**Subclass**
3”	75000	0	0	0	100	Gravel	
2”	50000	0	0	0	100	Gravel	
1.5”	37500	0	0	0	100	Gravel	
1”	25000	0	0	0	100	Gravel	
3/4”	19000	0	0	0	100	Gravel	
1/4”	6300	403.9	429.3	25.4	81.39	Gravel	
#4	4750	405	409.3	4.3	78.24	Gravel	
#10	2000	368.1	381.3	13.2	68.57	Sand	Coarse
#20	850	303.6	313.2	9.6	61.54	Sand	Medium
#40	425	269.9	276.4	6.5	56.78	Sand	Medium
#60	250	245.6	250.9	5.3	52.9	Sand	Fine
#80	180	246.3	249.6	3.3	50.48	Sand	Fine
#100	150	234.3	236.4	2.1	48.94	Sand	Fine
#200	75	314.1	320.1	6	44.55	Sand	Fine

Mt (g)*	136.51

Pi	**ln(di,g)**	**Piln(di,g)**	**Dlng (um)**	**effective porosity (n_e)**
0.00	10.0	151.4	310.8	**0.200**
18.61	9.3	173.0		
3.15	8.6	27.1		
9.67	8.0	77.7		
7.03	7.2	50.4		
4.76	6.4	30.5		
3.88	5.8	22.5		
2.42	5.4	13.0		
1.54	5.1	7.8		
4.40	4.7	20.5		

Uniformity Coefficient (D_{60}/D_{10})
281

Notes:

D_{10} - particle size where 10 percent of the total particles are smaller

D_{60} - particle size where 60 percent of the total particles are smaller

Dlng - the geometric particle size diameter

g - gram

ln(di,g) - natrual log of the geometric mean of the referential grain size

Mt - total mass of dry sample

Pi - percentile of the sieve residue mass in the total mass of the sample

um - micrometer

* Total sample mass is taken as the oven dried weight provided in the laboratory report

Table N-28

Summarized Grain Size Analysis and Calculated Effective Porosity Values from Deep Soil Sample LYS07007

Groundwater Model Development Report

Former Loring Air Force Base, Limestone, Maine

LYS07007 18-20 feet							
Sample Fraction	Size (um)	Pan Tare (g)	Pan+Sample (g)	Sample (g)	%Finer	Classification	Subclass
3”	75000	0	0	0	100	Gravel	
2”	50000	0	0	0	100	Gravel	
1.5”	37500	0	0	0	100	Gravel	
1”	25000	0	0	0	100	Gravel	
3/4”	19000	0	0	0	100	Gravel	
1/4”	6300	403.9	429	25.1	82.08	Gravel	
#4	4750	405	409.9	4.9	78.58	Gravel	
#10	2000	368.1	380	11.9	70.09	Sand	Coarse
#20	850	303.6	314	10.4	62.67	Sand	Medium
#40	425	269.9	276.8	6.9	57.74	Sand	Medium
#60	250	245.6	250.9	5.3	53.96	Sand	Fine
#80	180	246.3	249.5	3.2	51.67	Sand	Fine
#100	150	234.3	236.2	1.9	50.32	Sand	Fine
#200	75	314.1	319.9	5.8	46.18	Sand	Fine

Mt (g)*	140.08

Pi	ln(di,g)	Piln(di,g)	Dlng (um)	effective porosity (n_e)
0.00	10.0	0.0	60.4	**0.180**
17.92	9.3	166.6		
3.50	8.6	30.1		
8.50	8.0	68.2		
7.42	7.2	53.3		
4.93	6.4	31.5		
3.78	5.8	21.9		
2.28	5.4	12.2		
1.36	5.1	6.9		
4.14	4.7	19.3		

Uniformity Coefficient (D_{60}/D_{10})
337

Notes:

D_{10} - particle size where 10 percent of the total particles are smaller

D_{60} - particle size where 60 percent of the total particles are smaller

Dlng - the geometric particle size diameter

g - gram

ln(di,g) - natrual log of the geometric mean of the referential grain size

Mt - total mass of dry sample

Pi - percentile of the sieve residue mass in the total mass of the sample

um - micrometer

* Total sample mass is taken as the oven dried weight provided in the laboratory report

Table N-29

Summarized Grain Size Analysis and Calculated Effective Porosity Values from Shallow Soil Sample LYS12010

Groundwater Model Development Report

Former Loring Air Force Base, Limestone, Maine

LYS12010 0-3 feet							
Sample Fraction	Size (um)	Pan Tare (g)	Pan+Sample (g)	Sample (g)	%Finer	Classification	Subclass
3”	75000	0	0	0	100	Gravel	
2”	50000	0	0	0	100	Gravel	
1.5”	37500	0	0	0	100	Gravel	
1”	25000	0	0	0	100	Gravel	
3/4”	19000	0	0	0	100	Gravel	
1/4”	6300	403.7	436.8	33.1	75.45	Gravel	
#4	4750	405	412.5	7.5	69.89	Gravel	
#10	2000	368.3	389.7	21.4	54.02	Sand	Coarse
#20	850	303.7	320.9	17.2	41.26	Sand	Medium
#40	425	269.7	279.5	9.8	33.99	Sand	Medium
#60	250	245.6	250.5	4.9	30.36	Sand	Fine
#80	180	246.3	248.3	2	28.87	Sand	Fine
#100	150	234.5	235.5	1	28.13	Sand	Fine
#200	75	314.2	316.9	2.7	26.13	Sand	Fine

Mt (g)*	99.6

Pi	ln(di,g)	Piln(di,g)	Dlng (um)	effective porosity (n_e)
0.00	10.0	0.0	343.1	**0.322**
24.55	9.3	228.3		
5.56	8.6	47.9		
15.87	8.0	127.5		
12.76	7.2	91.5		
7.27	6.4	46.5		
3.63	5.8	21.0		
1.48	5.4	7.9		
0.74	5.1	3.8		
2.00	4.7	9.3		

Uniformity Coefficient (D_{60}/D_{10})
314

Notes:

D_{10} - particle size where 10 percent of the total particles are smaller

D_{60} - particle size where 60 percent of the total particles are smaller

Dlng - the geometric particle size diameter

g - gram

ln(di,g) - natrual log of the geometric mean of the referential grain size

Mt - total mass of dry sample

Pi - percentile of the sieve residue mass in the total mass of the sample

um - micrometer

* Total sample mass is taken as the oven dried weight provided in the laboratory report

Table N-30

Summarized Grain Size Analysis and Calculated Effective Porosity Values from Intermediate Soil Sample LYS12010

Groundwater Model Development Report

Former Loring Air Force Base, Limestone, Maine

LYS12010 6-8 feet							
Sample Fraction	**Size (um)**	**Pan Tare (g)**	**Pan+Sample (g)**	**Sample (g)**	**%Finer**	**Classification**	**Subclass**
3”	75000	0	0	0	100	Gravel	
2”	50000	0	0	0	100	Gravel	
1.5”	37500	0	0	0	100	Gravel	
1”	25000	0	0	0	100	Gravel	
3/4”	19000	0	0	0	100	Gravel	
1/4”	6300	403.9	428.6	24.7	82.14	Gravel	
#4	4750	405	411.9	6.9	77.15	Gravel	
#10	2000	368.1	380.7	12.6	68.04	Sand	Coarse
#20	850	303.6	313.2	9.6	61.1	Sand	Medium
#40	425	269.9	275.9	6	56.76	Sand	Medium
#60	250	245.6	250.3	4.7	53.36	Sand	Fine
#80	180	246.3	249	2.7	51.41	Sand	Fine
#100	150	234.3	236.1	1.8	50.1	Sand	Fine
#200	75	314.1	319.9	5.8	45.91	Sand	Fine

Mt (g)*	74.8

Pi	ln(di,g)	Piln(di,g)	Dlng (um)	effective porosity (n_e)
0.00	10.0	0.0	64.2	**0.180**
17.86	9.3	166.1		
4.99	8.6	42.9		
9.11	8.0	73.2		
6.94	7.2	49.8		
4.34	6.4	27.8		
3.40	5.8	19.7		
1.95	5.4	10.5		
1.30	5.1	6.6		
4.19	4.7	19.6		

Uniformity Coefficient (D_{60}/D_{10})
654

Notes:

D_{10} - particle size where 10 percent of the total particles are smaller

D_{60} - particle size where 60 percent of the total particles are smaller

Dlng - the geometric particle size diameter

g - gram

ln(di,g) - natrual log of the geometric mean of the referential grain size

Mt - total mass of dry sample

Pi - percentile of the sieve residue mass in the total mass of the sample

um - micrometer

* Total sample mass is taken as the oven dried weight provided in the laboratory report

Table N-31

Summary of Calculated PFOA and PFOS Saturated Distribution Coefficients

Groundwater Model Development Report
Former Loring Air Force Base, Limestone, Maine

Sample ID	Calculated Linear Kd (L/kg)	
	PFOA	PFOS
2208376	0.3	15.3
2208377	0.5	0.6
2208378	0.4	1.8
2208379	0.5	0.4
Average	0.43	4.5

Notes:

Kd - distribution coefficient

L/kg - liters per kilogram

Table N-32
LEAF PFOA Source Term Power Functions

Groundwater Model Development Report
Former Loring Air Force Base, Limestone, Maine

Source Area	LEAF Analysis	Liquid to Solid Ratio (L/S)	Time (yrs)	PFOA (ng/L)	log (time)	log (PFOA)
Nose Dock. No 44 Area	LORG_LYS12010_0-3_080422T01	0.2	4.9	279	0.7	2.4
	LORG_LYS12010_0-3_080422T02	0.5	12.4	164	1.1	2.2
	LORG_LYS12010_0-3_080422T03	1.0	24.7	55.8	1.4	1.7
	LORG_LYS12010_0-3_080422T04	1.5	37.1	16.9	1.6	1.2
	LORG_LYS12010_0-3_080422T05	2.0	49.4	8.9	1.7	0.9
	LORG_LYS12010_0-3_080422T06	4.5	111.2	3.6	2.0	0.6
	LORG_LYS12010_0-3_080422T07	5.0	123.5	1.9	2.1	0.3
	LORG_LYS12010_0-3_080422T08	9.5	234.7	2.6	2.4	0.4
	LORG_LYS12010_0-3_080422T09	10	247.0	2.6	2.4	0.4
			Fitted Power Function Parameters			
			Slope (exponent b)	Intercept log(a)	a	a_{adj}
			-1.369	3.473	2970	NA

Source Area	LEAF Analysis	Liquid to Solid Ratio (L/S)	Time (yrs)	PFOA	log (time)	log (PFOA)
Crash Fire Station	LORG_LYS07007_8-10_080522T01	0.2	5.2	4250	0.7	3.6
	LORG_LYS07007_8-10_080522T02	0.5	12.9	2010	1.1	3.3
	LORG_LYS07007_8-10_080522T03	1.0	25.9	1060	1.4	3.0
	LORG_LYS07007_8-10_080522T04	1.5	38.8	540	1.6	2.7
	LORG_LYS07007_8-10_080522T05	2.0	51.8	441	1.7	2.6
	LORG_LYS07007_8-10_080522T06	4.5	116.5	259	2.1	2.4
	LORG_LYS07007_8-10_080522T07	5.0	129.4	178	2.1	2.3
	LORG_LYS07007_8-10_080522T08	9.5	245.9	98.5	2.4	2.0
	LORG_LYS07007_8-10_080522T09	10	258.8	72.7	2.4	1.9
	Deep Lysimeter Median			7260		
			Fitted Power Function Parameters			
			Slope (exponent b)	Intercept log(a)	a	a_{adj}
			-1.013	4.398	25022	7260

Source Area	LEAF Analysis	Liquid to Solid Ratio (L/S)	Time (yrs)	PFOA	log (time)	log (PFOA)
Fire Training Area	LORG_LYS01007_11-13_080422T01	0.2	6.2	843	0.8	2.9
	LORG_LYS01007_11-13_080422T02	0.5	15.4	301	1.2	2.5
	LORG_LYS01007_11-13_080422T03	1.0	30.8	68.8	1.5	1.8
	LORG_LYS01007_11-13_080422T04	1.5	46.3	14.1	1.7	1.1
	LORG_LYS01007_11-13_080422T05	2.0	61.7	6.3	1.8	0.8
	LORG_LYS01007_11-13_080422T06	4.5	138.8	7.4	2.1	0.9
	LORG_LYS01007_11-13_080422T07	5.0	154.2	4.7	2.2	0.7
	LORG_LYS01007_11-13_080422T08	9.5	293.0	5	2.5	0.7
	LORG_LYS01007_11-13_080422T09	10	308.4	4.8	2.5	0.7
	Deep Lysimeter Median			1220		
			Fitted Power Function Parameters			
			Slope (exponent b)	Intercept log(a)	a	a_{adj}
			-1.381	3.833	6805	1220

Source Area	LEAF Analysis	Liquid to Solid Ratio (L/S)	Time (yrs)	PFOA	log (time)	log (PFOA)
Structural Fire Station	LORG_LYS05012_0-3_080522T01	0.2	2.6	419	0.4	2.6
	LORG_LYS05012_0-3_080522T02	0.5	6.4	110	0.8	2.0
	LORG_LYS05012_0-3_080522T03	1.0	12.8	30.7	1.1	1.5
	LORG_LYS05012_0-3_080522T04	1.5	19.1	15	1.3	1.2
	LORG_LYS05012_0-3_080522T05	2.0	25.5	11.3	1.4	1.1
	LORG_LYS05012_0-3_080522T06	4.5	57.4	10.3	1.8	1.0
	LORG_LYS05012_0-3_080522T07	5.0	63.8	5.3	1.8	0.7
	LORG_LYS05012_0-3_080522T08	9.5	121.2	5.9	2.1	0.8
	LORG_LYS05012_0-3_080522T09	10	127.6	5.9	2.1	0.8
	Deep Lysimeter Median			1124.5		
			Fitted Power Function Parameters			
			Slope (exponent b)	Intercept log(a)	a	a_{adj}
			-1.063	2.803	635	1125

Notes:

Greater than the target soil porewater concentration (C_{pw}) from SSL analyses

a - is the power function intercept fitted to the LEAF results

a_{adj} -is the power function intercept fitted to the LEAF results adjusted to the lysimeter median concentration

b - is the power function exponent and fitted slope to the LEAF results

LEAF - Leaching Environmental Assessment Framework

ng/L - nano grams per liter

PFOA - Perfluorooctanoic acid

yrs - years

Table N-33
LEAF PFOS Source Term Power Functions

Groundwater Model Development Report
Former Loring Air Force Base, Limestone, Maine

Source Area	LEAF Analysis	Liquid to Solid Ratio	Time (yrs)	PFOS (ng/L)	log (time)	log (PFOS)
Nose Dock. No 44 Area	LORG_LYS12010_0-3_080422T01	0.2	4.941	1030	0.7	3.0
	LORG_LYS12010_0-3_080422T02	0.5	12.4	755	1.1	2.9
	LORG_LYS12010_0-3_080422T03	1.0	24.7	1220	1.4	3.1
	LORG_LYS12010_0-3_080422T04	1.5	37.1	1340	1.6	3.1
	LORG_LYS12010_0-3_080422T05	2.0	49.4	1130	1.7	3.1
	LORG_LYS12010_0-3_080422T06	4.5	111.2	662	2.0	2.8
	LORG_LYS12010_0-3_080422T07	5.0	123.5	371	2.1	2.6
	LORG_LYS12010_0-3_080422T08	9.5	234.7	155	2.4	2.2
	LORG_LYS12010_0-3_080422T09	10	247.0	125	2.4	2.1
			Fitted Power Function Parameters			
			Slope (exponent b)	Intercept log(a)	a	a_{adj}
			-0.509	3.626	4230	NA

Source Area	LEAF Analysis	Liquid to Solid Ratio	Time (yrs)	PFOS (ng/L)	log (time)	log (PFOS)
Crash Fire Station	LORG_LYS07007_8-10_080522T01	0.2	5.2	20900	0.7	4.3
	LORG_LYS07007_8-10_080522T02	0.5	12.9	15300	1.1	4.2
	LORG_LYS07007_8-10_080522T03	1.0	25.9	9930	1.4	4.0
	LORG_LYS07007_8-10_080522T04	1.5	38.8	6770	1.6	3.8
	LORG_LYS07007_8-10_080522T05	2.0	51.8	5320	1.7	3.7
	LORG_LYS07007_8-10_080522T06	4.5	116.5	3340	2.1	3.5
	LORG_LYS07007_8-10_080522T07	5.0	129.4	2530	2.1	3.4
	LORG_LYS07007_8-10_080522T08	9.5	245.9	1260	2.4	3.1
	LORG_LYS07007_8-10_080522T09	10	258.8	1030	2.4	3.0
	Deep Lysimeter Median			13300		
			Fitted Power Function Parameters			
			Slope (exponent b)	Intercept log(a)	a	a_{adj}
			-0.772	5.009	102152	13300

Source Area	LEAF Analysis	Liquid to Solid Ratio	Time (yrs)	PFOS (ng/L)	log (time)	log (PFOS)
Fire Training Area	LORG_LYS01007_11-13_080422T01	0.2	6.2	20700	0.8	4.3
	LORG_LYS01007_11-13_080422T02	0.5	15.4	7550	1.2	3.9
	LORG_LYS01007_11-13_080422T03	1.0	30.8	4750	1.5	3.7
	LORG_LYS01007_11-13_080422T04	1.5	46.3	1340	1.7	3.1
	LORG_LYS01007_11-13_080422T05	2.0	61.7	591	1.8	2.8
	LORG_LYS01007_11-13_080422T06	4.5	138.8	274	2.1	2.4
	LORG_LYS01007_11-13_080422T07	5.0	154.2	186	2.2	2.3
	LORG_LYS01007_11-13_080422T08	9.5	293.0	115	2.5	2.1
	LORG_LYS01007_11-13_080422T09	10	308.4	92.2	2.5	2.0
	Deep Lysimeter Median			4855		
			Fitted Power Function Parameters			
			Slope (exponent b)	Intercept log(a)	a	a_{adj}
			-1.449	5.554	358027	4855

Source Area	LEAF Analysis	Liquid to Solid Ratio	Time (yrs)	PFOS (ng/L)	log (time)	log (PFOS)
Structural Fire Station	LORG_LYS05012_0-3_080522T01	0.2	2.6	10200	0.4	4.0
	LORG_LYS05012_0-3_080522T02	0.5	6.4	14900	0.8	4.2
	LORG_LYS05012_0-3_080522T03	1.0	12.8	5430	1.1	3.7
	LORG_LYS05012_0-3_080522T04	1.5	19.1	3090	1.3	3.5
	LORG_LYS05012_0-3_080522T05	2.0	25.5	2440	1.4	3.4
	LORG_LYS05012_0-3_080522T06	4.5	57.4	1340	1.8	3.1
	LORG_LYS05012_0-3_080522T07	5.0	63.8	975	1.8	3.0
	LORG_LYS05012_0-3_080522T08	9.5	121.2	475	2.1	2.7
	LORG_LYS05012_0-3_080522T09	10	127.6	374	2.1	2.6
	Deep Lysimeter Median			1250		
			Fitted Power Function Parameters			
			Slope (exponent b)	Intercept log(a)	a	a_{adj}
			-0.930	4.670	46769	1250

Notes:

Greater than the target soil porewater concentration (C_{pw}) from SSL analyses

a - is the power function intercept fitted to the LEAF results

a_{adj} -is the power function intercept fitted to the LEAF results adjusted to the lysimeter median concentration

b - is the power function exponent and fitted slope to the LEAF results

LEAF - Leaching Environmental Assessment Framework

ng/L - nano grams per liter

PFOS - Perfluorooctanesulfonic acid

yrs - years